THE REGULATION OF CARBAMOYL PHOSPHATE SYNTHETASE-ASPARTATE TRANSCARBAMOYLASE-DIHYDROOROTASE (CAD) BY PHOSPHORYLATION AND PROTEIN-PROTEIN INTERACTIONS

Eric M. Wauson

A dissertation submitted to the faculty of the University of North Carolina at Chapel Hill in partial fulfillment of the requirements for the degree of Doctor of Philosophy in the Department of Pharmacology.

Chapel Hill
2007

Approved by:

Lee M. Graves, Ph.D.

T. Kendall Harden, Ph.D.

Gary L. Johnson, Ph.D.

Aziz Sancar M.D., Ph.D.

Beverly S. Mitchell, M.D.

ABSTRACT

Eric M. Wauson: The Regulation of Carbamoyl Phosphate Synthetase-Aspartate Transcarbamoylase-Dihydroorotase (CAD) by Phosphorylation and Protein-Protein Interactions
(Under the direction of Lee M. Graves, Ph.D.)

Pyrimidines have many important roles in cellular physiology, as they are used in the formation of DNA, RNA, phospholipids, and pyrimidine sugars. The first rate-limiting step in the *de novo* pyrimidine synthesis pathway is catalyzed by the carbamoyl phosphate synthetase II (CPSase II) part of the multienzymatic complex Carbamoyl phosphate synthetase, Aspartate transcarbamoylase, Dihydroorotase (CAD). CAD gene induction is highly correlated to cell proliferation. Additionally, CAD is allosterically inhibited or activated by uridine triphosphate (UTP) or phosphoribosyl pyrophosphate (PRPP), respectively. The phosphorylation of CAD by PKA and ERK has been reported to modulate the response of CAD to allosteric modulators. While there has been much speculation on the identity of CAD phosphorylation sites, no definitive identification of *in vivo* CAD phosphorylation sites has been performed. Therefore, we sought to determine the specific CAD residues phosphorylated by ERK and PKA in intact cells. We observed the PKA-induced phosphorylation of Ser^{1406} and Ser^{1859} HEK-293 cells. Surprisingly, while ERK phosphorylated CAD on multiple residues *in vitro*, CAD was not an ERK substrate in HEK-293 cells. We determined the identity of a previously unknown phosphopeptide in CAD isolated from HEK-293 cells. We also observed that the phosphorylation of CAD in HEK-293 cells is important for the maintenance of

CPSase II activity. In addition to investigating the regulation of CAD by phosphorylation, we have identified a novel protein-protein interaction between CAD and the human cell cycle checkpoint protein hRad9. The interaction was mapped to the CPSase II portion of CAD, and the binding of hRad9 to CAD induced a significant activation of CPSase II activity. Taken together, these studies demonstrate novel mechanisms of CAD regulation in mammalian cells.

ACKNOWLEDGEMENTS

I want to thank my advisor, Lee Graves, for mentoring me. I enjoyed working with everyone in the Graves Lab. I want to thank Matthew Higgins, Brian Dewar, and Andrea Leisewitz for all of their support and for being great friends. Additionally, it was quite enjoyable working with Aziz Sancar and Laura Lindsey-Boltz. I learned a lot from them and they were great role models. My wife, Stephanie Wauson, and my two children, Madelyn and Alexander Wauson, have supported me throughout my graduate school career with their unconditional love. They have helped me stay grounded, and have taught me that family is the most important thing in my life. I want to give a special thanks to Stephanie for editing my dissertation, even though I gave it to her at the last moment. I also want to thank my mother and father, Mary and Peter Wauson, who have lovingly encouraged me to pursue my dreams and have always been there for me during the tough times. They fostered my intellectual curiosity by always engaging my brother and sister and I in stimulating conversations and debates on a wide variety of topics. My big brother, Matthew Wauson, has been a great friend and role model throughout my life. My relationship with my little sister, Molly Wauson, has brought me great joy throughout my life. I want to thank my Grandfather, Raymond Jennett (Doc). Doc has shared his intense curiosity of numerous subjects, including biology and history, with me ever since I can remember. His influence on me has helped to shape the person and scientist that I have become. My Grandmother, the late Bettie Jennett, also was very important in

shaping the person that I am today. Her enthusiasm for life was infectious and I loved her very much.

TABLE OF CONTENTS

LIST OF TABLES

LIST OF FIGURES

LIST OF ABBREVIATIONS

AC	adenylyl cyclase
ATCase	aspartate transcarbamoylase
ATM	ataxia-telangiectasia mutated
ATP	adenosine triphosphate
ATR	ATM and Rad 3-related
CAD	Carbamoyl phosphate synthetase, Aspartate transcarbamoylase, Dihydroorotase
cAMP	cyclic adenosine monophosphate
CDP-lipids	cytidine diphosphate-lipids
CMP	cytidine monophosphate
CNTs	concentrative nucleoside transporters
CPSase II	carbamoyl phosphate synthetase II
CTP	cytidine triphosphate
dCTP	deoxycytidine diphosphate
DHO	dihydroorotate
DHOase	dihydroorotase
DHODH	dihydroorotase dehydrogenase
DMSO	dimethylsulfoxide
dNTPs	deoxynucleoside triphosphates
dTTP	deoxythymidine triphosphate
dUDP	deoxyuridine diphosphate

dUTP	deoxyuridine uridine 5'-triphosphate
EGF	epidermal growth factor
ENTs	equilibrative nucleoside transporters
ERK	extracellular signal regulated kinase
ERK1/2	extracellular signal-regulated kinase1/2
FBS	fetal bovine serum
HEK	human embryonic kidney
HIF-1alpha	hypoxia inducible factor-1 alpha
HPLC	high performance liquid chromatograph
IMP	inosine 5`-monophosphate
KGF	keratinocyte growth factor
MALDI	matrix assisted laser desorption/ionization
MAP	mitogen-activated protein
MAPKs	mitogen-activated protein kinases
MBP	myelin basic protein
MKK	MAP kinase kinase
MKKK	MAP kinase kinase kinase
NLS	nuclear localization sequence
NTPs	ribonucleoside triphosphates
OMP	outer-membrane protein
PALA	phosphonacetyl-L-aspartate
PBS	phosphate buffered solution

PDGF	platelet derived growth factor
PHA	phytohemagglutinin
PKA	protein kinase A
PMA	phorbol 12-myristate 13-acetate
PMSF	phenylmethylsulfonyl fluoride
PRPP	phosphoribosyl pyrophosphate
RNR	ribonucleotide reductase
TFA	trifluoroacetic acid
TLC	thin layer chromatography
UCK	uridine/cytidine kinase
UDP	uridine diphosphate
UDP	uridine diphosphate
UMP	uridine monophosphate
UTP	uridine triphosphate
WT	wild type

CHAPTER I

GENERAL INTRODUCTION

1.1 Significance

The pyrimidines cytosine, uracil, and thymine are the heterocylic aromatic nitrogenous bases that, when attached to ribose sugars, compose the pyrimidine nucleosides cytidine, uridine, and thymidine, respectively. When these nucleosides contain one, two, or three phosphate groups, they are referred to as pyrimidine nucleotides. In addition to being the basic building blocks for RNA and DNA, pyrimidine nucleotides also are used in the synthesis of numerous other cellular components including glycoproteins, glycolipids, and phospholipids. Additionally, uridine nucleotides can function as ligands for cell surface receptors, as discussed below. Furthermore, pyrimidine nucleotides can exert anti-apoptotic effects by binding to cytochrome C, and thereby inhibiting apoptosome formation (Chandra et al., 2006).

The nucleotide uridine triphosphate (UTP) is incorporated directly into the synthesis of RNA polymers, or used as a substrate in the synthesis of cytidine triphosphate (CTP). Uridine diphosphate (UDP) is a substrate for ribonucleotide reductase (RNR), which forms deoxyuridine diphosphate (dUDP). The cell then converts dUDP to deoxythymidine triphosphate (dTTP), a necessary molecule for DNA synthesis (Figure 1.1). Additionally, UTP is used in the synthesis of UDP-glucose and UDP-N-acetylglucosamine. These UDP-sugars are used in the glycosylation of proteins and the formation of UDP-sugar derivatives, which are substrates for the synthesis of disaccharides and polysaccharides such as glycogen. Furthermore, UDP can be converted to uridine triphosphate (UTP) by nucleoside diphosphate kinase (Reviewed in (Huang and Graves, 2003).

Uridine nucleotides and UDP-sugars function as ligands for numerous members of the G-protein coupled P2Y receptors. Signaling through these receptors has been reported to elicit diverse physiological consequences, such as the induction of chemotaxis in dendritic cells (Idzko et al., 2002), the vasodilation or vasoconstriction of blood vessels (reviewed in Brunschweiger and Muller, 2006), and the enhanced proliferation of human neural stem precursor cells (Milosevic et al., 2006). Hence, the biosynthesis of pyrimidine nucleotides may influence cell signaling through the regulation of these receptors.

The cytidine nucleotides (CTP and dCTP) are incorporated into both RNA and DNA polymers. Additionally, CTP is a substrate for the formation of cytidine diphosphate-lipids (CDP-lipids), which are used by cells to make phospholipids. Phospholipids are important components of cellular membranes and act as second messengers. Moreover, cytidine monophosphate (CMP) is used in the synthesis of sialic acid. Sialic acids are nine carbon sugars, which are commonly attached to the ends of glycoproteins. Some of the functions of sialic acids have been elucidated, including the creation of recognition signals on receptors for sugar binding protein ligands, such as the selectins and various interleukins. Additionally, sialic acids form the most commonly found ligands for receptors on pathogenic viruses, bacteria, and protozoa (reviewed in Lehmann et al., 2006; Schauer, 2000).

Mammals obtain pyrimidine nucleotides by either *de novo* synthesis from basic cellular molecules including ATP, glutamine, and bicarbonate, or through an alternative salvage pathway that uses the nucleosides uridine and cytidine to make pyrimidine nucleotides. The relative importance of these two pathways is dependent on the cell type

and physiological state, but in general, slower growing or quiescent cells tend to rely on salvage synthesis of pyrimidines, while rapidly growing cells, such as mitogen-stimulated lymphocytes, require the *de novo* synthesis of pyrimidines (Ruckemann et al., 1998). Since the salvage and *de novo* synthesis pathways both form UMP, this is the point of convergence between these two pathways. UMP is the common precursor for all other pyrimidine nucleotides. UDP and UTP can be formed by the phosphorylation of UMP by UMP kinase and the phosphorylation of UDP by nucleoside diphosphate kinase. CTP is formed when CTP-synthetase transfers the amide from glutamine and transfers it to UTP (Figure 1.1) (reviewed in Huang and Graves, 2003).

1.2. Salvage pyrimidine synthesis

A major source of uridine and cytidine for the salvage synthesis of pyrimidine nucleotides is the degradation of nucleic acids and nucleotides. An important class of enzymes involved with the degradation of UTP, UDP, and UMP into uridine is the 5′-nucleotidases. Cytidine is converted to uridine by the action of cytidine deaminase. The catabolism of uridine and uracil is accomplished by the activities of uridine phosphorylase and dihydropyrimidine dehydrogenase, which catalyze the conversion of uridine to uracil and uracil to dihydrouracil, respectively (reviewed in Anderson and Parkinson, 1997). In most tissues, uridine is the starting point for the pyrimidine salvage pathway. The human blood plasma levels of uridine are strictly regulated at 3-5 μM, and the liver functions to keep this level constant by either degrading or synthesizing uridine as the need arises (reviewed in Connolly and Duley, 1999; Traut, 1994).

The uridine and cytidine in the blood plasma and other extracellular fluids are transported across cellular membranes by nucleoside transporters. These transporters are

critical homeostatic regulators of intra- and extracellular concentrations of nucleosides and nucleotides. The two major families of nucleoside transporters identified in numerous species, including mammals, are the equilibrative (sodium-independent) nucleoside transporters (ENTs) and the concentrative (sodium-dependent) nucleoside transporters (CNTs) (reviewed in Zhang et al., 2007). Increased ENT expression is highly correlated with rapid cellular proliferation, and the mitogen stimulation of lymphocytes causes a significant increase in ENT expression (Smith et al., 1989; Wiley et al., 1989). Once uridine or cytidine is transported into cells, uridine/cytidine kinase (UCK) phosphorylates them creating UMP and CMP. The activity of UCK, which has been reported to be the rate-limiting step in the salvage synthesis of pyrimidines, can be increased by serum growth factors and insulin. Furthermore, UCK activity is significantly elevated in various tumor cell models (reviewed in Huang and Graves, 2003).

1.3 *De Novo* pyrimidine synthesis

De novo pyrimidine synthesis is a cellular process where glutamine, ATP, bicarbonate and aspartate are converted to uridine monophosphate by three proteins containing six enzymatic activities (Figure 1.2). The multifunctional protein CAD catalyzes the first three reactions in this pathway. CAD is an acronym derived from the three enzymatic activities contained within this protein: Carbamoyl phosphate synthetase II (CPSase-II)-Aspartate transcarbamoylase (ATCase)-Dihydroorotase (DHOase). CPSase-II is the rate-limiting step in the *de novo* pyrimidine synthesis pathway, and is highly regulated by multiple mechanisms (Figure 1.5.). Dihydroorotate, the final product created by CAD, is thought to diffuse through the cytoplasm to the mitochondria where it

serves as a substrate for the fourth enzyme in the de novo pyrimidine synthesis pathway dihydroorotate dehydrogenase (DHODH) (reviewed in Jones, 1980).

DHODH is a mitochondrial integral membrane protein that catalyzes the oxidation of dihydroorotate (DHO) to orotate. Since electrons released during the oxidation of DHO are transferred to ubiquinone, DHODH is an important component of the mitochondrial respiratory chain (Loffler et al., 1997). The interrelatedness of pyrimidine synthesis and cellular respiration was nicely demonstrated when chemically induced respiratory chain dysfunction was shown to inhibit DHODH activity causing a reduction in de novo pyrimidine synthesis (Beuneu et al., 2000; Gattermann et al., 2004). DHODH is a relevant drug target, since it was observed by Simmonds and colleagues that the DHODH inhibitor leflunomide (Arava™) prevented mitogen-induced lymphocyte expansion. Leflunomide is currently being used clinically as an immune suppressant in the treatment of rheumatoid arthritis (reviewed in Herrmann et al., 2000).

The final two steps in de novo pyrimidine biosynthesis are catalyzed in the cytoplasm by the bifunctional enzyme UMP-synthetase. The mammalian protein consists of the orotate phosphoribosyltransferase domain, which catalyzes the transfer of the phosphoribosyl group of 5-phosphoribosyl 1- pyrophosphate (PRPP) to orotate creating OMP, and the orotidine-5′-phosphate decarboxylase domain, which catalyses the formation of UMP from OMP (reviewed in (Evans and Guy, 2004; Jones, 1980).

Early studies demonstrated that UMP-synthetase formed dimers in the presence of OMP, leading to an increase in enzymatic activity (Traut and Jones, 1977). The activity of UMP-synthetase was observed to be elevated in rapidly dividing cells, such as regenerating liver cells (Pausch et al., 1972) or murine leukemia cells (Reyes and

Guganig, 1975). Furthermore, a study performed by Mitchell and Hoogenraad demonstrated the activity profile of the orotate phosphoribosyl transferase activity of UMP-synthetase in synchronized rate hepatoma cells that were induced to enter the cell cycle. They observed that activity of this enzyme was low in G1, rose rapidly during S-phase, but declined rapidly during the G2/M phase (Mitchell and Hoogenraad, 1975).

1.4 CAD

1.4.1 Enzymatic Domains in CAD and Mechanisms of Reactions

While early research demonstrated that the three enzymatic reactions that CAD performed were present in mammalian cells, it was not until 1970 that Jones speculated that these enzymes might be combined in one polypeptide chain (Jones, 1970). This speculation was based on genetic data that demonstrated that a single protein in *Neurospora* and yeast had both ATCase and CPSase enzymatic activities. Subsequent experiments demonstrated that the CPSase and ATCase enzymatic activities were contained within single complexes in Ehrlich ascites cells, mouse spleen, human lymphocytes (Hoogenraad et al., 1971; Ito and Uchino, 1973; Shoaf and Jones, 1971; Shoaf and Jones, 1973). Finally, in 1977, Stark and colleagues demonstrated that the CPSase, ATCase, and DHOase activities were on a single, approximately 220,000 dalton protein by isolating CAD from a hamster cell line that was induced to overexpress all three enzymatic activities (Coleman et al., 1977).

1.4.1.a CPSase II

Brzozowski and colleagues first purified the bacterial CPSase from *E. coli* in 1966, and enzymatic data suggested that CPS catalyzed multiple steps during the formation of carbamoyl phosphate (Kalman et al., 1965). The *E. coli* CPSase enzyme

was determined to consist of a small subunit that liberated ammonia from glutamine and transferred it to the large subunit where the formation of carbamoyl phosphate occurred (Trotta et al., 1974). Both subunits had significant amino acid sequence homology with the large subunit of the *E. coli* CPSase (Simmer et al., 1990a), and much of what we know about the reaction mechanisms of the synthetase regions of CPSase II was derived from studies designed to investigate the *E. coli* CPSase.

The N-terminal section of the CPSase II domain of CAD contains the GLNase subdomain, and its sequence is highly similar to the sequence of the small subunit of *E. coli* CPSase (Simmer et al., 1990b). The GLNase subdomain is linked to the CPS.A and CPS.B subdomains by a 29-amino acid segment (Figure 1.3) (Bein et al., 1991; Maley and Davidson, 1988; Simmer et al., 1990a). Numerous studies suggest that the catalytic mechanism of GLNase is similar to cysteine proteases in that a nucleophilic histidine residue removes a proton from the sulfhydryl group of a cysteine residue in the active site. This cysteine residue then forms a γ-glutamyl thioester intermediate with glutamine and the subsequent release of ammonia occurs. Finally, in the rate limiting step, the thioester is hydrolyzed causing the regeneration of the active form of GLNase (Chaparian and Evans, 1991; Miran et al., 1991; Wellner et al., 1973).

When the hamster GLNase subdomain of CPSase II was cloned, expressed, and purified from *E. coli*, it was observed to have minimal glutaminase activity by itself. However, the activity was increased to normal levels when the GLNase subdomain was mixed with the *E. coli* CPSase large subunit (which is highly similar in sequence with the CPS.A and CPS. B subdomains of CPSase II) suggesting a functional linkage between the two subdomains (Guy and Evans, 1994b). Furthermore, Evans and colleagues

demonstrated that the GLNase activity of CAD was significantly lowered when ATP and HCO_3^-, the substrates for the CPS.A and CPS.B subdomains, are absent. Therefore, the authors hypothesized that the linkage of these domains allowed for a synchronization between the GLNase activity and the CPS.A and CPS.B. activities, allowing for the efficient use of substrates (Hewagama et al., 1999).

The large subunit of *E. coli* CPSase corresponds to the CPS (A) and CPS (B) subdomains of CAD (CPSase II synthetase regions) (Figure 1.3). Powers and Meister determined that the *E. coli* CPSase bound 2 molecules of ATP at two separate active sites where the formation of the unstable intermediates, carboxy phosphate and carbamate were synthesized (Powers et al., 1977; Powers and Meister, 1978). Numerous biochemical studies have contributed to the elucidation of the catalytic mechanism of *E. coli* CPSase. As described above, there are three active sites contained within the CPSase complex. The first active site is located within the small subunit, and is where glutamine is hydrolyzed to liberate ammonia molecules. The second active site, which is located within the CPS.A region of the large subunit, phosphorylates bicarbonate, creating carboxyphosphate. Carbamate then is formed from ammonia via a nucleophilic attack on the carboxyphosphate intermediate. Finally, the third active site, located in subdomain B (CPS.B), catalyzes the formation of carbamoyl phosphate by phosphorylating carbamate (Reviewed in Holden et al., 1999). Studies using positional isotope exchange demonstrated that the kinetic reaction mechanisms of the CPSase II of mammalian CAD were similar to the reaction mechanisms of *E. coli* CPSase (Meek et al., 1987).

Since the half-lives of carboxyphosphate and carbamate at neutral pH are quite short, the synchronization of the three reactions catalyzed by CPSase is important for the

efficient use of these unstable intermediates. It was demonstrated that the initiation event of the CPSase reaction cascade was the phosphorylation of bicarbonate at the second active site in the CPS.A region. This event caused a conformational change to the first active site in the small subunit; thereby, inducing a significant increase in the rate of glutamine hydrolysis. This ensures that there is ammonia immediately available to react with carboxyphosphate to form carbamate (Miles and Raushel, 2000).

The crystal structure of the *E. coli* CPSase was solved and found to consist of heterotetramer of the small and large CPSase subunits. Analysis of the crystal structure demonstrated the existence of a molecular tunnel in the interior of the protein that allowed unstable ammonia, carboxyphosphate, and carbamate to be channeled from the first through the third active site over a distance of approximately 100 angstroms (Thoden et al., 1997). Evidence supporting the hypothesis that the molecular tunnel allowed the channeling of intermediates was demonstrated by measuring CPSase enzymatic parameters in enzymes that had holes and blockages engineered into different points along the length of the tunnel (Huang and Raushel, 2000a; Huang and Raushel, 2000b; Kim et al., 2002; Kim and Raushel, 2004).

1.4.1.b ATCase and DHOase

The carbamoyl phosphate that is formed by the CPSase II domain is used by the ATCase domain of CAD to form carbamoyl aspartate. The approximately 40, 000 dalton fully active ATCase domain was isolated from hamster CAD elastase digests (Grayson and Evans, 1983). Subsequent experiments demonstrated that the ATCase domain had a molecular weight of 34,323 daltons, and its sequence was highly homologous with the sequence of the *E. coli* ATCase (Simmer et al., 1989). Studies on the *E. coli* ATCase

have suggested that the binding of carbamoyl phosphate occurs first, followed by aspartate (Porter et al., 1969). Furthermore, additional reports suggested that the binding of carbamoyl phosphate induced a conformational change in both *E. coli* ATCase and the ATCase domain of CAD, which was necessary for the subsequent binding of aspartate (Porter et al., 1969; Qiu and Davidson, 2000). While the *E. coli* ATCase is allosterically regulated by ATP, CTP, and UTP, the ATCase domain of CAD is not regulated by allosteric effectors (reviewed in Evans and Guy, 2004; Lipscomb, 1994).

The carbamoyl aspartate synthesized by the ATCase domain of CAD is used as a substrate by the DHOase domain to catalyze the reversible formation of dihydroorotate. Early work by Christopherson and Jones on the mouse DHOase suggested that the catalytic mechanism involved a zinc ion and a histidine residue (Christopherson et al., 1979). Evans and colleagues determined that the 44,000 dalton DHOase region of CAD was folded into an autonomously functioning domain when they excised DHOase from CAD by treating with elastase. It was determined that the isolated DHOase domain formed homodimers in solution. Furthermore, atomic absorption spectroscopy confirmed that each DHOase subunit contained a single zinc ion. (Kelly et al., 1986).

The crystal structure of the *E. coli* ATCase was solved and the active enzyme was determined to consist of two catalytic trimers in complex with three regulatory dimers (Stevens et al., 1991). The crystal structure of the *E. coli* DHOase demonstrated the existence of two catalytic zinc ions, while, as described above, the DHOase of CAD only has one zinc ion per subunit. While the crystal structure of the DHOase domain of CAD has yet to be solved, Christopherson and colleagues have grown and analyzed crystals of this domain (Maher et al., 2003).

1.4.2 CAD Enzymatic Properties and Structure

Studies using controlled proteolysis, and the cloning and expression of the separate domains of CAD have demonstrated that each of the three domains in CAD can exist as separately folded autonomously functional enzymes. Furthermore, these experiments allowed for the elucidation of the order of the domains in CAD polypeptide, which is as follows: NH_2-CPSase II-DHOase-ATCase-COOH (Kim et al., 1992; Williams et al., 1990).

The discretely folded functional domains of CAD are linked by interdomain linker regions. The length of the linker region that connects the DHOase and ATCase domains (DA linker) is conserved in all eukaryotes (Figure 1.3). Studies by Guy and Evans demonstrated that while DA linker deletion mutants of CAD had kinetic parameters similar to wild-type CAD, there was a reduced thermal stability of CPSase II activity. Additionally, it was observed that exogenously added carbamoyl phosphate could dilute the carbamoyl phosphate made by CPSase II to a much greater extent in the DA linker deletion mutant of CAD when compared to wild-type CAD. Therefore, it appeared that the DA linker facilitates carbamoyl phosphate channeling and enzyme stability (Guy and Evans, 1994a; Guy and Evans, 1994c).

Stark and colleagues observed that most of the CAD in cells was composed of trimers and hexamers of the 243-kDa polypeptide (Coleman et al., 1977). Crosslinking studies done by Evans and colleagues demonstrated that CAD monomers gradually formed cyclic hexamers with open planar appearances and that a portion of these hexamers formed larger oligomeric structures possibly representing the association of hexamers (Lee et al., 1985). Additional studies demonstrated that the hamster CAD

residues Asp^{2009} and Arg^{2187}, which are located in the ATCase domain (Figure 1.3), were critical for the formation of CAD hexamers. The site-directed mutagenesis of these residues to alanines caused a significant reduction in the V_{max} of ATCase, suggesting that, like the *E. coli* ATCase, oligomerization of this enzyme was important for catalytic activity.

All CAD substrates were observed to have Michaelis-Menten kinetics and the apparent affinity of each of the substrates was determined by Christopherson and Jones. The CPSase II activity was demonstrated to be the slowest of the three enzymes as the maximum velocities for CPSase II, ATCase, and DHOase were observed to be 329, 18,600 and 2,910 (pmol/min/μg), respectively (Christopherson and Jones, 1980).

The activity of CPSase II is unstable in aqueous buffers, and the addition of dimethylsulfoxide (DMSO) and glycerol was shown to stabilize this enzyme during storage and assay conditions (reviewed in Jones, 1980). A study by Tatibana and colleagues demonstrated that DMSO actually decreased the apparent K_m for MgATP (Ishida et al., 1977). Therefore, since DMSO is commonly used in CAD activity assays, the DMSO concentration should be noted when trying to compare the kinetic parameters of CAD between separate studies.

1.4.2.a Allosteric regulation of CAD

CPSase is the rate-limiting step of *de novo* pyrimidine biosynthesis and is allosterically regulated in all organisms tested. However, since the *E. coli* CPSase is used in both pyrimidine and arginine synthesis, and the CPSase II in animals is involved solely in pyrimidine synthesis, the two enzymes have evolved to use different regulatory ligands. The E. *coli* enzyme is activated by NH_3, IMP, and ornithine and inhibited by

UMP, while the mammalian CPSase II is inhibited by UTP, UDP, UDP-glucose, CTP, dUDP, and dUTP and activated by PRPP. The allosteric ligands activate or inhibit CPSase II activity by decreasing or increasing the affinity of the enzyme for ATP respectively. Furthermore, the polyamines spermine and spermidine inhibit the PRPP-induced increase in CAD activity (reviewed in Jones, 1980).

It was determined by Rubio and colleagues that UMP was bound to a 20-kDa fragment on the C-terminus of *E. coli* CPSase (Cervera et al., 1996). To determine if this regulatory domain region of *E. coli* corresponded to the homologous region in CPSase II of CAD, Evans and colleagues created an *E. coli*/hamster chimeric CPSase that consisted of most of the *E. coli* CPSase, except that the 20-kDa regulatory domain (B3 subdomain) was replaced with the homologous hamster CPSase II region. Interestingly, this chimera became insensitive to UMP and IMP, but was now able to be modulated with PRPP and UTP. Therefore, it was concluded that both PRPP and UTP bound in the CAD B3 subdomain (amino acids 1265-1461) (Figure 1.3) (Liu et al., 1994). By using the crystal structure to make predictions about the CPSase II domain of mammalian CAD, Davidson and colleagues performed site-directed mutagenesis studies that demonstrated that both PRPP and UTP could bind in a noncompetitive manner to the B3 subdomain. Furthermore, it appeared that PRPP activation dominates when both allosteric effectors were bound simultaneously (Simmons et al., 2004).

Cellular levels of PRPP can have significant effects on pyrimidine metabolism as it is used both as a substrate for UMP-synthetase, and as an allosteric activator of CPSase. PRPP synthetase catalyzes the formation of PRPP from ribose-5-phosphate and ATP. The average cellular concentration of PRPP was reported to be 0.1 mM (Jones,

1980), but fluctuations in this level can be caused by perturbations of ribose-5-phosphate levels and mitogens, such as insulin and epidermal growth factor (EGF), which induced an increase in PRPP-synthetase activity (Ishijima et al., 1988). Furthermore, Brand and colleagues demonstrated that PRPP levels increased through the G1-phase and reached maximum levels in the S-phase of concanavalin A stimulated rat thymocytes (Schobitz et al., 1991).

The allosteric regulation of CAD has been observed to be modified by both CAD phosphorylation (as discussed below) and a single point mutant discovered in the *Drosophila melanogaster* CAD gene rudimentary (*r*). The *Drosophila black* (b) mutation causes a dark cuticle color, a phenotype that is thought to be caused by lowered concentrations of β-alanine due to an abnormal increase in the catabolic enzyme β-alanine transaminase. The suppressor of black ($r^{sub(b)}$) mutation, which is found within the *r* gene, causes the dark cuticle phenotype of the (b) mutation to be restored to the normal color. Davidson and colleagues demonstrated that ($r^{sub(b)}$) phenotype was caused by the Glu^{1153} to Lys^{1153} (numbers represent corresponding residues in hamster CAD) (E1153K) mutation in the CPS.B2 domain of CAD (Figure1.4). It was further demonstrated that the E1153K mutation caused a significant reduction in the UTP-induced inhibition of CPSase II activity without affecting other enzymatic parameters (Simmons et al., 1999).

Carrey and colleagues have proposed that in addition to the allosteric regulation of CAD induced by PRPP and UTP, there exists a reciprocal allosteric mechanism that allows the substrates of CPSase II to activate ATCase and the substrates for ATCase to activate CPSase II. The binding of aspartate to ATCase caused CPSase II to be less

inhibited by its product carbamoyl phosphate. Furthermore, the binding of substrates to CPSase II caused an increase in the affinity ATCase for carbamoyl phosphate and aspartate. It was proposed reciprocal allostery evolved to increase the efficient use of the unstable substrate intermediates during the passage between active sites in CAD (Irvine et al., 1997).

1.5 CAD Evolution

While the first three steps in the *de novo* pyrimidine synthetic pathway are identical in bacteria, yeast, protozoa, and animals, the organization of the enzymes responsible for these steps vary from the single enzymatic proteins of the bacteria to the multienzymatic protein of animals (Figure 1.4). The evolution of the multifunctional characteristic of CAD appears to have involved gene duplication, gene translocation, and gene fusion events. The *E. coli* carA gene encodes the small subunit of the *E. coli* CPSase (described previously). Like the GLNase region of CAD, the small CPSase subunit (GLNase) catalyzes the formation of ammonia from glutamine. The small subunit forms interactions with the large CPSase subunit (encoded by the carB gene) allowing for the efficient transfer of glutamine

The large *E. coli* CPSase subunit is a 120 kDa enzyme that consists of highly homologous amino- and carboxy-terminal halves, which appear to have arisen from the duplication of a smaller ancestral gene (Nyunoya and Lusty, 1983). The two halves of CPSase II gene CPS.A and CPS.B (Figure 1.3) are highly homologous to the corresponding sections of the *E. coli* enzyme. Interestingly, although it appears that the CPS.A and CPS.B domains of CAD perform separate distinct functions as described above, when they were cloned and expressed separately, they were both observed to

catalyze the complete formation of carbamoyl phosphate (Guy and Evans, 1996). These data seem to further support the hypothesis that the CPS.A and CPS.B arose from the duplication and fusion of a smaller ancestral gene.

The carA and carB genes are separated by cistrons on a single operon in E. *coli* and other bacteria. Davidson and colleagues have hypothesized that a mutation of a stop codon between the carA and carB genes caused the formation of a CPSase II gene, which encoded a protein carrying the enzymatic activities of both the small and large subunits (reviewed in Davidson et al., 1993).

It is thought that after the eukaryotes split into animal and plant kingdoms that the ATCase and DHOase genes fused to the CPS gene creating the CAD gene. However, the duplication of the DHOase gene probably occurred prior to this fusion since yeast have a gene (URA4) that encodes the DHOase protein separated from the gene that encodes a protein with the CPSase and ATCase activities (URA2). Interestingly, the URA2 gene contains a region that is homologous to the sequences from DHOase from mammals and *E. coli*, but it is not catalytically active (reviewed in Davidson et al., 1993).

The selective advantages of the formation of multienzymatic protein CAD have been investigated. One hypothesis is that the close proximity of active sites on CAD allowed substrates of each enzyme to be channeled from one active site to the other without being degraded by catabolic enzymes. Jones and colleagues suggested that this "substrate channeling" occurred in CAD when they observed low cellular concentrations of carbamoyl phosphate and carbamoyl aspartate (Christopherson and Jones, 1980). Further evidence for the existence of substrate channeling in CAD was demonstrated when it was observed that endogenously-added carbamoyl phosphate was not

significantly used in the synthesis of carbamoyl aspartate, suggesting that the active sites were inaccessible to carbamoyl phosphate in the bulk solvent (Guy and Evans, 1994a). An additional selective advantage in having three enzyme activities in one protein is that the activities are coordinately regulated preventing the energetically wasteful process of creating substrates for subsequent enzymes in a pathway before those enzymes have been synthesized (Christopherson and Jones, 1980; Christopherson et al., 1981).

1.6 CAD and embryological development

Although currently little is known about the regulation of CAD during mammalian embryogenesis, studies with other organisms have demonstrated the importance of CAD activity during development. Studies using *Drosophila* showed that the unfertilized egg and early embryos had the highest activity of CAD, while enzymatic activity decreased rapidly during the first 24 hours after egg laying, reaching a minimum at the start of the first-instar larval stage. Between the first- and second-instar larval stages, CAD activity increased significantly. However, CAD activity began to decrease again until the end of the third instar larval stage. CAD activity then rose slightly but steadily through the pupa stages and into the adult stage (Mehl and Jarry, 1978). The molecular mechanisms by which CAD activity was regulated during *Drosophila* development have not been determined; these changes might result from transcriptional regulation and/or posttranslational modification of CAD, such as phosphorylation and/or caspase-mediated degradation (reviewed in Huang and Graves, 2003).

Mutations in *Drosophila* (*r)* that inhibited enzymatic activity have been identified (Jarry and Falk, 1974; Norby, 1973; Rawls and Fristrom, 1975). The rudimentary mutation caused lethality when the flies were grown on pyrimidine-deficient media;

however, when grown on media containing normal levels of pyrimidines, the flies exhibited small and abnormally shaped wings. Additionally, females homozygous for the rudimentary mutation were sterile when grown on normal pyrimidine containing media (Norby, 1970). These results demonstrated that CAD had tissue specific roles during *Drosophila* development.

As in *Drosophila*, CAD function is critical for the normal embryological development of zebrafish. It was found that CAD transcripts were maternally supplied to the egg since CAD mRNA was present before the start of zygotic transcription. During development, CAD mRNA levels appeared to be highest in the cells that were rapidly proliferating or initiating differentiation. When CAD mRNA levels were reduced using antisense oligonucleotides during zebrafish embryogenesis, tissue specific abnormalities were observed. The most dramatic phenotypes were the reduced eye size and inhibition of the differentiation of jaw and fin cartilage. Interestingly, the data suggested that the normal retinal development required CAD activity for the formation of nucleotides for RNA and DNA synthesis; whereas, UDP-dependent glycosylation was necessary for the normal differentiation of cartilage (Willer et al., 2005).

The role of CAD in the development of *C. elegans* was investigated when Okkema and colleagues discovered that a spontaneous mutation in the DHOase domain of *C. elegans* CAD (pyr-1 (cu8)) caused a loss of DHOase activity. The pyr-1 (cu8) mutation caused morphological defects and maternal effect lethality, as was seen in rudimentary mutations observed in *Drosophila* (described above). While this mutation was lethal to 95% of late stage embryos, the 5 % that survived had defects in pharyngeal morphogenesis and were shorter when compared to wild-type worms. As was found with

the *Drosophila* rudimentary mutations, the embryogenic lethality could be prevented by supplying exogenous pyrimidines to the growth media (Franks et al., 2006)

1.7 CAD gene transcription

CAD activity is well correlated with cellular growth, as rapidly growing tissues, such as fetal liver, spleen, testis and clonally expanding lymphocytes, have much higher CPSase II activity than slower growing tissues including lung, uterus, heart, brain and muscle. Additionally, various types of tumor cells display elevated CPSase II activity (Aoki et al., 1982a; Aoki and Weber, 1981; Ito and Uchino, 1971; Yip and Knox, 1970). One mechanism by which CPSase II activity is increased is through elevated transcription and expression of CAD. CAD mRNA levels are low in quiescent cells such as unstimulated lymphocytes (Wauson, unpublished data), serum starved cells and contact growth inhibited cells (Liao et al., 1986; Rao and Davidson, 1988). Following serum stimulation of quiescent cells, CAD mRNA levels increased approximately 10-fold at the G_1/S boundary (Rao and Church, 1988). Werner and colleagues observed that CAD mRNA increased within 5 hours of both KGF or EGF treatment of quiescent keratinocytes (Gassmann et al., 1999). Moreover, Snow and colleagues observed that CAD transcription was induced as B cells moved into and through the G_1 cell cycle phase after stimulation with PMA and ionomycin, LPS, or anti-IgM plus Il-4. Another earlier study showed that CAD specific activity was induced 5-fold over 70 hours in PHA-stimulated primary human lymphocytes. Since this increase was dependent on the synthesis of both RNA and protein, it was concluded that PHA induced CAD transcription (Ito and Uchino, 1971).

The mechanisms behind the growth-induced induction of CAD gene transcription have been investigated extensively. The CAD promoter contains transcription factor consensus binding sequences for E2f, Sp1, Myc, Max, and USF transcription factors (Boyd and Farnham, 1997; Miltenberger et al., 1995). While it has not been determined which transcription factor maintains the basal gene transcription, the large growth-induced increase in CAD transcription was mediated by the E-box at +65 in the CAD promoter (Miltenberger et al., 1995). Additionally, it was determined that although the transcription factors USF, Myc, and Max bind to the CAD E-box *in vivo,* it was the Myc-Max heterodimer that was responsible for growth-regulated CAD expression (Boyd and Farnham, 1997). Studies in c-myc null cells confirmed that CAD was a c-Myc target gene (Bush et al., 1998). Further studies have shown that the CAD gene is induced in estrogen receptor positive breast cancer cells by estrogen receptor/Sp1 complexes in response to17β-estradiol. Moreover, mutational analysis of the CAD promoter showed that the E-box is not necessary for 17β-estradiol induced or basal CAD transcription in the breast cancer cell line (Khan et al., 2003). Thus, it appears that in some cell types, Myc is necessary for mitogen-induced CAD gene transcription, while in other cell types, transcription factors such as Sp1 are required.

Cellular cues, such as serum removal, induction of differentiation, and hypoxia, can induce a decrease in cellular levels of CAD mRNA. Two studies demonstrated that 12 hours incubation of cells in low serum growth conditions, CAD RNA levels remained unchanged, but by 24 hours, the cells displayed a ten-fold decrease in CAD mRNA when compared to cells growing in normal levels of serum (Liao et al., 1986; Rao and Davidson, 1988). Furthermore, CAD mRNA levels in HL-60 (human promyelocyte

leukemic cell line) cells drop significantly within 12 hours of the application of a differentiation stimulus (Rao et al., 1987). Additionally, data from our laboratory suggests that CAD levels decrease after the differentiation of myoblasts into myocytes (Lee Graves unpublished data). While the mechanism for the decrease of CAD gene transcription is not known, it may be due decreased c-Myc expression that occurs during serum starvation and myoblast and HL-60 differentiation (Reitsma et al., 1983; Wisdom and Lee, 1990; Yeilding et al., 1998). However, Mac and Farnham observed that CAD expression was not deregulated in Burkitt's lymphoma cell lines that overexpressed c-Myc, suggesting that mechanisms other than c-Myc expression also regulate CAD gene expression (Mac and Farnham, 2000). Indeed, Sif and colleagues observed that the repression of c-Myc-induced CAD transcription was caused by chromatin remodeling and histone deacetylation (Pal et al., 2003). Another mechanism for the downregulation of CAD transcription appears to be the direct interaction of hypoxia inducible factor-1 alpha (HIF-1alpha) with the CAD promoter (Chen et al., 2005).

1.8 Chemical Inhibitors of CAD

In 1971, Collins and Stark reported on the synthesis of the rationally designed ATCase inhibitor N-(phosphonacetyl)-L-aspartate (PALA). The structure of PALA resembles the two natural substrates of ATCase, carbamoyl phosphate and aspartate, and inhibits the carbamoyl phosphate binding and aspartate binding to ATCase in a competitive and noncompetitive manner, respectively (reviewed in (Grem et al., 1988)). 100 μM PALA was observed to prevent cellular division and kill the majority of the cells in a culture of SV40-transformed hamster kidney. This cytotoxicity was attributed to the inhibition of *de novo* pyrimidine synthesis since 100 μM of exogenously added uridine

completely inhibited the cell death and cell cycle arrest. During these studies it was observed that a small number of the hamster cells were resistant to 100 μM PALA (Swyryd et al., 1974). In subsequent studies, PALA-resistant cells were subjected to incremental increases in the PALA concentrations up to 25 mM. It was concluded that the resistance was due to the increase in CAD mRNA and protein and the subsequent 100-fold increase in ATCase activity (Kempe et al., 1976; Padgett et al., 1979). Stark and colleagues determined that the increase in CAD levels in PALA resistant cells was due to the amplification of the CAD gene (Wahl et al., 1979). Phase I and II clinical trials were performed with PALA; however, dose-limiting gut toxicities and tumor resistance due to CAD gene amplification prevented the use of PALA as a treatment option (reviewed in Grem et al., 1988).

Acivicin was another compound observed to inhibit CPSase II activity. Acivicin is a naturally occurring L-glutamine antagonist antibiotic discovered to be released from *Streptomyces sviceus* (Jayaram et al., 1975). Cooney and colleagues determined that the combined treatment of mice bearing tumors consisting of a PALA resistant Lewis Lung cell line with acivicin and PALA effectively inhibited CPSase II and ATCase activity respectively, causing tumor growth arrest and increased life spans (Kensler et al., 1981). However, since acivicin is a glutamine antagonist, it can inhibit numerous glutamine transferase enzymes, making the determination of the mechanisms by which it inhibits tumor growth difficult. In fact, Christopherson and colleagues observed that acivicin was a potent inhibitor of CTP-synthetase and GMP-synthetase, but not CPSase II, in intact leukemia cells (Lyons et al., 1990).

Current research is underway to investigate ways of inhibiting CPS II activity to treat diseases caused by the protozoa such *P. falciparum* (the malarial parasite). Stewart and colleagues observed that there was a significant decrease in viability of *P. falciparum* when in *vitro* cultures were treated with hammerhead ribozymes that targeted regions of the CPS II gene. Another protozoan that is sensitive to the inhibition of CPS II is the toxoplasmic encephalitis causing parasite *T. gondii.* Fox and Bzik created *T. gondii* strains that were CPS II null, and thus lacked detectable CPSase II activity. When mice were injected with the normal CPS II containing strains of *T. gondii*, they succumbed to the infection within 9 days. However, the mice that were injected with the CPS II null strains of *T. gondii* survived for greater than 6 months with no apparent parasite infection (Fox et al., 2002).

1.9 Post-translational regulation of CAD

1.9.1 CAD Phosphorylation

Early studies by Tatibana and colleagues showed that CAD was phosphorylated *in vitro* by the purified catalytic subunit of cyclic adenosine monophosphate (cAMP)-dependent protein kinase (PKA) (Otsuki et al., 1981). PKA was first discovered to be an effector of cAMP by Krebs and colleagues (Walsh et al., 1968). cAMP is synthesized from ATP by the adenylyl cyclase (AC) enzyme in response to numerous cellular signaling molecules, such as hormones, neurotransmitters, and growth factors. Ligand bound G-protein coupled receptors release $G_s\alpha$ or $G_i\alpha$ subunits that activate or inhibit the membrane bound adenylyl cyclase (AC), respectively. Ten isoforms of AC have been identified in mammals with noted differences in tissue distribution (reviewed in Tasken and Aandahl, 2004).

The cAMP-modulated increase in PKA has been extensively studied. PKA is a holoenzyme consisting of two catalytic subunits (C) and a dimer of two regulatory subunits (RI and RII). cAMP binds each of the RI and RII subunits at sites A and B in a cooperative manner. The binding of cAMP molecules induces a conformational change that allows the catalytic subunits to be released into active monomers (reviewed in (Kim et al., 2006). The active PKA monomers then can phosphorylate serine and threonine residues on numerous substrate proteins (reviewed in (Tasken and Aandahl, 2004). PKA is known to phosphorylate serine and threonine residues on over 100 different proteins with the optimal amino acid consensus motif being R-R-X-S^*/T^* (* denotes phosphorylated residue) (reviewed in Shabb, 2001).

The first study to show that CAD was phosphorylated by PKA demonstrated that this kinase induced an incorporation of 2.2 mol $^{32}P_i$/mole of CAD. Additionally, they observed that PKA-mediated CAD phosphorylation caused a slight increase in CPSase II activity by decreasing the apparent Km value for MgATP (Otsuki et al., 1981). Hardie and colleagues subsequently confirmed that CAD was phosphorylated by PKA *in vitro* and further showed that the sites of *in vitro* phosphorylation were Ser^{1406} and Ser^{1859} (Figure 1.6). Additionally, while they confirmed that there was a slight increase in CPSase II activity after PKA phosphorylation, they observed that the ability of UTP to inhibit CPSase II activity was significantly reduced (Carrey et al., 1985). A further study showed that while the *S. cerevisiae* enzyme URA2 (described above) was phosphorylated *in vitro* by PKA, its enzymatic activity or allosteric regulation was not affected (Denis-Duphil et al., 1990).

To further investigate the effect of PKA phosphorylation on allosteric regulation, Evans and colleagues constructed an *E. coli*/hamster CPSase chimeric protein that had the *E. coli* CPSase A1 and A2 subdomains fused to the hamster CAD CPSase B3 subdomain (the subdomain that binds the allosteric regulators UTP and PRPP as described above) (Figure 1.4). They reported that PKA phosphorylation of the chimera caused it to become insensitive to UTP inhibition as previously demonstrated by Carrey and colleagues (Carrey et al., 1985). No change in the response to saturating levels of PRPP was observed between the phosphorylated or unphosphorylated chimera; however, it was reported that phosphorylation of chimera by PKA did cause a significant decrease in the affinity for PRPP (Sahay et al., 1998).

As described above, Carrey and colleagues discovered that Ser^{1859} was phosphorylated in the amino acid linker region between the DHOase and ATCase CAD domains (Figure 1.6). To investigate the function of this linker region and the phosphorylation of Ser^{1859}, Guy and Evans examined the effect of the deletion of this amino acid segment on CAD activity, allosteric regulation, and substrate channeling. They demonstrated that both the deletion of the linker region, or the PKA-induced phosphorylation of wild-type CAD, caused a significant decrease in channeling of carbamoyl phosphate between the CPSase and ATCase when compared to unphosphorylated wild-type CAD. Additionally, they determined that the PKA induced-phosphorylation of the deletion mutant (which lacks Ser^{1859}) induced a decrease in UTP inhibition and PRPP activation of CAD. Therefore, the authors concluded that the effect of the phosphorylation of Ser^{1406} was decreased UTP inhibition and reduced PRPP

stimulation and that the phosphorylation of Ser^{1859} caused a decrease in substrate channeling (Guy and Evans, 1994c).

Davidson and colleagues performed the first studies designed to investigate the PKA-induced CAD phosphorylation in vivo. CAD was observed to be phosphorylated in cells after the stimulation of PKA with 8-Br-cAMP. Furthermore, the phosphorylation was reduced in cells that were pretreated with the PKA inhibitor H89. Since PKA phosphorylated Ser^{1406} *in vitro*, it was hypothesized that this was the CAD site phosphorylated in intact cells. However, these authors reported no decrease in the phosphorylation of CAD that had Ser^{1406} mutated to Ala^{1406} (S1406A) (a residue not able to be phosphorylated) when compared to wild-type CAD. While these data suggested that Ser^{1406} was not the *in vivo* PKA-induced CAD phosphorylation site, the authors noted that the basal level of CAD phosphorylation in the absence of PKA stimulation may have prevented them from observing the loss of CAD phosphorylation in the S1406A mutant (Banerjei and Davidson, 1997).

Interestingly, when the Ser^{1406} CAD residue was mutated to the phospho-mimetic Glu^{1406} (S1406E) residue, there was an increase in CAD activity and a decrease in the UTP-induced allosteric inhibition. Furthermore, there was no observed effect on the PRPP-induced stimulation of CPSase II (Banerjei and Davidson, 1997). Using a Glu as a phospho-mimetic suggested that the function of the phosphorylation of Ser^{1406} was to increase CAD activity and decrease UTP inhibition. However, no catalytic or allosteric affect was observed in a subsequent study in which the *Drosophila* CAD rudimentary (*r*) serine residue corresponding to Ser^{1406} was mutated to the Glu (Simmons et al., 1999). Moreover, the CAD activity or allosteric regulation was not measured from forskolin-

treated cells that displayed PKA-induced CAD phosphorylation (Banerjei and Davidson, 1997). Therefore, the role of PKA-induced CAD phosphorylation in cells remained unclear.

During studies designed to determine substrates of the extracellular signal-regulated kinase1/2 (ERK1/2), Graves and colleagues demonstrated that ERK1/2 phosphorylated CAD *in vitro*. ERK1/2 is a member of the mitogen-activated protein kinases (MAPKs) and is activated in response to numerous physiological stimuli. Well-characterized activators of ERK are the growth factors, platelet derived growth factor (PDGF) and epidermal growth factor (EGF). By binding cell membrane receptors, EGF and PDGF activate a kinase cascade causing MAP kinase kinase kinases (MKKKs) to phosphorylate and activate MAP kinase kinases (MKKs). The MKKs, MEK1 and MEK2 then activate ERK1/2 by phosphorylating tyrosine and threonine residues in the activation domain. ERK1/2 phosphorylates numerous substrates, which are involved in diverse cellular processes such as proliferation, differentiation, and apoptosis (reviewed (Cuevas et al., 2007; Raman et al., 2007).

ERK1/2 were observed to phosphorylate CAD *in vitro* on Thr^{456}. Furthermore, the stimulation of ERK activity in the liver cell line GN4 by platelet derived growth factor (PDGF) induced CAD phosphorylation. It appeared that the phosphorylation of CAD caused a decrease in UTP inhibition and an increase in PRPP stimulation. However, the authors noted that it remained to be determined whether Thr^{456} was a major *in vitro* or *in vivo* ERK phosphorylation site (Graves et al., 2000).

To investigate the role of PKA- and ERK- mediated phosphorylation of CAD *in vivo*, Guy and colleagues performed studies using BHK 165-23 cells, a cell line that was

induced to overexpress CAD over 100-fold by selecting cells that were resistant to treatments with PALA. To determine if CAD phosphorylation was affected during cellular growth, CAD was immunoprecipitated from cells that were harvested every 24 hours for six days after plating. SDS-PAGE and immunoblotting using general phospho-threonine and phospho-serine antibodies was performed. They reported that CAD had increased threonine phosphorylation during exponential cellular growth when ERK was active and more serine phosphorylation as the growth of the cells slowed and there was higher PKA activity. Furthermore, the authors demonstrated that during times of high ERK activity and low PKA activity PRPP could stimulate CAD activity by 22-fold; however, when there was low ERK activity and high PKA activity, PRPP could only stimulate CAD by 6-fold. There was an observed increase in *de novo* pyrimidine synthesis during the exponential cellular growth when ERK levels were high. Therefore, the authors concluded that the physiological function of ERK-mediated CAD phosphorylation was to cause an increase in CAD activity thereby increasing pyrimidine pools needed for cellular growth. Additionally, they hypothesized that the role of PKA phosphorylation of CAD was to inhibit enzyme activity by decreasing PRPP stimulation during slowed cellular growth when high levels of pyrimidines were not needed (Sigoillot et al., 2002b).

To further investigate the role of ERK phosphorylation of CAD, Guy and colleagues used an antibody designed to recognize CAD pThr^{456} to determine if higher levels of pThr^{456} correlated with the increased CAD activity in the MCF7 breast cancer cell line. In this study it was reported that MCF7 cells had higher levels of active ERK and higher levels of phosphorylated CAD residue Thr^{456}, and U0126, a MEK-1 inhibitor,

appeared to decrease the pThr^{456} levels in MCF7 cells (Sigoillot et al., 2004). In more recent studies the pThr^{456} specific antibody was used to demonstrate that levels of CAD phosphorylated on Thr^{456} were enriched in the insoluble nuclear fraction of numerous cell types including MCF7 and HEK-293. It was proposed that CAD was most active in the nucleus where it was phosphorylated on Thr^{456} by ERK. Furthermore, it was hypothesized that nuclear localization of active CAD allowed for more efficient pyrimidine biosynthesis since the perinuclear region is enriched with mitochondria, and that dihydroorotate (the product of CAD) could be channeled directly to the mitochondrial DHODH without having to equilibrate into the cytoplasm (Sigoillot et al., 2005).

In addition to being phosphorylated by ERK and PKA, Evans and colleagues proposed that CAD was autophosphorylated. This proposal was based on the demonstration that the incubation of CAD, purified from BHK 165-23 cells, with [γ-^{32}P]ATP caused a 0.97 mol of phosphate incorporated per mol of CAD. Additionally, the authors reported that unpublished mass spectrometry data suggested that Thr^{1037} was the autophosphorylation site in CAD. Moreover, since CAD that was pre-incubated with ATP and kinase buffer had greater CPSase II activity and responded differently to allosteric effectors when compared to CAD that was not pre-incubated with ATP and kinase buffer, the authors concluded that these enzymatic changes were the result of the autophosphorylation of Thr^{1037} (Sigoillot et al., 2002a). Whether or not Thr^{1037} is an *in vivo* CAD phosphorylation site remains to be determined.

By performing a mass spectrometric global analysis of phosphorylation sites in proteins from HELA cells stimulated with EGF, Mann and colleagues discovered 6,600

putative phosphorylation sites on 2,244 proteins. According to the published database from this work (PHOSIDA.COM), CAD was phosphorylated on residues Ser^{1823}, Ser^{1859}, Ser^{1900}, Ser^{1920}, Ser^{1928}, and Thr^{1933} (Figure 1.6). Furthermore, an EGF-induced increase in the phosphorylation of Ser^{1900}, Ser^{1920}, Ser^{1928}, and Thr^{1933} was noted (Olsen et al., 2006). In a tyrosine specific global phosphorylation analysis performed by Comb and colleagues, it was reported that CAD isolated from pervanadate and calyculin treated Jurkat or K562 cells was phosphorylated on Tyr^{735}, Tyr^{1884}, and Tyr^{1890} (Identified with Phosphosite at www.phosphosite.org) (Rush et al., 2005). In additional studies, Evans and colleagues reported that the PKC phosphorylation of CAD at Ser^{1873} and the PKA phosphorylation of CAD at Ser^{1406} stimulate or inhibit ERK phosphorylation at Thr^{456} respectively (Kotsis et al., 2007; Sigoillot et al., 2007).

1.9.2 CAD Proteolysis

The apoptotic proteolytic enzyme caspase-3 was observed to cleave CAD during apoptosis. The cleavage sites were determined to be at Asp^{1143} and Asp^{1371} in the B2 and B3 subdomains of CPSase II respectively (Figure 1.4). The withdrawal of interleukin-3 from a myeloid precursor cell line or the addition of staurosporine caused caspase-3-mediated degradation of CAD that preceded the appearance of annexin-5 and DNA fragmentation, both late occurring events in cellular apoptosis. A decrease in activity and allosteric activation of CAD, as well as a decrease in intracellular pyrimidine pools, paralleled the cleavage of CAD (Huang et al., 2002). Tang and colleagues demonstrated in a recent study that physiological levels of nucleoside triphosphates (NTPs) bound to lysine residues on cytochrome C thereby preventing their interaction with Apaf-1, a key step in the subsequent activation of caspase-9 and the eventual cell death (Chandra et al.,

2006). Therefore, an interesting hypothesis is that the degradation of CAD and the consequent lowering of intracellular pyrimidines is necessary for cells to undergo efficient apoptosis.

1.10 Protein-Protein Interactions

A study performed by Angeletti and Engler demonstrated that CAD was present in adenovirus replicative complexes on the nuclear matrix of cells infected with adenovirus. More specifically, CAD formed a protein-protein interaction with the precursor of the terminal protein (pTP), the protein that initiates the stimulation of viral DNA chain extension. Although BrdU staining demonstrated that the CAD-pTP complex was present at sites of active replication, the function of this complex was not determined. Furthermore, large-scale protein-protein interaction screens have identified 14-3-3 zeta (Meek et al., 2004) and the postreplicative mismatch repair enzyme PMS2 (Cannavo et al., 2007) as CAD interacting proteins. A study performed by Carrey and colleagues suggested that CAD was associated with the actin cytoskeleton in sperm (Carrey et al., 2002). An additional protein-protein interaction between CAD and the human checkpoint protein hRad9 was found by our laboratory and is the subject of chapter III of this dissertation.

1.11 Intraceullar location of CAD

While the majority of CAD protein is reported to be cytoplasmic, CAD was observed in the nucleus in numerous studies (Angeletti and Engler, 1998; Carrey et al., 2002; Sigoillot et al., 2003). The function of nuclear CAD is currently unknown. As described above, Evans and colleagues have reported that nuclear CAD is more efficient than cytoplasmic CAD in providing dihydroorotate to the mitochondrial DHODH

enzyme. Therefore, they propose that the function of nuclear CAD is to increase the supply of cellular pyrimidine nucleotides. The signal that induces the trafficking of CAD to the nucleus in mammalian cells is not known. However, studies performed by Nagy and colleagues suggest that the yeast CAD homolog (Ura2) contains a bipartite nuclear localization sequence that directs it to the nucleus. Furthermore, studies in our laboratory demonstrated that CAD became almost entirely nuclear when hRad9 was cotransfected with CAD in HELA and HEK-293 cells (Brown and Graves, unpublished data).

1.12 Rad9

DNA damage can be caused by the exposure of cells to ionizing radiation, UV radiation, and numerous types of chemicals during the course of cellular growth. Since DNA damage can cause genomic instability leading to cellular death and pathological conditions such as cancer, the recognition and repair of this damage is critically important. Cell cycle checkpoints have evolved to cause the inhibition of the progression of the cell cycle so that damaged DNA can be repaired. Clearly defined checkpoints have been identified as the G1/S, intra-S, and G2/M checkpoints (reviewed in Sancar et al., 2004)). The recognition of DNA damage must first occur before the subsequent events leading to the eventual repair of DNA or the induction of apoptosis can occur. This recognition step is performed by the DNA damage sensors, which include the kinases ATM and ATR, the Rad17-RFC complex, and the 9-1-1 complex. The 9-1-1 complex is a homotrimer consisting of the hRad9, hRad1, and hHus1 proteins (reviewed in Sancar et al., 2004). The N-terminus of hRad9 and the C-terminus of the PCNA-like region of hRad9 are the regions on hRad9 responsible for the interaction with hRad1 and hHus1 respectively (Burtelow et al., 2001). This complex forms a ring-like structure that is

loaded onto damaged DNA by the hRad17-RFC protein complex (Bermudez et al., 2003; Griffith et al., 2002; Lindsey-Boltz et al., 2001). The 9-1-1 complex encircles damaged DNA and recruits other checkpoint proteins called mediators to the sites of damage. These mediators then activate the signal transducers, such as the checkpoint kinase Chk1, which subsequently inhibits cell cycle progression by targeting Cdc25 for ubiquitin-mediated degradation (reviewed in Sancar et al., 2004). In addition to the DNA damage sensor role of 9-1-1, this complex appears to also participate in DNA repair by directly binding to and activating DNA ligase I (Wang et al., 2006).

hRad9 can bind other cellular proteins outside the 9-1-1 complex. A BH3 domain in the N-Terminal portion of Rad9 allows Rad9 to bind to the prosurvival proteins BCL-2 and Bcl-x_L (Komatsu et al., 2000). The susceptibility to DNA damage-induced apoptosis was measured in cells transfected with either wild-type hRad9 or a BH3 deletion mutant of hRad9 that could not interact with BCL-2 or Bcl-x_L. The results suggested the function of Rad9 BCL-2/Bcl-x_L interaction was the promotion of apoptosis (Komatsu et al., 2000). Subsequent studies demonstrated that DNA damage caused the c-Abl tyrosine kinase to phosphorylate hRad9 on Tyr^{28} thereby inducing the hRad9/ Bcl-x_L interaction (Yoshida et al., 2002). In addition, Kufe and colleagues provided evidence that suggested that the hRad9 interaction with BCL-2/Bcl-x_L was also regulated by the direct phosphorylation of hRad9 by PKC delta (Yoshida et al., 2003).

The cellular localization of hRad9 has been investigated. Transiently transfected hRad9 in HeLa cells was expressed throughout the cells with highest expression being in the nucleus (Komatsu et al., 2000). Rad9 was primarily localized in the nucleus of the leukemia cell line K526 and in HEK 293 cells and hRad9 formed discrete nuclear foci

upon DNA damage (Burtelow et al., 2000). Subsequent studies by Davey and colleagues demonstrated that hRad9 colocalized with other DNA damage sensing proteins at double stranded DNA breaks within 2 minutes of damage induction (Greer et al., 2003). A nuclear localization sequence (NLS) located towards the C-terminus of the C-terminal domain of hRad9 was determined to be necessary for the DNA damage-induced cell cycle arrest at G2/M phase. Furthermore, it appeared that the NLS of hRad9 was necessary for the nuclear localization of other 9-1-1 components (Hirai and Wang, 2002). Therefore, it appears that the NLS of hRad9 is critical for the checkpoint function of hRad9. Since hRad9 bound to Bcl-2 and Bcl-xL outside the nucleus, the mechanism that allowed hRad9 to remain outside the nucleus was unclear. However, studies by Wang and colleagues suggested that during apoptotic signals, caspase-3 cleavage of hRad9 caused the cytoplasmic accumulation of hRad9 (Lee et al., 2003).

While hRad9 is required for the normal response to DNA chemically and radiation induced DNA damage, the deletion of the mouse version of this gene, Mrad9, demonstrated that Rad9 was also necessary for normal embryogenesis. The $Mrad9^{-/-}$ mouse embryos died between E9.5 and E12.5. Additionally, fibroblasts taken from $Mrad9^{-/-}$ embryos were not viable (Hopkins et al., 2004). Experiments performed with $Mrad9^{-/-}$ embryonic stem cells demonstrated that the primary role of Mrad9, at least in ES cells, was to protect cells against DNA damage induced apoptosis (Loegering et al., 2004).

Rad9 has been reported to have roles in addition to the direct checkpoint and apoptotic functions described above. hRad9 was determined to be a transcription factor able to directly activate the transcription of the cyclin-kinase inhibitor p21 (Yin et al.,

2004). Further studies suggested that the mechanism by which Rad9 activated p21 transcription was by forming a complex with the p53 protein and binding to the p21 promoter (Ishikawa et al., 2007). Additionally, hRad9 bound to and downregulated the activity of the androgen receptor (Liu et al., 2004). Data presented in chapter 3 of this dissertation suggests that an additional role of hRad9 is the regulation of nucleotide synthesis by binding to CAD and activating CPSase II activity (Lindsey-Boltz et al., 2004).

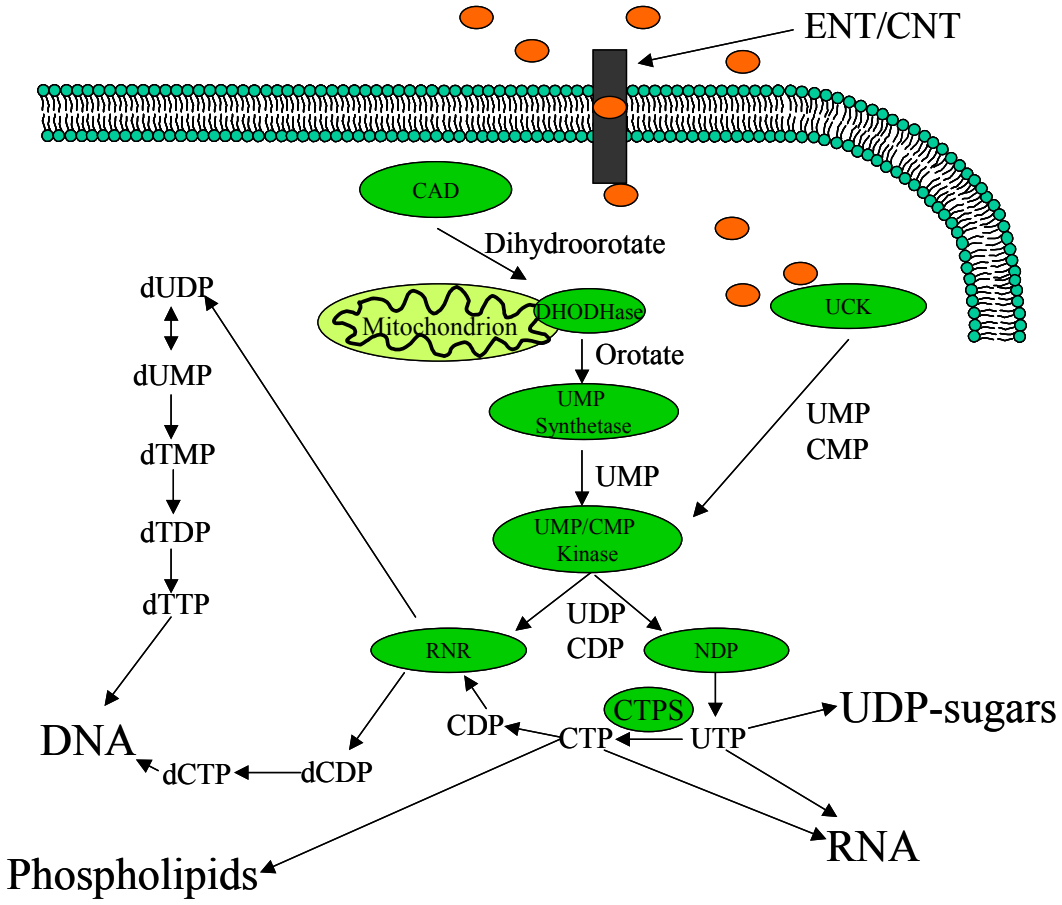

Figure 1.1. Cellular Pyrimidine Synthesis. Pyrimidines nucleotides can be synthesized *de novo* from basic cellular molecules, or by the salvage of preexisting nucleosides. The multifunctional protein CAD catalyzes the first three reactions in *de novo* pyrimidine biosynthesis. Dihydroorotate, the product of CAD, is then used by the mitochondrial membrane protein dihydroorotate dehydrogenase (DHODHase) to form orotate. Orotate then is used by the multienzymatic protein UMP-synthetase to form UMP. The extracellular nucleosides uridine and cytidine can be imported into cells by the equilibrative nucleoside transporters (ENTs) and the concentrative nucleoside transporters (CNTs). Once inside the cell, uridine and cytidine are phosphorylated to UMP and CMP by uridine/cytidine kinase (UCK). UMP/CMP kinase then phosphorylates UMP and CMP creating UDP and CDP, respectively. Nucleoside diphosphate kinase (NDPK) catalyzes the formation of UTP and CTP. While CTP can be formed by NDPK, CTP-Synthetase also catalyzes the formation of CTP from UTP. UTP is used in the formation of RNA and UDP-sugars, while CTP is incorporated into RNA and converted into phospholipids. Additionally, CDP is converted to deoxycytidine diphosphate (dCDP) by ribonucleotide reductase (RNR). dCDP then is used to make dCTP and is incorporated into DNA. RNR also converts UDP to dUDP. dUDP is transformed in a series of steps into dTTP, which is also used in the synthesis of DNA.

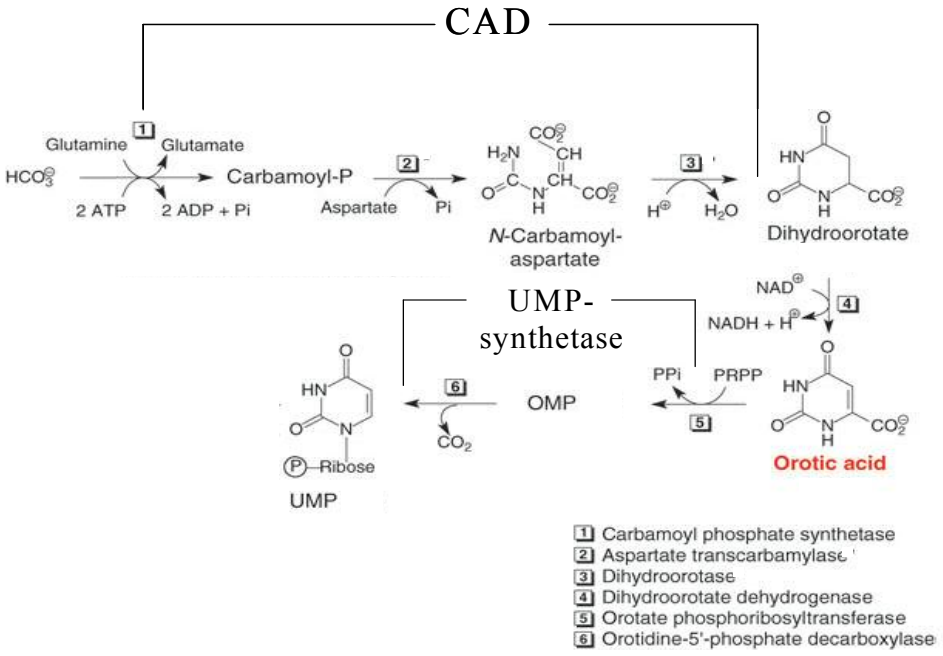

Figure 1.2. Chemical reactions in *de novo* pyrimidine synthesis. The CPSase II portion of CAD catalyzes the formation of carbamoyl phosphate. Carbamoyl aspartate transcarbamoylase then uses aspartate and ATP to form N-Carbamoyl-aspartate. N-Carbamoyl-aspartate catalyzes the condensation of N-Carbamoylaspartate to dihydroorotate. Dihydroorotate dehydrogenase then oxidizes dihydroorotate to orotic acid. The orotate phosphoribosyltransferase domain of UMP-synthetase uses PRPP and orotate to form Orotidine monophosphate (OMP). OMP is decarboxylated into UMP by the orotidine-5′-phosphate decarboxylase, which is the second enzymatic domain of UMP-synthetase. This image is from (Lagoja, 2005) and reproduced with permission. Copyright Wiley-VCH Verlag GmbH & Co. KgaA.

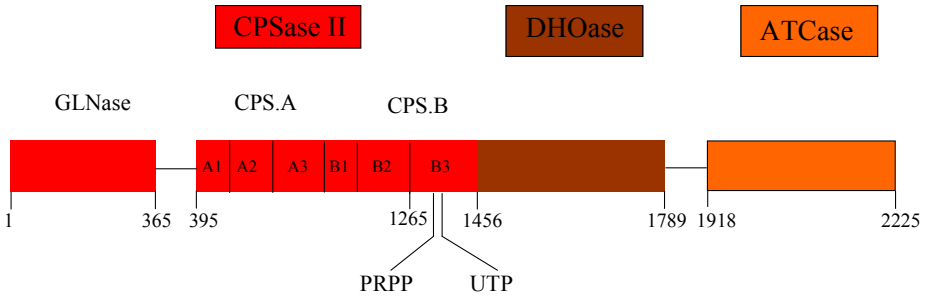

Figure 1.3. Domain structure of CAD. The numbers represent hamster amino acids (Kim et al., 1992). The amino acid numbers CAD is a modular protein consisting of three distinct domains: Carbamoyl phosphate synthetase II (CPSase II), Dihydroorotase (DHOase), and Aspartate transcarbamoylase (ATCase). The CPSase II is further divided into the subdomains glutaminase (GLNase), CPS.A, and CPS.B. The GLNase is on the N-terminal end of CAD, and is linked to the CPS.A. subdomain by a 30 amino acid linker region (amino acids 366-395). CPS.A and CPS.B are the highly homologous subdomains of CPSase II. The B3 region of CPS.B is the site of binding for the allosteric effectors PRPP and UTP. The DHOase and ATCase domains are connected via the 129 amino acid linker region (DA).

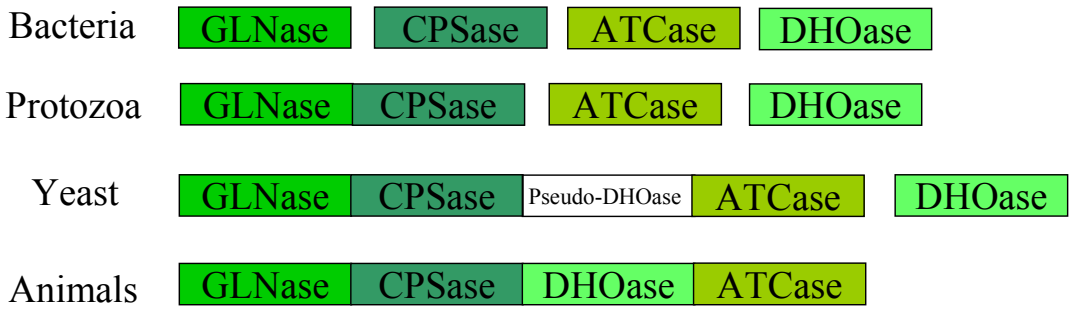

Figure 1.4. Evolution of CAD. The evolution of the multifunctional protein CAD is hypothesized to have occurred from gene duplications and gene fusions. Bacteria have four separate gene products that encode the four proteins: Glutaminase (GLNase), Carbamoylphosphate synthetase (CPSase), Aspartate Transcarbamoylase (ATCase), and Dihydroorotase (DHOase). Protozoa have a multifunctional protein that contains the GLNase and CPSase enzymatic activities. Yeast have evolved the multifunctional protein that contains the GLNase, CPSase and ATCase enzymatic activities. Finally, animals express the CAD protein, which contains all four of the enzymatic activities.

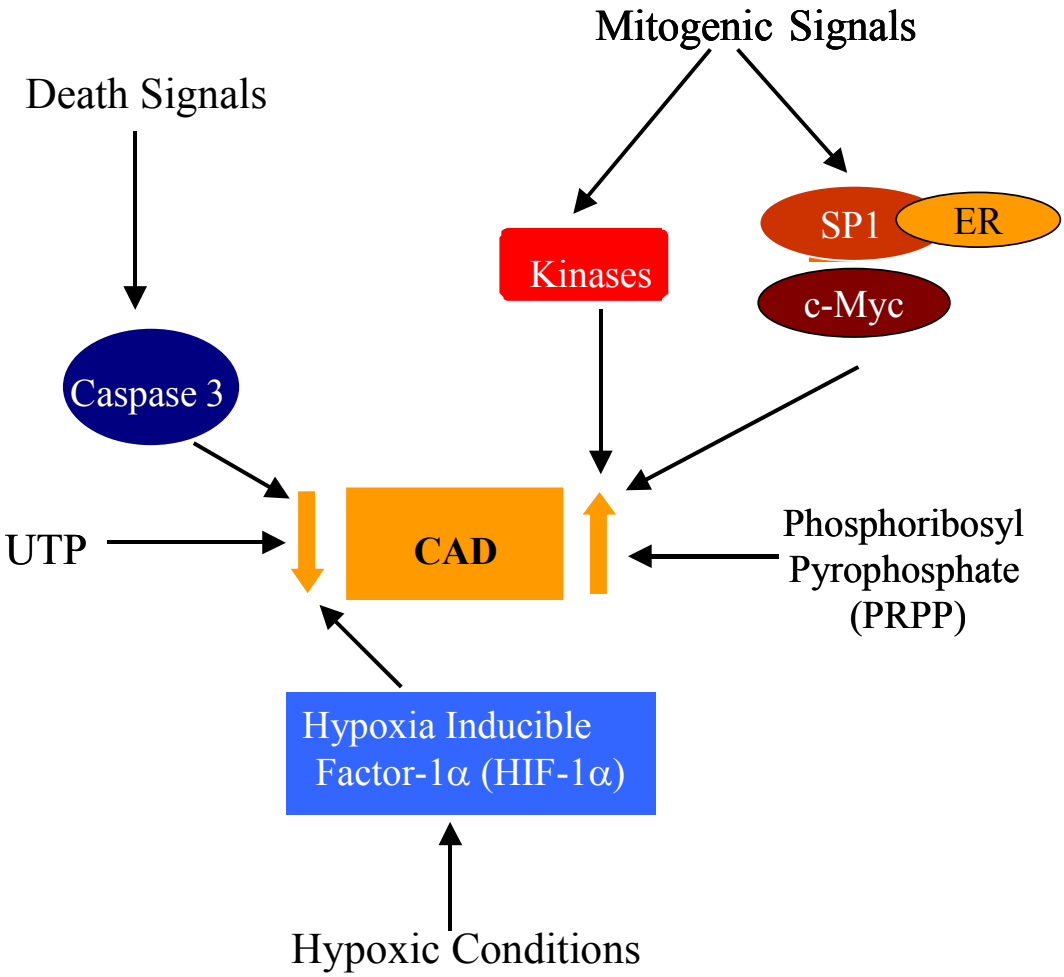

Figure 1.5. CAD Regulation. Since CAD catalyzes the rate-limiting step in *de novo* pyrimidine biosynthesis, it is regulated at multiple levels. Growth stimulatory signals can increase CAD transcription by increasing the activities of the c-Myc, SP1, and estrogen receptor (ER) transcription factors. Additionally, kinases induced by growth factors have been reported to phosphorylate and activate CAD. The hypoxia inducible factor-1α (HIF-1α) can decrease CAD transcription during cellular hypoxic conditions. CAD activity is allosterically activated by phosphoribosyl pyrophosphate (PRPP) and allosterically inhibited by UTP. During apoptosis, CAD is degraded by caspase 3-induced proteolysis.

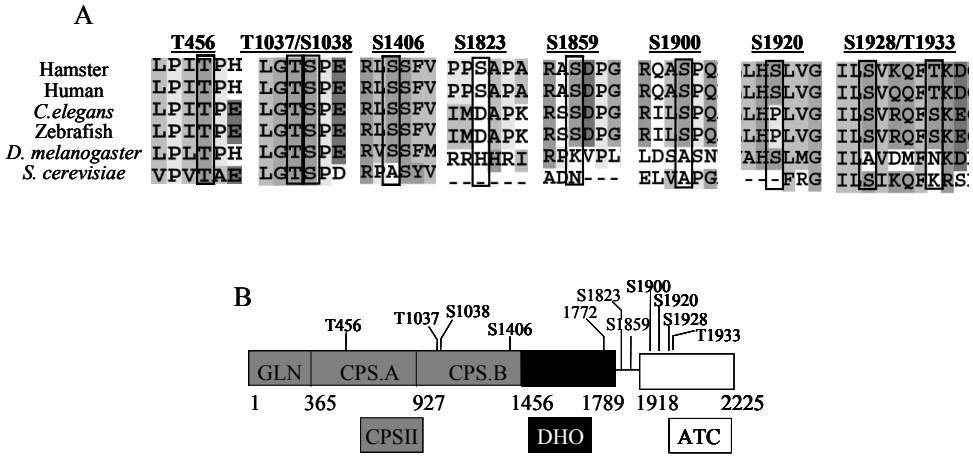

Figure 1.6. Proposed CAD phosphorylation sites and the conservation of these sites in various species. (A) A sequence alignment showing the degree of conservation between phosphorylation sites reported in hamster or human CAD and CAD from other species. The sequences that were used have the following NCBI Accession numbers: Hamster (P08955); Human (P27708); *C. elegans* (NP_495838); Zebra fish (CAI20956); *D. melanogaster* (NP_523377); *S. cerevisiae* (CAA89425). (B) The proposed CAD phosphorylation sites are found within the CPS.A, CPS.B, and ATCase subdomains and within the solvent exposed linker region between the DHOase and ATCase domains.

CHAPTER II

REGULATION OF CAD BY PHOSPHORYLATION

2.1 Introduction

Pyrimidine nucleotides are used by cells to make complex molecules such as RNA, DNA, phospholipids, glycosylated proteins and are used as ligands for numerous members of the G protein-coupled P2Y receptor family (reviewed in (Connolly and Duley, 1999). A recent study suggested that an additional role for pyrimidine nucleotides was the inhibition of apoptosis by binding to cytochrome C and inhibiting the apoptosome formation (Chandra et al., 2006). *De novo* pyrimidine biosynthesis is important for rapidly proliferating cells and the robust increase in intracellular pyrimidine nucleotides is required for the mitogen-induced clonal expansion of lymphocytes (Ruckemann et al., 1998).

CAD, the 243-kDa protein that initiates *de novo* pyrimidine synthesis, contains three enzymatic domains: carbamoyl phosphate synthetase II (CPSII), aspartate transcarbamoylase (ATCase), and dihydroorotase (DHOase). The CPSII activity of CAD is the rate-limiting step and is allosterically activated by phosphoribosyl pyrophosphate (PRPP) and inhibited by the product of pyrimidine-nucleotide synthesis, uridine 5′-triphosphate (UTP). CAD activity is increased in tumor cells (Aoki and Weber, 1981; Denton et al., 1982) and mitogen-stimulated lymphocytes (Ruckemann et al., 1998). In addition to allosteric regulation, total CAD activity can be elevated by gene amplification and increases in transcription in response to growth stimulatory signals (Gassmann et al., 1999; Rao and Church, 1988; Reardon et al., 1987). Furthermore, the acute regulation of CAD activity via post-translational modifications, such as caspase cleavage and phosphorylation, have been described (reviewed in (Evans and Guy, 2004; Huang and Graves, 2003).

CAD can be phosphorylated by protein kinase A (PKA) *in vitro* on the amino acids Ser^{1406} and Ser^{1859}. The phosphorylation of CAD by PKA increased enzymatic activity due to increased affinity for ATP and a decreased UTP inhibition (Carrey et al., 1985; Otsuki et al., 1981). Further studies showed that CAD was phosphorylated in intact cells, on an undetermined amino acid residue, after the cells were treated with 8-Br-cAMP, an activator of PKA. Additionally, H89, a PKA inhibitor, prevented the 8-Br-cAMP-induced phosphorylation of CAD. The mutation of Ser^{1406} to Glu^{1406}, to mimic phosphorylation, caused the apparent K_m (ATP) to be reduced and the IC_{50} of UTP to be increased; however, the mutation of Ser^{1406} to an Ala^{1406} did not alter the biochemical properties of CAD. Furthermore, Evans and colleagues proposed that the physiological role of PKA phosphorylation of CAD is to decrease overall enzyme activity since they showed that PKA-induced phosphorylation of an *E. coli*/human chimera of CAD *in vitro* diminished the PRPP-induced increase in CAD activity (Sahay et al., 1998).

CAD was shown to be phosphorylated *in vitro* by MAP kinase on Thr^{456}. The *in vitro* phosphorylation of CAD by ERK and the stimulation of cells with epidermal growth factor (EGF) or platelet derived growth factor (PDGF) appeared to modulate the allosteric regulation of CAD (Graves et al., 2000). While Thr^{456} could be phosphorylated *in vitro* by ERK, it remained to be determined whether this was the only site phosphorylated by this kinase *in vitro* and whether this site was phosphorylated *in vivo*. Guy and colleagues have reported an antibody that recognized phosphorylated Thr^{456}. Data using this antibody suggested that CAD isolated from a breast cancer cell line had higher levels of phosphorylated Thr^{456} than CAD from non-cancerous control cells (Sigoillot et al., 2004). However, the specificity of this antibody was not reported.

In addition to PKA and ERK phosphorylating CAD, there is a report that CAD partially isolated from the cell line BHK-165-23, was autophosphorylated on Thr^{1037} (Sigoillot et al., 2002a). BHK 165-23 is a hamster kidney cell line that was induced to overexpress CAD over 100-fold by exposing the cells to the ATCase inhibitor, N-phosphonacetyl-L-aspartate (Padgett et al., 1979). CAD reportedly "autophosphorylated" when incubated with ATP and a kinase buffer. Additionally, it was reported that autophosphorylated CAD had a 2-fold increase in CPSase II activity, a decrease in the activation by PRPP and an increase in sensitivity to the allosteric inhibitor UTP (Sigoillot et al., 2002a).

The physiological relevance of CAD phosphorylation is not well understood. Guy and colleagues reported that the phosphorylation of serine and threonine sites on CAD fluctuate with the cell cycle and that these phosphorylation events modulated the allosteric regulation of CAD. Since Ser^{1406} and Thr^{456} were shown to be *in vitro* PKA and MAP kinase phosphorylation sites, respectively, this group used phospho-serine antibodies to measure the PKA-induced phosphorylation of Ser^{1406} and the MAP kinase-induced phosphorylation of Thr^{456}. Using this premise, Guy and colleagues proposed that increased CAD allosteric activation during the S-phase of hamster kidney cells was due to MAP kinase phosphorylation and that this was responsible for the 1.9 fold increase in the pyrimidine biosynthetic pathway observed during S phase. Furthermore, they proposed that the PKA-induced phosphorylation of CAD accounted for the decrease in CAD activity that was observed in cells following S-phase.

While it has been proposed that CAD is phosphorylated by ERK solely on Thr^{456}, and by PKA on Ser^{1406} and Ser^{1859} in cells, these sites have not been confirmed in CAD

from intact cells. Furthermore, there are reports of additional phosphorylation sites in CAD (Olsen et al., 2006; Sigoillot et al., 2007). Therefore, a major objective in this study was to perform a comprehensive identification of the *in vivo* CAD phosphorylation sites by using 2D-phosphopeptide mapping, site-directed mutagenesis, and a variety of mass spectrometric approaches. Additionally, we tested the ability of ERK and PKA to phosphorylate CAD in HEK-293 cells. While we determined that forskolin-induced PKA activity increased the phosphorylation of Ser^{1406} and Ser^{1859}, surprisingly, we observed that CAD was not a substrate for ERK in HEK-293 cells. To investigate the effect of CAD phosphorylation on enzymatic activity, we measured CPSase II activity from CAD isolated from forskolin treated HEK-293 cells, from phosphorylation-null mutants, and from CAD isolated from HEK-293 cells treated with a phosphatase.

2.2 Materials and Methods

2.2.1 Materials

Antibodies that recognized the indicated antigens were as follows: $pThr^{456}$ and pERK2 from Santa Cruz Biotechnology, mouse anti-Flag M2 from Sigma, and the secondary HRP antibodies from Santa Cruz Biotechnology. The MEK-1 inhibitor U0126 and the adenylyl cyclase activator forskolin were purchased from CalBiochem. Both compounds were dissolved in DMSO and stored at –20 °C. The anti-Flag M2 resin was purchased from Sigma and the Ni-NTA resin was purchased from Qiagen. The PRPP was purchased from Sigma, dissolved in H_2O to a concentration of 75 mM and stored at –70 °C. The [^{32}P]-orthophosphate and [^{14}C]-sodium bicarbonate were purchased from MP Biomedicals. The [γ^{32}P]ATP was purchased from Perkin Elmer. The GST-14-3-3ζ

expression vector was a gift from Dr. Helen Piwnica-Worms and is described in (Meek et al., 2004).

2.2.2 Cell Growth and Transfection

Human embryonic kidney (HEK-293) cells were grown in Dulbecco's modified Eagle's medium (Invitrogen) supplemented with 10% heat inactivated fetal bovine serum (FBS) and 100 U/ml of penicillin and streptomycin (Invitrogen) in an atmosphere of 5% CO_2 at 37 °C. Cells were plated at a density of approximately 2.5 * 10^6 cells per 100 mm tissue culture plate the day before the cells were transfected with 5.6 μg of the various constructs using Lipofectamine (Invitrogen) per manufacturer's protocol. Cells were grown in 10 % FBS (normal growth media) for either 24 hours after transfection or placed in 0.2 % FBS (low serum growth media) for an additional 18-24 hours before subsequent treatments.

2.2.3 Mutagenesis

The wild type CAD used in this study was hamster CAD cDNA that was subcloned into PCDNA3.1 HIS (Invitrogen) described previously (Graves et al., 2000). An additional 3X-FLAG sequence was placed on the N-terminus. We used a Quickchange™ XL II kit (Stratagene, La Jolla, CA) to make the CAD mutants T456A, T1037A, T1037E, S1038A, S1406A, S1823A, S1859A, S1900A, S1920A, S1928A, and T1933A per manufacturer's instructions. Each mutation was verified by DNA sequencing.

2.2.4 Metabolic labeling with [^{32}P]-orthophosphate, cell treatments, and immunoprecipitation

After HEK-293 cells were transfected and grown in either low serum or normal growth media as described above, the cells were rinsed once in 5 ml of phosphate free DMEM (sodium phosphate and sodium pyruvate free with sodium pyruvate (Invitrogen Inc.) added to a final concentration of 110 mg/ml of sodium pyruvate. 3 ml of phosphate free DMEM with either 10 %, or 0.2 % dialyzed FBS (Invitrogen Inc.) was added to the plates and the cells were allowed to incubate for 30 min. in the normal cell growth conditions described above. Then to each plate 1-2 mCi of [^{32}P]-orthophosphate (0.33 mCi/ml, MP Biomedical) was added. The cells were treated with 20 μM forskolin, or stimulated with 10 % fetal bovine serum 3-4 hours after the addition of the [^{32}-P]-orthophosphate. 15 min after the addition of forskolin or 10 min, 30 min, or 60 min after the addition of 10 % serum, the plates were placed on ice, the media was removed, and the cells were rinsed twice in 10 ml of ice-cold phosphate buffered solution (PBS). 125 μl of ice-cold cell lysis buffer (20 mM Tris-HCl (pH 7.5), 137 mM $NaCl_2$ 10% glycerol, 5 μg/ml leupeptin, 250 μM phenylmethylsulfonyl fluoride (PMSF) 100 nM microcystin, 200 μM Na_3VO_4, and 2 mM ATP) was added to each plate and the cells were removed by scraping. The cell lysates then were centrifuged at 18,000 x g for 15 minutes at 4 °C, Flag-CAD was immunoprecipitated by adding 6 μl of anti-Flag agarose resin (Sigma) (suspended in a 1:1 solution of agarose beads:lysis buffer) per 1 mg of protein to microfuge tubes and rolling the tubes end-over-end at 4 °C for 3-4 hours. The anti-Flag agarose then was washed twice in 1 milliliter of ice-cold lysis buffer, and Flag-CAD was

removed by boiling the beads for 4 minutes in 2X SDS sample buffer (0.5 M Tris pH 6.8, 4 % SDS, 20 % glycerol, 10 % β-mercaptoethanol, 0.002 g/ml bromophenol blue).

2.2.5 CAD activity assay

CPSase II activity was measured essentially as described previously (Huang et al., 2002). Briefly, all of the reaction components except the cold and [^{14}C]- labeled sodium bicarbonate (the initiation solution) were added to 1.7 ml microfuge tubes on ice. The reaction mixture contained 41 µl of Flag resin bound to the immunoprecipitated Flag-CAD suspended in cell lysis buffer (described above). 174 µl of CAD Reaction solution (87 mM Tris-HCl (pH 8.0), 87 mM KCl, 6.5% dimethyl sulfoxide, 2.2% glycerol, 0.87 mM dithiothreitol, 3.1 mM glutamine, 17.4 mM aspartate, 7 mM [^{14}C]$NaHCO_3$ (50 mCi/mmol), 2 mM excess of $MgCl_2$ over the nucleotide (ATP) and PRPP concentrations, and ATP concentrations (adjusted to ATP contained within the cell lysis buffer) was added to each reaction. These samples then were placed in a 37°C water bath for 5 minutes before the initiation mix was added to start the reaction. The 250 µl reaction was allowed to proceed for 30 minutes at 37°C before it was quenched by the addition of 125 µl of 80 % trichloroacetic acid. The unincorporated ^{14}C then was removed by gently heating the samples at 85° C for 2-3 hours. 5 ml of Scintisafe ™ Econo 2 was added to each sample and the incorporation of ^{14}C into the acid stable carbamoyl aspartate was measured by liquid scintillation counting. The CAD protein concentrations used in the assay were determined by comparison to bovine serum albumin standards on a coomassie stained gel after SDS-PAGE was performed using either a 6 % polyacrylamide gel or a 4-12% NuPAGE Bis-Tris gradient gel (Invitrogen).

2.2.6 Phosphatase treatment

Flag-CAD was immunoprecipitated from radiolabeled HEK-293 cells as described above. The Flag-resin was washed 2 times with 1 ml of cell lysis buffer without the addition of ATP or protease or phosphatase inhibitors to remove any remaining phosphatase inhibitors used in previous steps. The Flag-CAD bound to Flag-resin then was resuspended in phosphatase buffer (50 mM tricine pH 8.0, 5 mM KCl) and placed at 30 °C. The dephosphorylation of CAD was initiated by adding 20 µl of 1 unit/µl calf intestine alkaline phosphatase (CIP) (Roche). 20 µl of 50 % glycerol (CIP suspension buffer) was added to the untreated control samples. The reaction was stopped by adding 1 ml of ice-cold lysis buffer (20 mM Tris-HCl (pH 7.5), 137 mM $NaCl_2$ 10% glycerol, 5 µg/ml leupeptin, 250 µM phenylmethylsulfonyl fluoride (PMSF) 100 nM microcystin, 200 µM Na_3VO_4, and 2 mM ATP). The Flag resin-bound CAD was pelleted and the supernatant was removed. The immunoprecipitates were washed again with 1 ml of lysis buffer before they were used in CAD activity assays as described above. To determine the degree of dephosphorylation and to map the sites that were dephosphorylated, the above procedure was performed with [^{32}P]-labeled Flag-CAD isolated from metabolically labeled HEK-293 cells. The CAD from these samples then was separated using SDS-PAGE and the amount of dephosphorylation between the control and the CIP treated CAD was analyzed by performing autoradiography on the gel. 2D-phosphopeptide mapping then was performed on CAD as described below.

2.2.7 Kinase Assays

16 μl of immunoprecipitated Flag-CAD (resuspended 20 mM Tris-HCl (pH 7.5), 137 mM $NaCl_2$ 10% glycerol, 5 μg/ml leupeptin, 250 μM phenylmethylsulfonyl fluoride (PMSF) 100 nM microcystin, 200 μM Na_3VO_4) was combined with 6 μl of ERK kinase reaction buffer that had the final concentration of 40 μM ATP 50mM Tris-HCl, 10 mM $MgCl_2$, and 2 mM dithiothreitol), 4 μl of [γ-^{32}P]ATP (10 mCi/ml) and 4 μl of purified Erk2 (100 units/μl) (New England BioLabs) (final reaction volume was 30 μl). The reaction was allowed to proceed for 45 min at 37 °C. The reaction was stopped by adding 2X SDS sample buffer. PKA kinase assays were performed in essentially the same manner as the ERK kinase assays, except that PKA buffer (50 mM Tris HCl (pH 7.5), 10 mM $MgCl_2$), and 500 units of purified PKA catalytic subunit (New England BioLabs) was used.

2.2.8 Trypsin digestion of CAD

After Flag-CAD was immunoprecipitated as described above, SDS-PAGE was performed and the gel was stained with Coomassie. The gel then was placed in a destain solution of 5% methanol and 7% acetic acid and allowed to gently rotate until the Flag-CAD protein could be visualized. The destain solution was discarded and the gel was washed in water. The gel bands containing Flag-CAD were excised from the gel and chopped into small pieces with a razor blade. The gel pieces then were added to a microfuge tube and the Coomassie stain was removed by adding enough solution A (50 % acetonitrile and 50 % of 25 mM ammonium bicarbonate (pH 8.0) to cover the gel pieces and vortexing the tube for 5-10 min. Solution A then was removed from the gel

pieces and fresh solution A was added. The gel pieces were allowed to dehydrate by setting at room temperature in solution A for approximately 1 hour. Next, solution A was removed and the gel pieces were dried in a speed vacuum microcentrifuge for approximately 30 minutes. 20 µl of 25 mM ammonium bicarbonate containing 0.4 µg of sequence grade modified trypsin (Promega) was placed on top of the dried gel pieces. The trypsin then was allowed to soak into the gel pieces for 20 minutes before an additional 25 mM ammonium bicarbonate (enough to cover the gel pieces) was added. The tube then was incubated at room temperature for 18-24 hours. The supernatant was removed and placed into a new microfuge tube. The tryptic peptides were eluted from the gel pieces by adding 50 µl of elution solution (60 % acetonitrile and 5 % formic acid) and vortexing every 5 min for 30-45 minutes. Next, the supernatant was added to the previous supernatant and the above elution protocol was repeated. The combined eluate was dried down to approximately 5 µl in the speed-vac. The peptides then were washed twice with water to remove the ammonium bicarbonate. After the water was removed in the speed vacuum microcentrifuge, the peptides were resuspended in 10 µl of the pH 1.9 buffer (15 % v/v of acetic acid and 5 % v/v of 88 % formic acid). To determine the elution efficiency of the phosphopeptides from the gel (typically around 80 %), the amount of radioactivity in the eluate and the remaining gel pieces was determined by Cerenkov counting with a scintillation counter.

2.2.9 Ni-NTA Chromatography

After lysing 5 confluent 100 mm tissue culture plates of [^{32}P]-orthophosphate metabolically labeled HEK-293 cells transfected with a N-terminal 6X-His-CAD construct were lysed in cell lysis buffer (described above), the lysates were centrifuged

for 30 min at 100,000 X g. The supernatant of the cell lysate then was brought up to a volume of 10 ml in buffer A (20 mM Tris-HCl, (pH 8.5), 500 mM KCl, 20 mM imidazole, 5 mM 2-mercaptoethanol, and 10 % (v/v) glycerol). A gravity-flow chromatography column was filled with 0.5 ml bead volume of Ni-NTA resin (Qiagen). The column was equilibrated by allowing 5 ml of buffer A to flow through the resin before the supernatant was added to the column. The column was washed with 8 column volumes of buffer B (20 mM Tris-HCl (pH 8.5), 1 M KCl, 5 mM 2-mercaptoethanol, and 10% (v/v) glycerol). 6X-His-CAD then was eluted from the column using 10 column volumes of elution buffer (20 mM Tris-HCl (pH 8.5), 100 mM KCl, 200 mM imidazole, 5 mM 2-mercaptoethanol, and 10 % (v/v) glycerol). The eluates were spin concentrated using a BIOMAX 100 kDa cutoff 4 ml spin concentrator (Millipore). These eluates then were separated by SDS-PAGE and CAD was trypsin digested as described above.

2.2.10 Reverse Phase HPLC

Gel eluted tryptic peptides were brought up to a volume of 110 µl in 0.1 % HPLC grade trifluoroacetic acid (TFA) (Pierce). The peptides were separated by reverse phase chromatography using a Hewlett-Packard HP 1100 Series High Performance Liquid Chromatograph (HPLC) System connected to a Vydac C18 column (Cat # 218TP5115). The peptides were eluted with a linear gradient of 0-10% buffer B (90 % acetonitrile, 10 % H_2O, and 0.1 % TFA) over the first 10 minutes, from 10 % to 40 % buffer B from 10 minutes to 45 minutes, and from 40 % to 65 % buffer B from 45 minutes to 65 minutes. The flow rate was 0.250 ml/minute and fractions were collected every minute.

2.2.11 2-dimensional phosphopeptide mapping and mass spectrometry

The peptides in the pH 1.9 buffer (15 % v/v of acetic acid and 5 % v/v of 88 % formic acid) were spotted in the corner of a 10 X 10 cm cellulose, glass-backed thin layer chromatography (TLC) plate. The peptides then were electrophoresed at 1000 V for 25 minutes in pH 1.9 buffer in a Hunter thin-layer electrophoresis box. After the TLC plates were thoroughly dried, the peptides were separated in the second dimension by ascending chromatography by placing the TLC plates in a TLC chamber containing approximately 104 ml of Scheidtmann buffer (65 ml isobutyric acid, 5 ml pyridine, 3 ml acetic acid, 2 ml butanol, and 29 ml H_2O) (Scheidtmann et al., 1982). After drying the plates, the phosphopeptides were imaged by exposing the plates to X-ray film or a phosphoimager plate. The cellulose in the areas on the TLC plate containing the phosphopeptides was scraped off the plate. The peptides were eluted off the cellulose by adding 50 μl of pH 1.9 buffer and vortexing for approximately 1 min. This elution procedure was repeated. The volume of the peptides then was reduced to approximately 5 μl in a speed vac. Peptides then were either purified using C18 ziptips (Millipore) following manufactuer's protocol, or directly spotted onto MALDI-mass spectrometer sample target plates. The premixed dihydrobenzoic acid or α-cyano-4-hydroxy-cinnamic acid matrices then was added to the peptides on the target plate. The Bruker Daltronics Ultraflex MALDI-TOF/TOF or the ABI 4700 MALDI-TOF/TOF mass spectrometers operating in positive ion mode were used to analyze the mass of the peptides. Phosphatase treatment was performed on the MALDI target plate by adding 0.01 units of CIP (Roche) in 50 mM ammonium bicarbonate directly to the previously analyzed peptide sample. 15 min later

the peptides were analyzed again on the Ultraflex, MALDI-TOF/TOF mass spectrometer to identify ions that had an –80 m/z shift (characteristic of a loss of a phosphate group).

2.3 Results

2.3.1 Mapping of phosphorylation sites in CAD from intact cells

Considerable speculation into the identity of potential CAD phosphorylation sites has been made; however, a definite analysis of these sites has not been performed. Moreover, because of its large size, analysis of phosphopeptides from CAD is extremely challenging. To determine the identity of phosphorylated amino acids in CAD from intact cells, 6X-His-CAD was expressed and isolated from [^{32}P]-orthophosphate labeled human embryonic kidney cells (HEK-293) as described in Materials and Methods. The isolated CAD was trypsin digested, separated by C18 reverse-phase HPLC, and each fraction was analyzed on an ABI 4700 MALDI-TOF/TOF mass spectrometer. The mass spectra from a series of three fractions (fractions 48-50) are displayed in Figure 2.1. The identity of the CAD peptides that each ion represented was determined by matching them to the m/z of the predicted CAD tryptic peptide ions using Protein Prospector (http://prospector.ucsf.edu) (Clauser et al., 1999). The peak at m/z 2962.2724 corresponded to a singly charged CAD peptide Trp^{1812}-Arg^{1838} containing a single phosphate group. Additionally, the peak at 3090.3121 corresponded to the singly charged CAD peptide Lys^{1811}-Arg^{1838} containing a phosphate group. MS/MS analysis of the 3090.3121 ion was performed, and although not conclusive, the data suggested that the peptide was ^{1811}KWPQGAVPQPPPS*APATTITTTPERPRR^{1838}, with the asterisk representing the putatively phosphorylated Ser residue.

To further examine the identity of phosphorylated amino acids in CAD from intact cells, Flag-CAD was immunoprecipitated from [^{32}P]-orthophosphate labeled human embryonic kidney cells (HEK-293). CAD tryptic peptides were analyzed by 2D TLC as described in Materials and Methods. As seen in Fig. 2.2A, there were four major phosphopeptide spots (labeled 1-4) observed in CAD from HEK-293 cells. The phosphopeptides were scraped from the TLC plate, eluted from the scrapings, and analyzed by MALDI-MS and tandem MS. The MS spectrum from the eluate from spot 4 contained a peak at m/z 1696.7708, which corresponded to charged CAD peptide Ala^{1855}-Lys^{1869} containing a single phosphate group. MS/MS was performed and the sequence of this peptide was determined to be IHRAS*DPGLPAEEPK (1855-1869), where the asterisk represents the phosphorylated serine 1859 residue (Figure 2.2B). The eluate from spot 1 was determined to contain the phosphopeptide AS* DPGLPAEEPK (1857-1869), which was the same peptide found in spot 4, except that it had three less amino acids, corresponding to trypsin cleavage. Hence, spot 4 was determined to contain a missed trypsin cleavage peptide. Additionally, MALDI-MS spectrum of the eluate from spot 3 contained a peak at m/z 1526.531, which corresponded to the singly charged CAD peptide Ala^{1769}-Lys^{1780} containing a single phosphate group (Figure 2.3). While the MS/MS data of this ion was inconclusive, the treatment of this peptide with phosphatase caused the peak to be shifted by -80 m/z (the m/z of a phosphate moiety) to 1446.536, which matched the m/z of the unphosphorylated peptide (Figure 2.3). Since the sequence of this peptide is ^{1769}ARWTPFEGQKVK^{1780}, Thr^{1772} is the only residue that can be phosphorylated.

To corroborate the mass spectrometry data, we mutated Ser^{1859} to Ala^{1859} (S1859A) and transfected HEK-293 cells with either WT Flag CAD or the S1859A CAD mutant. 2D phosphopeptide maps were run to compare the phosphopeptide patterns from wild type (WT) CAD and the alanine mutant. As observed in Fig. 2.2C, spots 1 and 4 were absent in the 2D maps from the S1859A CAD mutant when compared to WT CAD. This confirmed our data from Fig. 2.2B that spots 1 and 4 contain the peptide with $pSer^{1859}$. We are currently making the Thr^{1772} to Ala^{1772} (T1772A) mutant to corroborate the mass spectrometry data displayed in Figure .2.3.

2.3.2 Effect of CAD phosphorylation on enzyme activity and allosteric regulation

Since CAD from HEK-293 cells growing in 10 % serum media was phosphorylated on multiple sites (Fig. 2.2A) and previous evidence suggested that the phosphorylation of CAD increased the allosteric activation by PRPP (Carrey et al., 1985; Graves et al., 2000; Sigoillot et al., 2002b), we hypothesized that dephosphorylation would decrease the allosteric activation or catalytic activity of CAD. Immunoprecipitated Flag-CAD from [^{32}P]-orthophosphate labeled HEK-293 cells was incubated with or without calf intestinal phosphatase (CIP). As seen in Fig. 2.5A, CIP treatment reduced the total amount of radioactive phosphate in into CAD. Furthermore, 2D phosphopeptide analysis of CIP-treated or control CAD demonstrated that CIP treatment reduced the phosphorylation of phosphopeptides 1-4 (Figure 2.5B) To determine if the reduction in CAD phosphorylation affected enzymatic activity, we performed CAD activity assays on immunoprecipitated Flag-CAD treated with or without CIP for 15, 30 or 45 minutes. 15 minutes after the addition of CIP, CAD activity was reduced by approximately 40 % compared to control. Treatment with CIP resulted in a

time-dependent loss of CAD activity that paralleled the loss of CAD phosphorylation (Fig.2.5C). Interestingly, CIP treatment did not affect the ability of PRPP to stimulate CAD activity (Fig 2.5D).

2.3.3 Ser^{1406} and Ser^{1859} phosphorylated by PKA in intact cells

Previous studies showed that CAD was phosphorylated by PKA *in vitro* on residues Ser^{1406} and Ser^{1859} (Carrey et al., 1985). CAD has also been reported to autophosphorylate (Sigoillot et al., 2002a). To determine if any of the sites observed in the 2D maps were from PKA phosphorylation or autophosphorylation, 2D-phosphopeptide mapping was performed on Flag-CAD incubated with either [γ-^{32}P]ATP alone or with the purified catalytic subunit of PKA. As shown in Fig. 2.6A, spots 1 and 4, which represented $pSer^{1859}$ peptide (as shown in Figure 2.2), was phosphorylated. Additionally, we observed a new phosphopeptide spot (labeled spot 5) present in CAD phosphorylated by PKA that was not seen in the 2D maps from CAD isolated from HEK-293 cells (Figure 2A). No evidence of CAD autophosphorylation was observed in these experiments.

To investigate the phosphorylation of CAD by PKA *in vivo*, WT Flag-CAD was immunoprecipitated from lysates from [^{32}P]-orthophosphate labeled HEK-293 cells that had been treated with vehicle (DMSO) or 20 μM forskolin for 15 minutes prior to cell harvesting and 2D-phosphopeptide mapping was performed. As shown in Figure 5B, forskolin treatment increased the phosphorylation of Ser^{1859} (spot 4) and induced the phosphorylation of spot 5. To determine if spot 5 contained the putative PKA phosphorylation site $pSer^{1406}$ (Carrey et al., 1985), we mutated Ser^{1406} to Ala^{1406} (S1406A) and transfected this mutant into HEK-293 cells. Cells were metabolically

labeled and treated with or without forskolin as described above. As observed in Figure 2.6C, spot 5 was absent from the forskolin-treated sample; whereas, it was observed in WT CAD (Figure 2.6B). This data demonstrated that spot 5 represented the phosphopeptide containing pSer^{1406}. Since we observed the Ser^{1859} peptide was phosphorylated in HEK-293 without forskolin stimulation, we hypothesized that there might be a basal level of PKA activity in HEK-293 cells that resulted in the phosphorylation of Ser^{1859}. To test this, we treated [^{32}P]-orthophosphate metabolically labeled HEK-293 cells with the PKA kinase inhibitor, H89. 2D-phosphopeptide mapping then was performed on the isolated Flag-CAD. As shown in Figure 2.6B, H89 caused a significant reduction in the phosphorylation of Ser^{1859}, confirming that this site was phosphorylated by PKA, or another H89-sensitive kinase.

2.3.4 Thr^{456} is not a major ERK-mediated phosphorylation site in CAD

Since phosphorylated Thr^{456} was not observed in our analysis of CAD phosphorylation (Fig. 2.2), we designed experiments to reevaluate whether Thr^{456} was a major CAD phosphorylation site. Since ERK had been reported to phosphorylate CAD *in vitro* on Thr^{456} (Graves et al., 2000), we performed 2D-phosphopeptide mapping on WT Flag-CAD or T456A Flag-CAD that was incubated with either [γ-^{32}P]ATP alone or in the presence of recombinant active ERK2. Erk2 activity was verified by MBP phosphorylation (data not shown). We were unable to detect phosphopeptides from WT Flag-CAD or T456A Flag-CAD incubated with [γ-^{32}P]ATP alone; however, both WT and T456A CAD contained numerous phosphopeptides when incubated with ERK2 (Fig. 2.7A). Surprisingly, none of the phosphopeptide spots were reduced in the 2D maps

from T456A CAD (Fig. 2.7A). This data suggested that Thr^{456} was not a major ERK-induced CAD phosphorylation site *in vitro*.

To determine if we could detect the ERK-induced CAD phosphorylation site *in vivo,* we transfected HEK-293 cells with WT-Flag CAD and serum-starved the cells overnight. The cells were radiolabeled with [^{32}P]-orthophosphate and incubated with or without 150 ng/ml of EGF for 15 minutes to activate ERK (described in Materials and Methods). ERK activation was verified by immunoblotting for active ERK (Figure 2.7B). CAD was immunoprecipitated and 2D-phosphopeptide mapping was performed. While we observed a robust phosphorylation of ERK (Fig. 2.7B right), indicating that ERK was activated under these conditions, the 2D maps from CAD isolated from the EGF-treated cells showed no apparent change in phosphorylation when compared to CAD isolated from the unstimulated control cells. This result suggested that CAD was not a substrate of ERK in intact cells under these conditions.

However, to further investigate if ERK phosphorylated CAD basally, we examined the affect of a MEK-1 inhibitor known to prevent ERK activation (U0126). U0126 was added to HEK-293 cells during the 3 hour incubation with [^{32}P]-orthophosphate and CAD was immunoprecipitated and 2D-phosphopeptide mapping performed. As seen in Fig. 2.7C (lower panel), U0126 reduced ERK phosphorylation as expected. However, no reduction in the phosphorylation of any of the phosphopeptides from CAD was observed when compared to CAD isolated from control and U0126 treated cells (Fig. 2.7C, upper panel).

Although ERK activation did not increase the phosphorylation of Thr^{456}, there remained a possibility that a peptide containing $pThr^{456}$ was present in the remaining

phosphopeptide spots. To test this, WT Flag-CAD or T456A Flag-CAD was transfected into HEK-293 cells, the cells were radiolabeled with [^{32}P]-orthophosphate, and 2D-phosphopeptide mapping was performed. As shown in Figure 2.7D, spots 1-4 were present in the maps from WT CAD and T456A CAD, suggesting that pThr^{456} was not a major CAD phosphorylation site in these cells.

In addition to investigating the effects of EGF stimulation on CAD phosphorylation, we wanted to determine if CAD was phosphorylated by serum-induced kinases, which contains numerous growth factors. HEK-293 cells were transfected with WT Flag-CAD, placed in low serum for 18 hours, labeled with [^{32}P]-orthophosphate, and stimulated with 10 % FBS for the indicated times (Figure 2.8). As shown in Figure 2.8, no increase in radioactivity incorporation into spots 1-4 occurred at the 10 min, 30 min, or 60 min time points when compared to the control. Interestingly, the overall radioactivity incorporation into all of the spots appeared to be slightly lower in both the 10 min and 30 min time points when compared to the 0 min and 60 min time points. Additionally, two minor phosphopeptide spots (indicated by arrows) were observed in the 0 min and 60 min time points (Figure 2.8).

It has been reported that the enhanced allosteric activation of CAD by phosphorylation of Thr^{465} by ERK in a human breast cancer cell line is the potential cause for the elevated level of pyrimidine synthesis in these cells. Additionally Guy and colleagues reported that pThr^{456} CAD is localized to the insoluble nuclear fractions of numerous different cell lines. The basis for the conclusions in both of these studies came from the data collected using an antibody designed to specifically recognize the pThr^{456} residue. However, the specificity of this antibody has not been reported. Since our data

suggested that pThr^{456} was not a major phosphorylation site in CAD, we designed two experiments to test the specificity of the pThr^{456} antibody. First, we performed immunoblots using lysates from CAD-deficient G9C cells (expressing either WT-CAD, the T456A mutant, or the empty vector (PCDNA 3.1) (described in (Graves et al., 2000)). The separation of soluble and insoluble cellular fractions was performed exactly as described earlier (Sigoillot et al., 2005). The proteins were separated by SDS-PAGE and an immunoblot was performed using the pThr^{456} antibody (Santa Cruz Biotechnology). We detected a protein that ran on SDS-PAGE at a molecular weight similar to where CAD was normally observed (~240 kDa) in the insoluble fractions from G9C cells transfected with WT-CAD. Additionally, we observed the same band in the G9C cells transfected with T456A CAD or the empty vector (Figure 2.9A). This suggested that this antibody was not specific for the Thr^{456} phosphorylation site. To further investigate the specificity of the anti-phospho Thr^{456} antibody, we immunoprecipitated WT Flag-CAD or T456A Flag-CAD from HEK-293 cells as described in Materials and Methods. SDS-PAGE was performed and western blots were performed. By immunoblotting with an α-Flag antibody we demonstrated that both WT and T456A Flag-CAD were expressed and immunoprecipitated at similar levels (Figure 2.9B lower panel). As seen in the top panel of Figure 2.9B, the α-pThr^{456} antibody reacts with either CAD or a protein that has an identical molecular weight to CAD in the lysates (input) and immunoprecipitates from both WT-Flag CAD and T456A Flag-CAD. Therefore, this data strongly suggests that the pThr^{456} antibody from Santa Cruz that was used in three prior studies (Kotsis et al., 2007; Sigoillot et al., 2005; Sigoillot et al., 2004), does not bind specifically to phosphorylated Thr^{456} CAD.

2.3.5 Forskolin stimulation of PKA in HEK-293 cells decreased CAD activity

Carrey and colleagues showed that PKA phosphorylation of CAD *in vitro* abolished UTP inhibition of enzymatic activity (Carrey et al., 1985). Furthermore, Guy and colleagues reported that there was a correlation between an increase in PKA activity and an increase in total serine phosphorylation of CAD in cells as they reached growth arrest (Sigoillot et al., 2002b). Moreover, the increase in CAD serine phosphorylation correlated with a decrease in the PRPP stimulation of CAD activity (Sigoillot et al., 2002b). To evaluate the effect of PKA activation in intact cells on CAD enzymatic activity and allosteric function, we stimulated HEK-293 cells transfected with Flag-CAD with forskolin or with the vehicle control DMSO. Since we observed increased CAD phosphorylation using this same treatment protocol (Figure 2.6B), we assumed that CAD phosphorylation was also increased in this experiment. Flag-CAD was immunoprecipitated and enzymatic activity assays were performed using multiple concentrations of ATP. Activation of PKA did not affect the affinity of CAD for ATP; however, there was a small decrease in the CPSase II activity isolated from forskolin treated cells when compared to compared CAD isolated from DMSO treated cells (Figure 2.10A). Additionally, there was a slight decrease in PRPP stimulation from CAD isolated from forskolin-treated cells when compared to CAD from DMSO treated cells (Figure 2.10B).

2.3.6 Effect of mutating CAD phosphorylation sites to alanines on the enzymatic activity and allosteric regulation of CAD

To begin to address potential importance of the phosphorylation of specific residues on CAD enzymatic function, we performed CPSase II activity assays on the

phosphorylation site mutants. WT Flag-CAD, T456A Flag-CAD, T1037E Flag-CAD, S1406A Flag-CAD, and S1859A Flag-CAD were expressed in HEK-293 cells and immunoprecipitated as described in Materials and Methods. CPSase II enzyme activity assays were performed on immunoprecipitated Flag-CAD constructs as described in Materials and Methods. As shown in Figure 2.11A, both WT Flag-CAD and S1859A Flag-CAD displayed an almost identical increase in activity as the ATP concentration was increased. When compared to both the WT-Flag CAD and S1859A-Flag CAD mutants, the T456A Flag CAD mutant had an approximate 6-fold reduction in CAD activity at the 20 mM ATP concentration. Additionally, the activity of the S1406A and T1037E Flag-CAD mutants was reduced approximately 20-fold when compared to the activity of both WT and S1859A Flag-CAD. Interestingly, 500 μM of PRPP stimulated the CPSase II activity of each of these Flag-CAD mutants to a level similar to that observed with WT Flag-CAD (Figure 2.11B).

While all of the mutants described above were activated by PRPP to a similar degree as wild-type Flag-CAD, interestingly, the CPSase II activity of the T1037A CAD mutant showed a significantly greater increase. To investigate this effect further, we performed a PRPP dose-response experiment. As seen in Figure 2.12B, the activity of the T1037A mutant was increased ~2000 % over no ligand by 125 μM PRPP, while the activity of WT-CAD increased ~1000 % at the same PRPP concentration. At 500 μM PRPP, T1037A was stimulated approximately 3-fold higher than WT-Flag CAD. Furthermore, 500 μM appeared to be the saturating concentration of PRPP for both WT Flag-CAD and T1037A Flag-CAD since neither displayed a further increase in CPSase II activity when the PRPP concentration was increased to 2 mM (Figure 2.12B). When the

CPSase II activity of WT-Flag CAD and T1037A Flag-CAD were measured as a function of increasing ATP concentrations, it was observed that the T1037A mutant had less CPSase II activity than WT-Flag CAD (Figure 2.12A). Thus these results suggested that mutation of Thr^{1037} affected both the PRPP-stimulation and basal CPSase II activity.

2.3.7 A caffeine sensitive kinase phosphorylates Ser^{1859}

Since CAD was phosphorylated on Ser^{1859}, Thr^{1772}, and on an unknown phosphopeptide represented by spot 2 (Figure 2.2A and 2.3), we wanted to determine the identity of the kinase(s) responsible for phosphorylating these sites. We hypothesized that the ionizing radiation from the [^{32}P]-orthophosphate might be inducing a checkpoint response, thereby activating the ATM/ATR and Chk1/2 kinases. A common drug used to inhibit ATM and ATR is caffeine (Sarkaria et al., 1999). Therefore, to test the hypothesis that ATM/ATR or their downstream substrate kinases Chk1/2 were leading to the phosphorylation of Ser^{1859}, Thr^{1772}, and/or the phosphopeptide spot 2, we treated cells labeled with [^{32}P]-orthophosphate with 5 mM caffeine. Interestingly, 2D phosphopeptide maps of the immunoprecipitated Flag-CAD from the caffeine treated cells demonstrated that Ser^{1859} phosphorylation was significantly reduced when compared to Flag-CAD from control cells (Figure 2.13). Thus this result suggests that a caffeine sensitive kinase phosphorylates Ser^{1859}.

2.3.8 14-3-3ζ forms a protein-protein interaction with CAD

CAD was identified as a 14-3-3ζ binding protein in a large scale mass spectrometry screen designed to detect 14-3-3ζ binding proteins (Meek et al., 2004). We sought to confirm this interaction and to determine if $pSer^{1406}$ (a predicted 14-3-3 binding

site according to the scansite sequence match program (Obenauer et al., 2003) bound 14-3-3ζ. To confirm that 14-3-3 could bind to CAD and to determine if Ser^{1406} was necessary for interaction with 14-3-3ζ, we incubated the lysates from HEK-293 cells transfected with either WT Flag-CAD, or S1406A Flag-CAD, with glutathione agarose beads bound to either GST alone, or GST-14-3-3. As seen in Figure 2.14, GST-14-3-3 bound to both WT Flag-CAD and S1406A CAD. While this data confirmed that 14-3-3 zeta bound to CAD (Meek et al., 2004), it suggested that a phosphorylation site in CAD other than Ser^{1406} was responsible for this protein-protein interaction.

2.4 Discussion

2.4.1 Identification of CAD phosphopeptides

Although CAD has been reported to be phosphorylated on several residues, this is the first comprehensive investigation to identify the phosphorylation sites in CAD isolated from intact cells. By using mass spectrometric analysis and 2D-phosphopeptide mapping, we determined there are a minimum of five major tryptic phosphopeptides in CAD (Figure 2.2A and 2.6B). Phosphopeptide spots 1 and 4 were identified as containing $pSer^{1859}$, spot 5 is the phosphopeptide containing $pSer^{1406}$, and spot 3 likely contains $pThr^{1772}$. While we have yet to identify the phosphopeptide in spot 2 (Figure 2.2), we did determine that this spot did not contain the previously proposed phosphorylated residues $pThr^{456}$, $pThr^{1037}$, or the putative CAD phosphorylation site Ser^{1823} that we found by other methods (Figures 2.1, 2.4, and 2.7.D). Furthermore, while the large-scale phosphorylation site analysis identified the CAD residues Ser^{1900}, $pSer^{1920}$, $pSer^{1928}$, and $pThr^{1933}$ as *in vivo* CAD phosphorylation sites (Olsen et al., 2006), these phosphorylated residues were not found in phosphopeptide spot 2. (Figure 2.4). While

this implies that there are additional unknown phosphopeptides in CAD, it does not necessarily demonstrate that the above phosphopeptides do not exist. One explanation for us not observing these phosphopeptides with the 2D phosphopeptide maps is that these sites are already maximally phosphorylated when the cells are metabolically labeled with [^{32}P]-orthophosphate and consequently do not incorporate radioactive phosphate. Furthermore, it is possible that low stoichiometry of phosphorylation prevents these phosphopeptides from appearing as major spots on our phosphopeptide maps. Indeed, we sometimes observed faint phosphopeptide spots as indicated by the arrows in Figures 2.2C, and 2.8 that could possibly represent low levels of these minor phosphopeptides.

To investigate the importance of these major CAD phosphopeptides (Figure 2.1) on CPSase II activity, we dephosphorylated CAD immunoprecipitated from HEK-293 cells with a phosphatase and measured enzymatic activity (Figure 2.5). Since we observed a reduction in the phosphorylation of all four phosphopeptides and a decrease in CPSase II activity after phosphatase treatment, we concluded that these phosphopeptides were important for catalytic activity. Furthermore, since spots 1 and 4 represent the phosphopeptide containing Ser^{1859} (Figure 2.2) and the phospho-null S1859A mutant did not affect CPSase II activity (Figure 2.11A), we have hypothesized that Thr^{1772} (spot 3) and/or the unknown phosphopeptide in spot 2 are important for the CPSase II catalytic activity.

2.4.2 PKA phosphorylation of CAD

Our studies were designed to determine the sites that were phosphorylated in CAD by PKA in HEK-293 cells. While we determined that PKA induced the phosphorylation of Ser^{1406} and Ser^{1859}, we demonstrated that there was a high basal level

of Ser^{1859} phosphorylation in HEK-293 cells growing in normal growth media (Figures 2.2 and 2.6). When H89, a chemical that inhibits PKA activity, was added to the cells, the phosphorylation of Ser^{1859} dropped to almost undetectable levels (data not shown). A potential explanation for these results is that there is a low level of PKA activity in HEK-293 cells (which was observed by Higgins and Graves (unpublished data)), which phosphorylates Ser^{1859}, and that only a significant increase in PKA activity induced by forskolin allows for the phosphorylation of Ser^{1406}. However, since H89 is a non-specific kinase inhibitor (Davies et al., 2000), another explanation is that Ser^{1859} can be phosphorylated by both PKA and another H89-sensitive kinase that is active in HEK-293 cells. Indeed, we discovered phosphorylation was also inhibited by caffeine (Figure 2.13), suggesting a potential role for the kinases ATM/ATR. It is interesting to speculate that phosphorylation of CAD by these kinases may relate to the function of the interaction of the checkpoint protein hRad9 with CAD (Lindsey-Boltz et al., 2004) (described in Chapter III).

The phosphorylation of CAD was reported to be important in modulating the allosteric regulation and enzyme activity of this multifunctional protein. Early work by Elizabeth Carrey and colleagues suggested that *in vitro* phosphorylation of CAD by PKA on residues Ser^{1406} and Ser^{1859} increased CAD activity in cells since it caused a decrease in UTP "feedback" inhibition of CAD. Guy and colleagues observed that the PKA phosphorylation of CAD caused a decrease in the PRPP-induced activation of CPSase II activity. As seen in Figure 2.11, our data demonstrate that forskolin induces both a slight decrease in CAD activity at high ATP concentration (20 mM) and a slight decrease in PRPP activation. At lower ATP concentrations, which are closer to physiological

amounts (2-5 mM ATP), forskolin did not affect CPSase II activity. Therefore, it has to be questioned whether or not the affect of forskolin-induced PKA activation on CPSase II activity is physiologically relevant. Furthermore, while the S1859A mutant did not affect CPSase II activity, the S1406A mutant significantly decreased enzymatic activity at all concentrations of ATP tested (Figure 2.11A). Interestingly, the allosteric activation of the S1406A CAD mutant activity by PRPP was similar to WT CAD, suggesting that allosteric activation by this ligand was unaffected (2.11B). Since the phosphorylation of this site by forskolin induced a slight decrease in CPSase II activity, the phosphorylation null alanine mutant would not be expected to decrease CPSase II activity. Therefore, it is possible that the S1406A mutation affects the catalytic activity in a manner not related to the loss of phosphorylation of this residue in the S1406A mutant.

2.4.3 ERK phosphorylation of CAD

Previous reports suggest that Thr^{456} was phosphorylated *in vitro* by ERK (Graves et al., 2000). However, it was not determined if this was the major site of ERK phosphorylation in CAD. Surprisingly, our 2D-phosphopeptide maps from WT-Flag CAD and T456A-Flag CAD phosphorylated *in vitro* by ERK (Figure 2.7A) showed no difference, suggesting that Thr^{456} was not a major ERK-induced CAD phosphorylation site. Although in our mass spectrometry analysis, we observed a peptide consistent with the phosphorylation of Thr^{456} (Jun Han, unpublished), our 2D-phosphopeptide data does not support the conclusion that Thr^{456} is a major phosphorylation site. Instead our studies suggest that multiple residues in CAD can be phosphorylated by ERK *in vitro*. An alternative explanation for Thr^{456} not being observed is that it was already phosphorylated in CAD isolated from HEK-293 cells. To address this concern, CAD isolated from HEK-

293 cells was treated with a phosphatase before being phosphorylated *in vitro* with ERK. We observed that there was the same amount of ERK-mediated phosphorylation on the phosphatase-treated CAD compared to the CAD not treated with a phosphatase (data not shown).

Although it had previously been reported that CAD was phosphorylated by ERK on Thr^{459} *in vivo* (Sigoillot et al., 2002a), our data in Figure 2.7B-D demonstrated that while EGF-stimulation induced a robust activation of ERK in HEK-293 cells, no increase in CAD phosphorylation was observed. Additionally, since there was some basal level of ERK activity in HEK-293 cells even after serum-starvation (Figure 2.7C), it could be argued that this active ERK could cause Thr^{456} to be already maximally phosphorylated before EGF-stimulation. To determine if this possibility was correct, we treated HEK-293 cells with the MEK-1 inhibitor U0126 to reduce the basal ERK activity. U0126 inhibited ERK, but did not reduce the phosphorylation of the CAD peptides represented on the 2D phosphopeptide map. Therefore, taken together, our data presented in Figure 2.7 clearly demonstrated that while CAD was phosphorylated by ERK on multiple sites *in vitro*, the activation of ERK in HEK-293 cells did not lead to the phosphorylation of CAD. This data is in contrast to the reports by Guy and colleagues that Thr^{456} was phosphorylated *in vivo* by ERK (Sigoillot et al., 2003; Sigoillot et al., 2002b; Sigoillot et al., 2007; Sigoillot et al., 2005; Sigoillot et al., 2004). The conclusion that ERK was phosphorylated on Thr^{456} by ERK *in vivo* by these authors was based on experiments using an antibody designed to recognize the phosphorylated Thr^{456} CAD residue (Sigoillot et al., 2005). However, this antibody was not shown to be specific for phosphorylated Thr^{456} and our data strongly demonstrates that this antibody is not

specific for pThr^{456} CAD (Figure 2.9). Therefore, the conclusions from studies using this antibody (Kotsis et al., 2007; Sigoillot et al., 2007; Sigoillot et al., 2005; Sigoillot et al., 2004) are highly questionable.

While our data (Figure 2.7) demonstrated that CAD was not phosphorylated by ERK in HEK-293 cells, a recent study by Guy and colleagues reported that the phosphorylation of CAD by PKA prevented the phosphorylation of CAD by ERK. Since there was the possibility that we did not observe ERK-induced CAD phosphorylation because of PKA activity in these cells, we pretreated metabolically labeled HEK-293 cells with the PKA inhibitor H89 before stimulating them with EGF. While H89 significantly decreased CAD phosphorylation, EGF did not induce CAD phosphorylation (data not shown).

2.4.4 EGF stimulation of CAD phosphorylation

While it was reported that EGF induced the phosphorylation of CAD residues Ser^{1900}, Ser^{1920}, Ser^{1928}, and Thr^{1933} in HeLa cells, as discussed above, we did not observe significant EGF-induced CAD phosphorylation in HEK-293 cells. Two major differences exist between these two studies. First, different cell types were used. The EGF-induced kinase in HeLa cells that is responsible for CAD phosphorylation may not be regulated in HEK-293 cells. Additionally, previous reports have suggested that there are CAD phosphorylation sites that inhibit the phosphorylation at other CAD sites (Kotsis et al., 2007; Sigoillot et al., 2007). Therefore, CAD may be phosphorylated on a residue in HEK-293 cells that prevents EGF-induced phosphorylation, while CAD in the HELA cells is not phosphorylated on this inhibitory residue. The second major difference between these two studies was the methods used to identify phosphopeptides. The mass

spectrometry method used by Mann and colleagues might be more sensitive than our method, allowing for the detection of minor CAD phosphorylation sites that we were unable to detect.

2.4.5 Autophosphorylation of CAD

As previously described, a study reported that CAD autophosphorylated on Thr^{1037} (Sigoillot et al., 2002a). Since CAD is not a kinase, this was a controversial finding. However, we were unable to detect any autophosphorylation on immunoprecipitated CAD from HEK-293 cells in our in vitro kinase assays (Figures 2.6A and 2.7A). A possible explanation for the discrepancies between our study and the one performed by Guy and colleagues is that what was reported to be autophosphorylation, was actually phosphorylation induced by a contaminating kinase in their isolated CAD. Another potential explanation is that we did not observe the autophosphorylation because we did not use high enough ATP concentrations in our kinase assays. However, this seems unlikely since they reported autophosphorylation using 50 μM ATP in their kinase assays and we used 40 μM ATP.

While our data suggest that Thr^{1037} is not an autophosphorylation site, and we did not detect the phosphorylation of Thr^{1037} on our 2D phosphopeptide maps, we did acquire data using the recently described technique of titanium dioxide phosphopeptide enrichment (reviewed in Bodenmiller et al., 2007) that suggested that Thr^{1037} was phosphorylated in CAD from HEK-293 cells (data not shown). Interestingly, we observed that while the T1037A mutant slightly reduced CPSase II activity, it displayed a significant increase in the fold-stimulation induced by PRPP (Figure 2.12B).

2.4.6 14-3-3ζ interaction with CAD

Additionally, we have confirmed that 14-3-3ζ binds to CAD (Meek et al., 2004). Since 14-3-3 typically binds to phosphorylated Ser/Thr residues in proteins (Aitken, 2006), and $pSer^{1406}$ matched a putative 14-3-3 binding according to the scansite sequence match program (Obenauer et al., 2003), we hypothesized that the phosphorylation of Ser^{1406} mediated the interaction of CAD with 14-3-3. However as seen in figure 2.14, 14-3-3 still bound to the S1406A Flag-CAD. While the amino acid sequence surrounding the other phosphorylation sites do not match known 14-3-3 binding consensus sequences, there are reports of novel 14-3-3 binding consensus sites (Ganguly et al., 2005; Shikano et al., 2005). Furthermore, it was shown that PKA phosphorylated a Thr residue in one of these novel 14-3-3 binding sequences (Ganguly et al., 2005). Therefore, it is interesting to speculate that the function of PKA phosphorylation of Ser^{1859} might be to facilitate the binding of 14-3-3 to CAD. Additionally, since there are proteins that bind 14-3-3 in a phosphorylation-independent manner (Clark et al., 2004; Macdonald et al., 2005), there is a possibility that the phosphorylation of CAD does not regulate the interaction with 14-3-3.

2.4.7 Conclusion

In conclusion, we have demonstrated that there are four major phosphopeptides observed on our 2D phosphopeptide maps of Flag-CAD isolated from HEK-293 cells. While spots 1 and 4 represent $pSer^{1859}$, and spot 3 represent Thr^{1772}, the identity of the phosphopeptide in spot 2 remains unknown. However, our 2D-phosphopeptide maps of our Ser/Thr to Ala CAD mutants demonstrate that spot 2 does not represent previously reported putative CAD phosphorylation sites (Olsen et al., 2006; Sigoillot et al., 2002a).

Our phosphatase treatment and activity data suggest that Thr^{1772} and/or the phosphopeptide represented by spot 2 are important for CPSase II activity. The mechanism by which the phosphorylation of CAD modulates CPSase II activity needs to be investigated. One possibility is that the phosphorylation increases the affinity of CPSase II for ATP. Additionally, since the functional unit of CAD is a hexamer (Coleman et al., 1977; Lee et al., 1985; Qiu and Davidson, 2000), the phosphorylation of CAD may function to enhance CPSase II activity by facilitating hexamer formation. In fact, precedence for this role of phosphorylation in a pyrimidine synthetic enzyme was demonstrated by Carman and colleagues. They observed that the dephosphorylation of CTP synthetase isolated from *Saccharomyces cerevisiae* prevented the formation of the active CTP synthetase tetramer. Additionally, the phosphorylation of CTP synthetase with PKA and PKC facilitated the tetramerization of this enzyme (Pappas et al., 1998).

A fifth phosphopeptide (spot 5), which represents Ser^{1406}, appears after HEK-293 cells are stimulated with forskolin. Moreover, CPSase II activity and allosteric activation by PRPP are only minimally reduced after forskolin treatment. Furthermore, while Thr^{456} and Thr^{1037} were not identified as a major phosphopeptides in CAD, the T1037A mutation caused a significant increase in the PRPP stimulation of CPSase II activity, and the T456A mutation significantly inhibited CPSase II activity. While we determined that ERK phosphorylated CAD on numerous sites in vitro, CAD was not a substrate for ERK in HEK-293 cells in our experimental conditions. Therefore, the model whereby ERK regulates the cellular levels of pyrimidines by phosphorylating CAD and increasing CPSase II activity (Sigoillot et al., 2003; Sigoillot et al., 2002b; Sigoillot et al., 2005; Sigoillot et al., 2004) needs to be reevaluated.

Other functions of CAD phosphorylation could be the mediation of the interaction of CAD with the hRad9 protein (which is described in Chapter III), or the regulation of CAD nuclear localization. In fact, Ser^{1406} is located in the sequence of mammalian CAD that corresponds to the nuclear localization sequence in yeast URA2 (Nagy et al., 1989). Since the phosphorylation of residues within nuclear localization sequences can regulate protein entry into the nucleus (reviewed in Jans and Hubner, 1996), the phosphorylation of CAD Ser^{1406} might cause CAD to be transported into the nucleus.

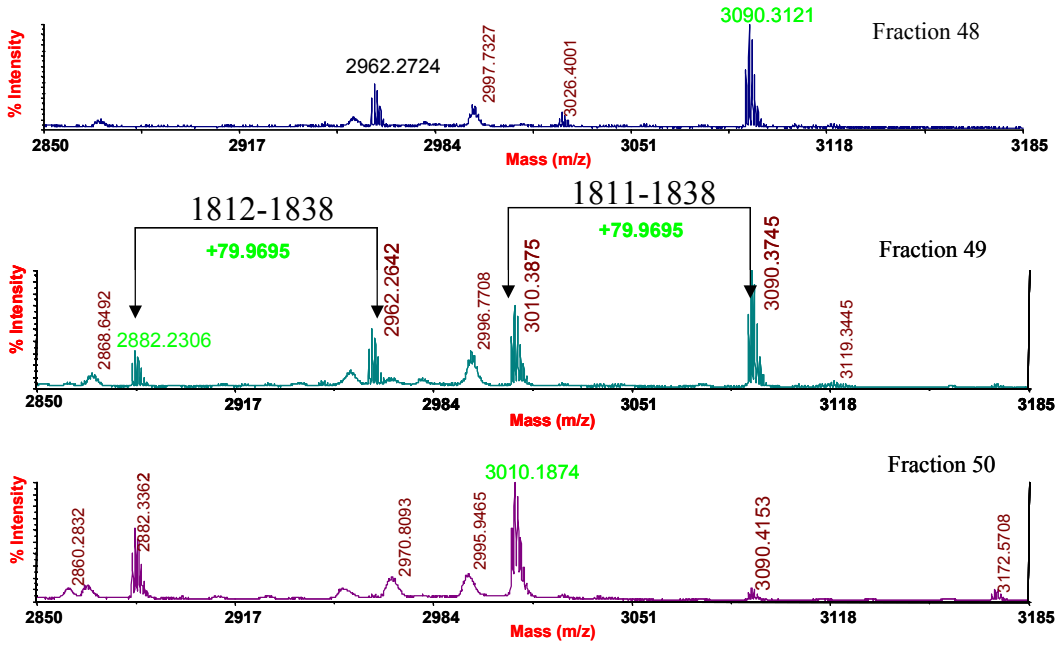

Figure 2.1. Identification of the tryptic-CAD phosphopeptide ^{1811}Lys-Arg^{1838}. His-CAD was isolated from HEK-293 cells and trypsin digested as explained in Materials and Methods. The tryptic peptides were separated by C18 reverse-phase HPLC, and each fraction was analyzed by the ABI 4700 MALDI-TOF/TOF mass spectrometer as described in Materials and Methods. The three mass spectra above were gathered from HPLC fractions 48, 49, and 50. The CAD peptide that each ion represented was determined by matching them to the m/z of the predicted CAD tryptic peptide ions using Protein Prospector (http://prospector.ucsf.edu) (Clauser et al., 1999). The peak in fraction 48 at m/z 3090.3121 corresponded to the singly charged peptide Lys^{1811}-Arg^{1838} containing a single phosphate group. The peak at m/z 2962.22724 in fraction 48 corresponded to Trp^{1812}-Arg^{1838} containing a single phosphate group. We observed both of these phosphopeptide ions in fraction 49, in addition to the peaks at m/z 2882.2306 and m/z 3010.3875, which corresponded to the Trp^{1812}-Arg^{1838}.

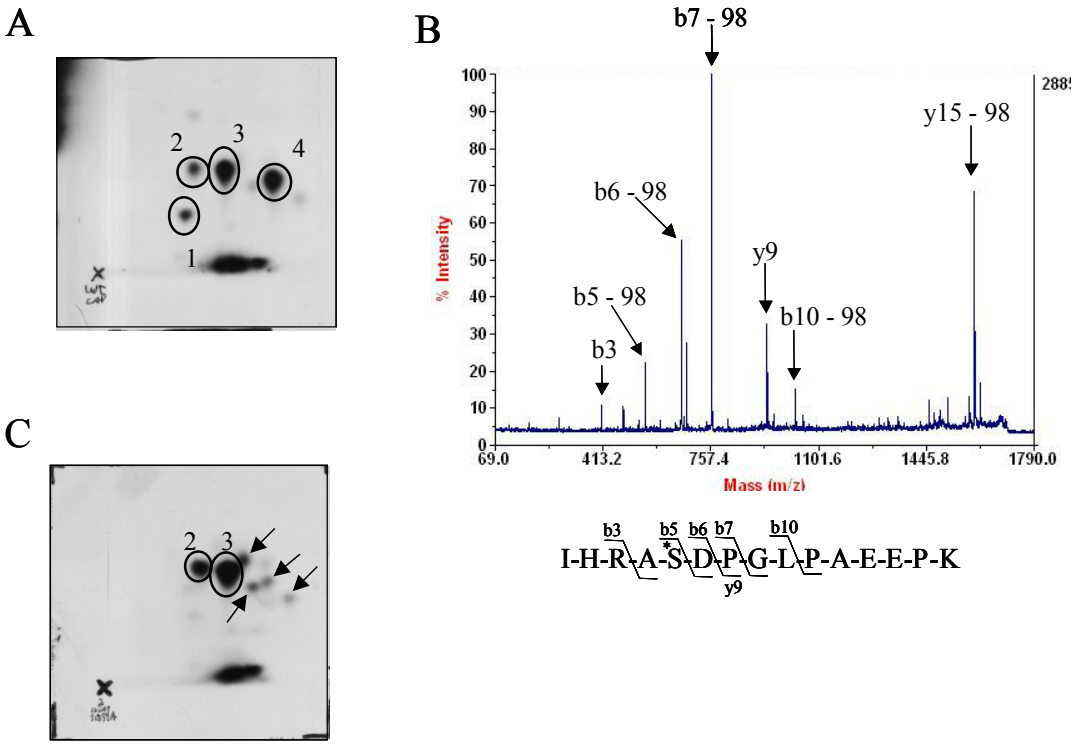

Figure 2.2. Identification of Ser[1859] as a phosphorylation site in CAD isolated from HEK-293 cells. (A) HEK-293 cells were transfected with Flag-CAD and maintained in 10% FBS. 24 hours after transfection, the cells were labeled with from [^{32}P]-orthophosphate. Lysates were prepared and Flag-CAD was isolated and trypsin digested in the gel as described in Materials and Methods. 2D-phosphopeptide mapping then was performed by separating the tryptic peptides on a cellulose backed TLC plate in two dimensions. The TLC plates then were exposed to film to identify the area containing phosphopeptides. **(B)** Spot four (A) was scraped and the peptides were analyzed using the 4700 (ABI) MALDI-TOF/TOF mass spectrometer. A peak at m/z of 1696.7708 on the MS spectrum corresponded to the predicted m/z of the singly charged Ala[1855]-Lys[1869] peptide with the addition of one phosphate group (data not shown). This peptide was fragmented using CID and the fragment ions whose m/z values correspond to y or b ions (some of which correspond to ions with the neutral loss of H_3PO_4 (-98)) are labeled. The asterisk indicates the phosphorylated Ser[1859] residue. **(C)** The CAD residue Ser[1859] was mutated to an alanine (S1859A) as described in Materials and Methods. HEK-293 cells were transfected with either WT-Flag CAD or S1859A-Flag CAD and 2D-phosphopeptide mapping was performed as in (A**)**. The arrows indicate minor phosphopeptides.

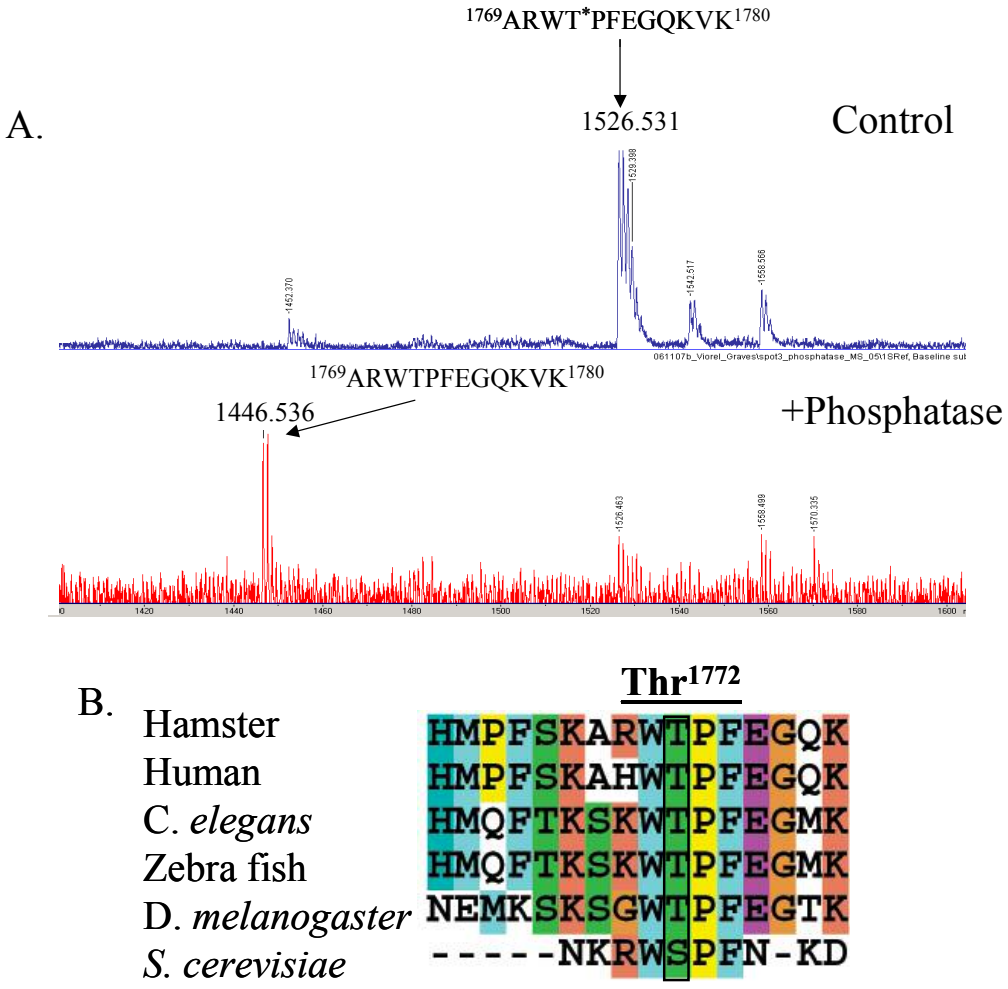

Figure 2.3. Identification of the CAD phosphopeptide 1769-1780. (A) Peptides from spot three (Figure 2.2A.) were eluted off the cellulose from the TLC plate. The peptides then were analyzed by MALDI-MS on a Bruker Daltonics Ultraflex mass spectrometer. The upper panel is the mass spectrum showing the peak at 1526.531 corresponding to the predicted m/z of the singly charged ^{1769}ARWTPFEGQKVK^{1780} CAD peptide with the addition of one phosphate group. The peptides then were treated with alkaline phosphatase on the MALDI plate and reanalyzed. The mass spectrum of the phosphatase treated peptides (bottom panel) shows a peak at 1446.536, which is 80 (the m/z of a phosphate moiety) less than the 1526.531 peak in the upper panel. Since Thr^{1772} is the only residue in this peptide able to be phosphorylated, we assigned this residue as a CAD phosphorylation site. (B) A sequence alignment using ClustalX was performed on CAD amino acid sequences from the indicated organisms. The sequences that were used have the following NCBI Accession numbers: Hamster (P08955); Human (P27708); *C. elegans* (NP_495838); Zebra fish (CAI20956); *D. melanogaster* (NP_523377); *S. cerevisiae* (CAA89425).

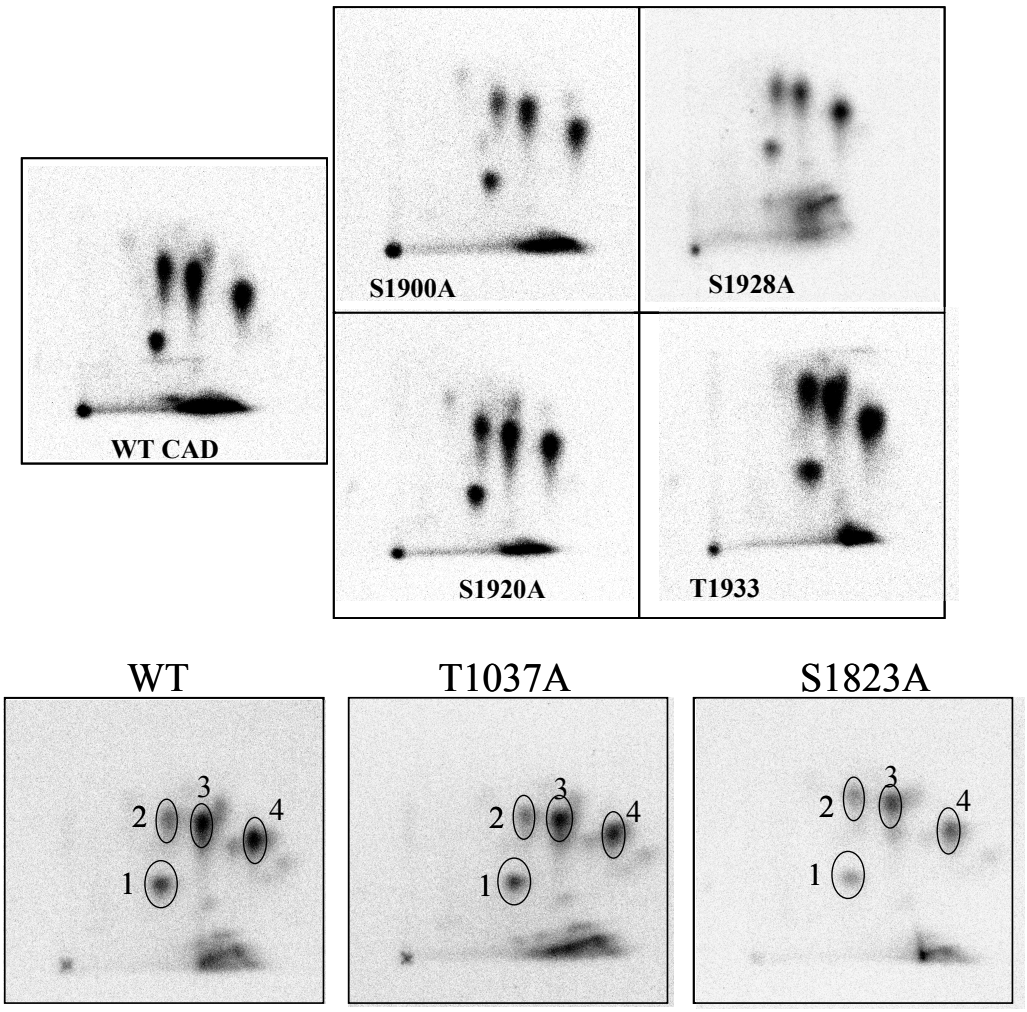

Figure 2.4. Phosphopeptide spot 2 is not one of the previously reported CAD phosphopeptides. Phosphopeptide mapping (described in Materials and Methods) was performed on either WT-Flag CAD, or the indicated Thr/Ser to Ala mutants isolated from [^{32}P]-orthophosphate labeled HEK-293 cells**.**

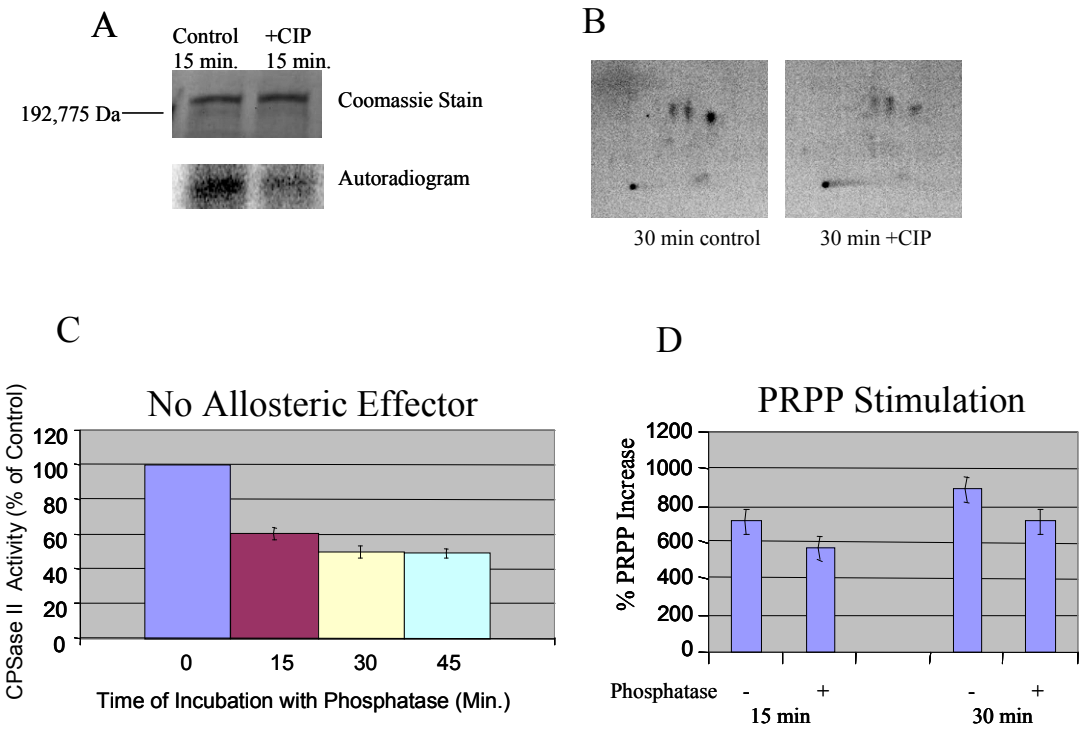

Figure 2.5. The Dephosphorylation of Flag-CAD from HEK-293 cells inhibits CPSase II activity. (A) CAD was immunoprecipitated from [^{32}P]-orthophosphate labeled HEK-293 cells. CAD was then dephosphorylated with calf intestinal alkaline phosphatase (CIP) and separated by SDS-PAGE as described in Materials and Methods. CAD was visualized by staining the gel with Coomassie stain, and an autoradiogram was performed. (B) The treatment of CAD with CIP was performed as in (A), and CAD was excised from the gel and 2D phosphopeptide mapping was performed as described in Materials and Methods. (C) Immunoprecipitated Flag-CAD was incubated with CIP for the indicated times, and CPSase II activity with the presence of 20 mM ATP was measured as described in Materials and Methods. The CPSase II activity at each time point is graphed as percent activity compared to the activity of CAD incubated without CIP under the same conditions (Materials and Methods). (D) CPSase II assays of CAD treated with or without CIP were performed in the presence of 500 μM PRPP and 2 mM ATP. The PRPP stimulation is plotted as percentage of total activity without added PRPP.

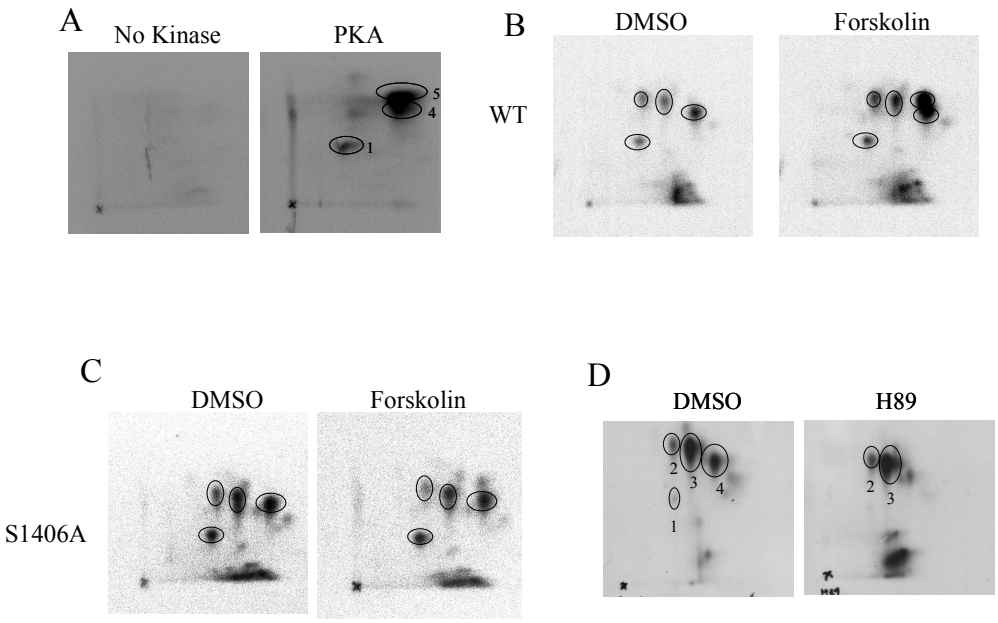

Figure 2.6. PKA phosphorylates CAD on Ser^{1406} and Ser^{1859} in HEK-293 cells. Flag CAD was immunoprecipitated from HEK-293 cells was incubated with or without the catalytically active PKA subunit and [γ-^{32}P]ATP (A). 2D phosphopeptide mapping was performed on WT Flag-CAD (B and D) or S1406A Flag-CAD (C) immunoprecipitated from [^{32}P]-orthophosphate labeled cells that were treated with either DMSO or 20 μM forskolin for 15 min (B and C), or DMSO or 20 μM H89 for three hours (D).

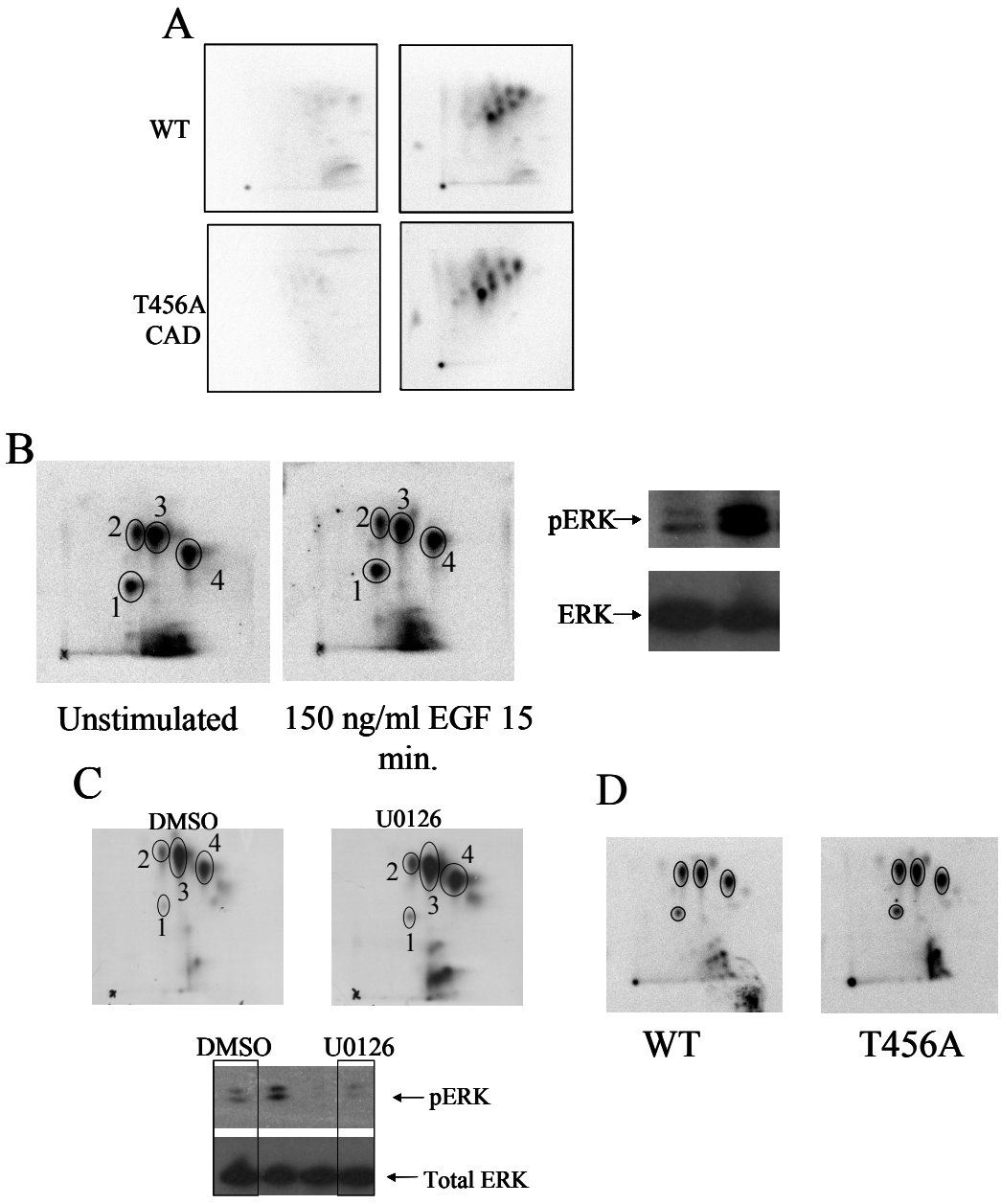

Figure 2.7. CAD was not significantly phosphorylated by ERK in HEK-293 Cells. Immunoprecipitated WT Flag CAD or T456A Flag-CAD was incubated with or without active ERK2 and [γ-^{32}P]ATP and 2D phosphopeptide mapping was performed as described in Materials and Methods (A). 2D phosphopeptide mapping was performed on immunoprecipitated WT-Flag CAD (B, C, and D) or T456A Flag-CAD (D) from metabolically labeled HEK-293 cells that were stimulated with or without 150 ng/ml EGF for 15 min (B), or with 10 μM U0126 or DMSO for three hours (C). Lysates from the unstimulated or EGF-stimulated (B) and the DMSO or U0126 (C) treated cells were separated by SDS-PAGE and ERK activity was measured by immunoblotting with an anti-phospho ERK antibody.

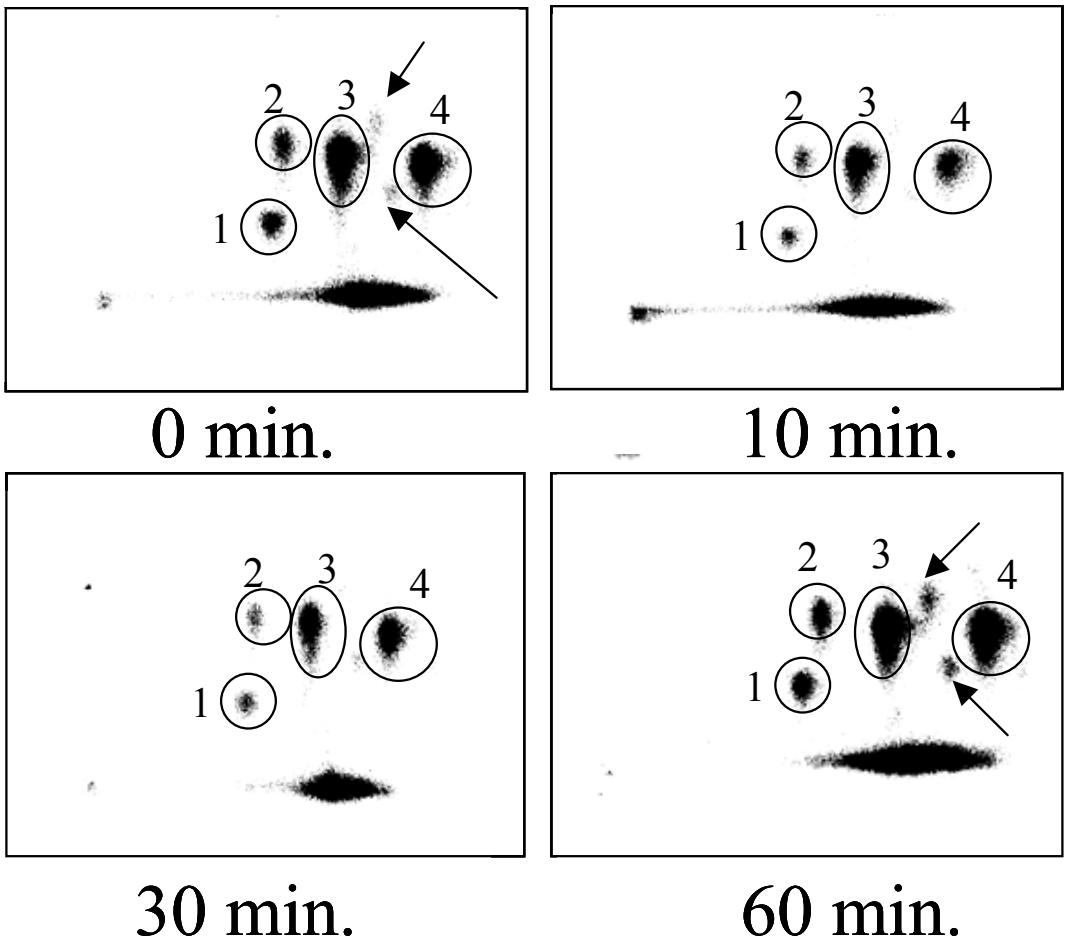

Figure 2.8. Serum does not stimulate CAD phosphorylation. 2D phosphopeptide mapping was performed on immunoprecipitated Flag-CAD isolated from HEK-293 cells that had been grown in low serum media for 18 hours prior to being stimulated with 10 % fetal bovine serum (FBS) for the indicated times (described in Material and Methods). The arrows indicate minor phosphopeptide spots.

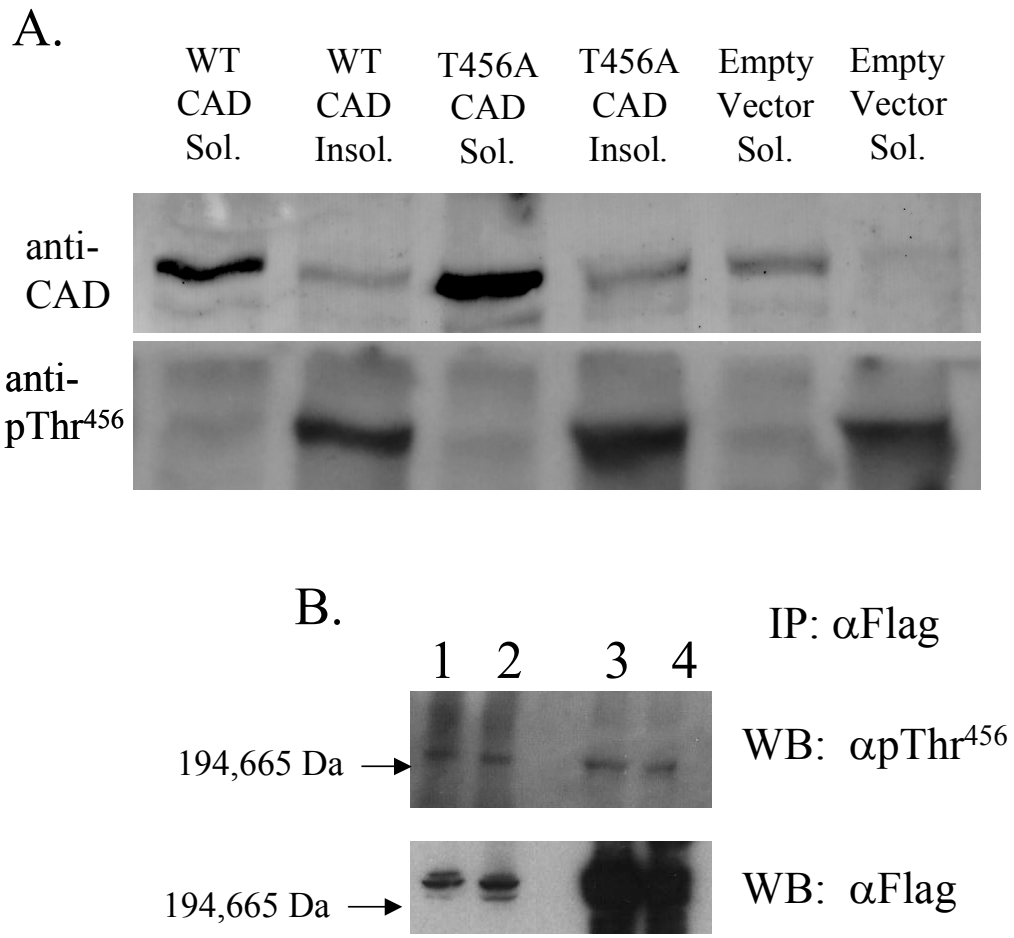

Figure 2.9. The pThr^{456} antibody is not specific for this CAD phosphorylation site. Cells with low CAD activities (G9C), were induced to stably express the vector PCDNA3.1, WT-CAD, or T456A-CAD in a previous report (Graves et al., 2000). G9C cells stably expressing WT-CAD, T456A-CAD, or PCDNA3.1 were lysed and separated into detergent soluble or insoluble as described in (Sigoillot et al., 2005). SDS-PAGE was performed and immunoblots using the Santa Cruz anti-pThr^{456} antibody (A, bottom panel), or an anti-CAD antibody (A, top panel) were performed. (B) WT Flag CAD (lane 3) or T456A Flag-CAD (lanes 4) were immunoprecipitated from HEK-293 cells. 20 μg of lysate from cells transfected with WT Flag-CAD (lane 1), or T456A Flag-CAD (lane 2). The proteins were analyzed by immunoblotting with the anti-pThr456 or anti-Flag antibodies as indicated.

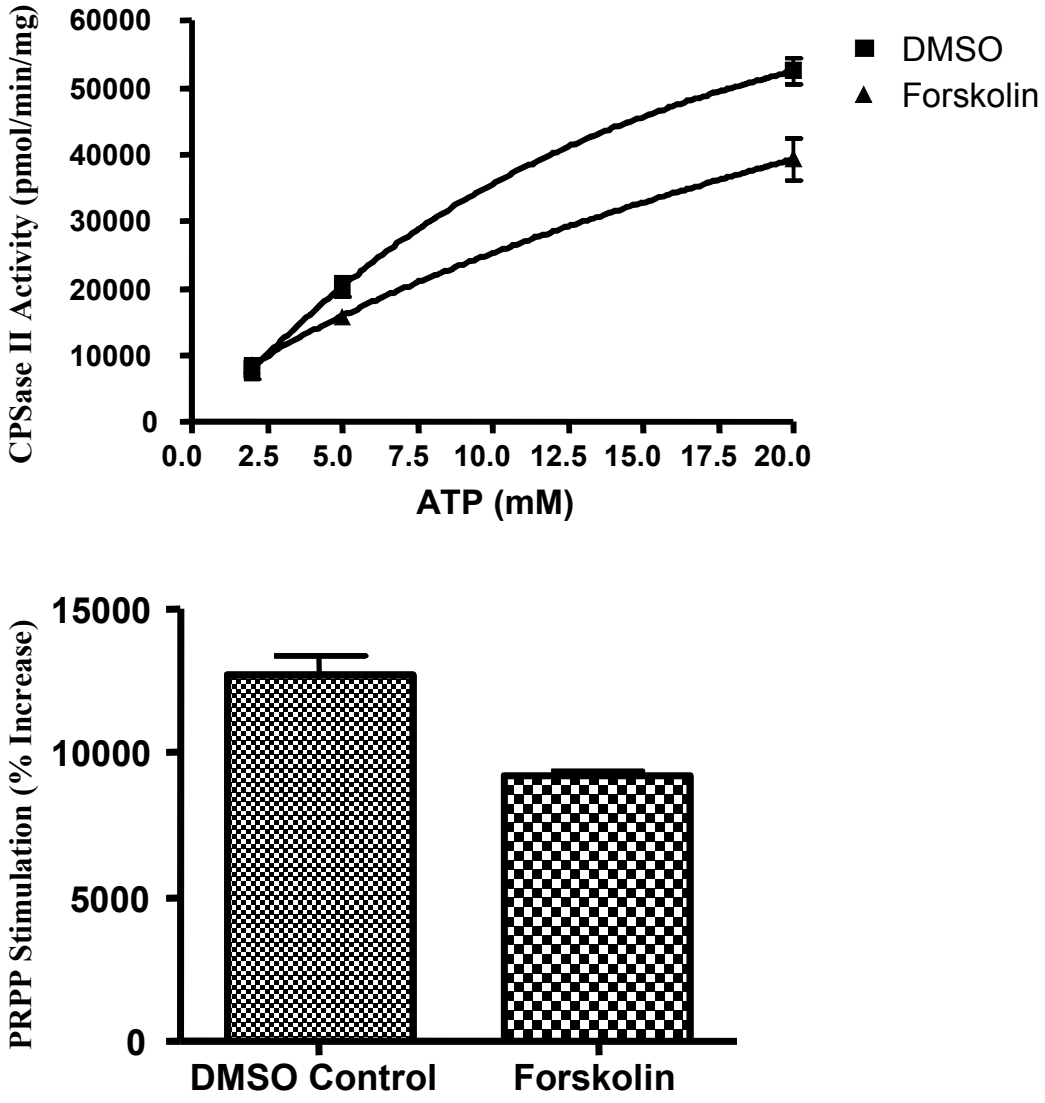

Figure 2.10. Forskolin treatment of HEK-293 cells causes a slight decrease both CPSase II activity and PRPP activation. HEK-293 cells were transfected with WT Flag-CAD and treated with the vehicle DMSO or 20 μM forskolin for 15 min prior to harvesting so that. This treatment was observed to induce the phosphorylation of Ser^{1406} in Figure 2.6. Flag-CAD was immunoprecipitated and CPSase II activity assay were with varying concentrations of ATP (A), or 2 mM ATP and 500 μM PRPP (B). The curves in (A) were generated using GraphPad Prism version 4.01 for Windows (GraphPAD Software, San Diego, CA, www.graphpad.com), by performing nonlinear regression analysis and fitting the raw data to the equation $Y = Vmax * X^h/(K + X^h)$ where h is the Hill coefficient and K is the apparent Km.. The PRPP stimulation is plotted as percentage of total activity without added PRPP (B).

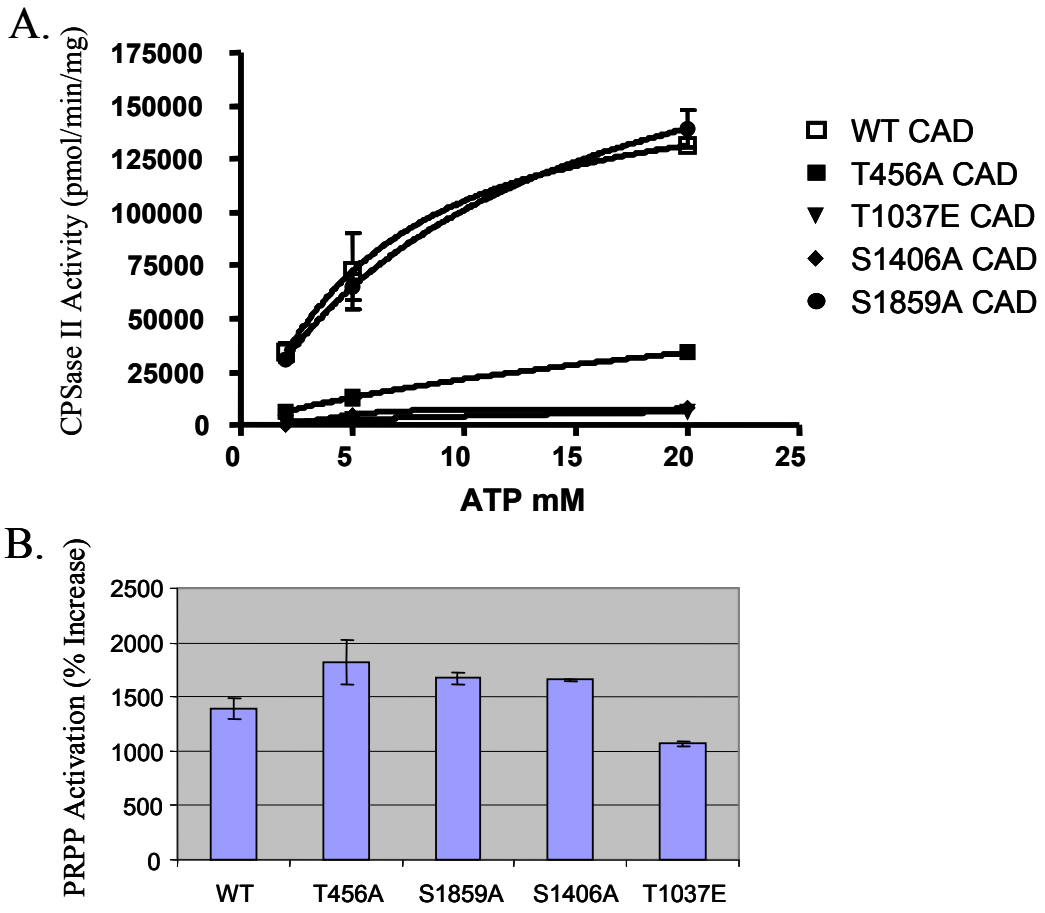

Figure 2.11. The effects of CAD phosphorylation site mutants on CPSase II activity and PRPP stimulation. (A) The CPSase II activity of the immunoprecipitated WT-Flag CAD, or the indicated Flag-CAD mutants, was measured at 2 mM. 5 mM, or 20 mM ATP as described in Materials and methods. The curves were generated using GraphPad Prism version 4.01 for Windows (GraphPAD Software, San Diego, CA, www.graphpad.com), by performing nonlinear regression analysis and fitting the raw data to the equation $Y = Vmax * X^h/(K + X^h)$ where h is the Hill coefficient and K is the apparent Km. (B) CPSase II activity of WT-Flag CAD or the indicated Flag-CAD mutants was measured in the presence or absence of 500 μM PRPP with 2 mM ATP. The PRPP stimulation is plotted as percentage of total activity without added PRPP.

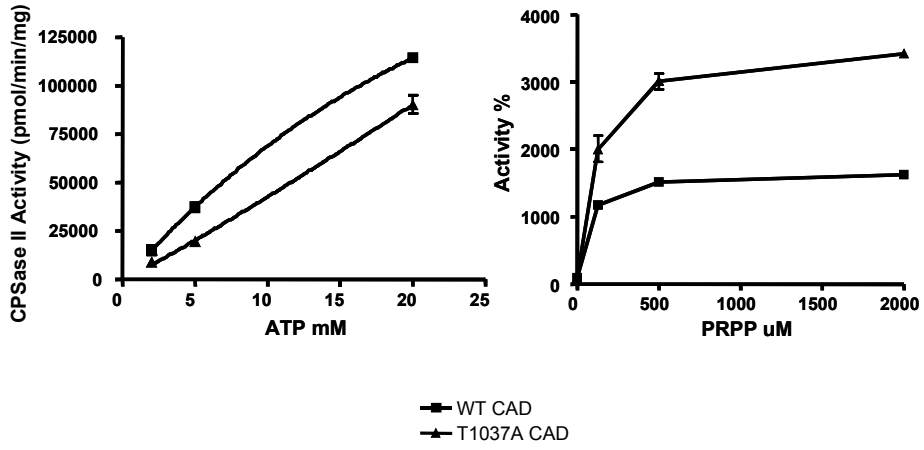

Figure 2.12. The T1037A CAD mutant decreases CPSase II activity, but increases PRPP stimulation of CPSase II activity. CPSase II activity was measured from immunoprecipitated WT-Flag CAD (square) or T1037A Flag-CAD (triangle) in the absence of PRPP with varying concentrations of ATP **(A)** or at 2 mM ATP in the presence of varying concentrations of PRPP (B)**.** The curves in (A), were generated using GraphPad Prism version 4.01 for Windows (GraphPAD Software, San Diego, CA, www.graphpad.com**),** by performing nonlinear regression analysis to fit the raw data to the equations $Y=Vmax * X^h/(K + X^h)$ where h is the Hill coefficient and K is the apparent Km. The PRPP stimulation in **(B)** is plotted as percentage of total activity without added PRPP.

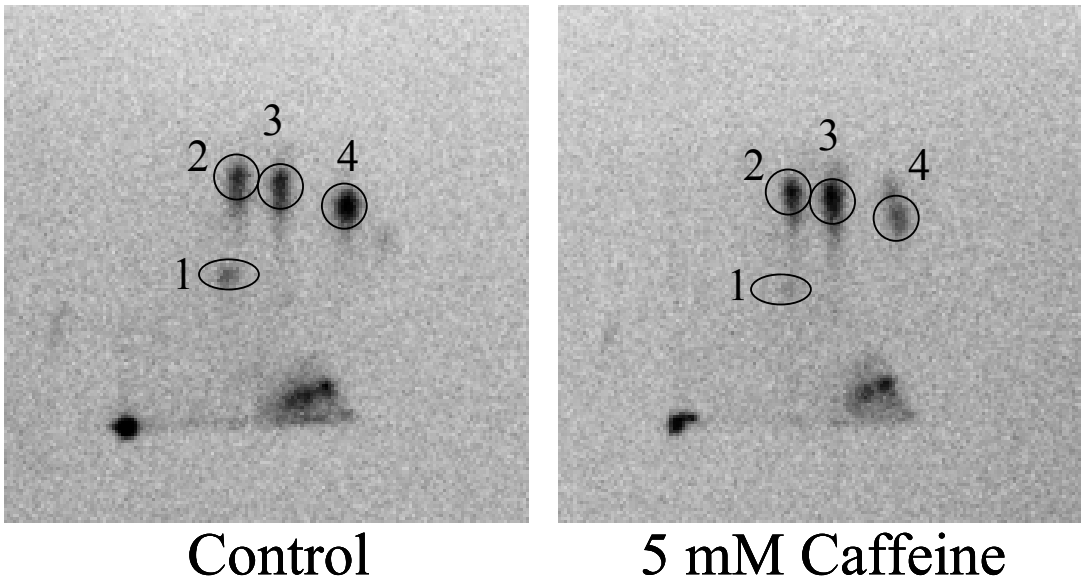

Figure 2.13. Caffeine inhibits CAD phosphorylation on Ser^{1859}. WT Flag-CAD was isolated from HEK-293 cells that were metabolically labeled with [^{32}P]-orthophosphate and treated with or without 5 mM caffeine for 3 hours prior to harvesting. 2D phosphopeptide maps then were performed as described in Materials and Methods.

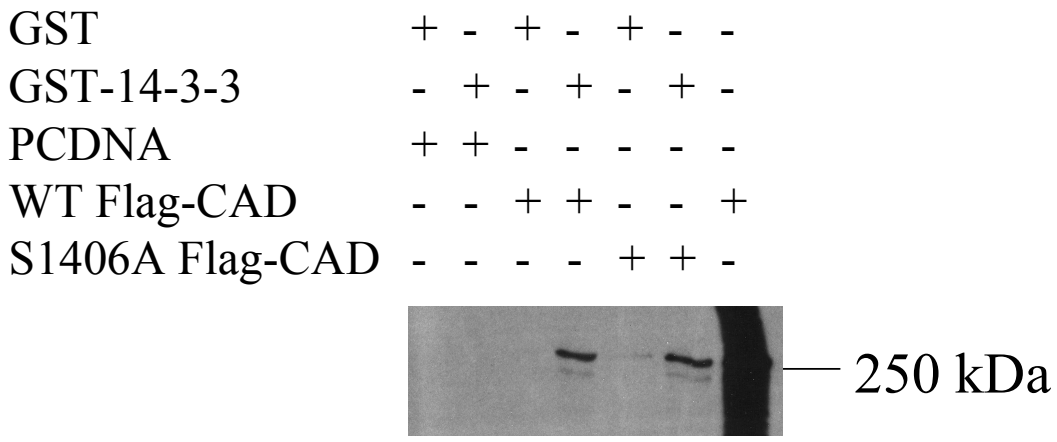

Figure 2.14. 14-3-3ζ interacts with Flag-CAD from HEK-293 cells, but does not require the CAD phosphorylation site Ser^{1406}. Lysates from PCDNA3.1, WT Flag-CAD, or S1406A Flag-CAD vector transfected cells were incubated with either GST-conjugated, or GST-14-3-3ζ conjugated glutathione beads. SDS-PAGE was performed and Flag-CAD was detected by immunoblotting with the anti-Flag antibody.

CHAPTER III

THE HUMAN RAD9 CHECKPOINT PROTEIN STIMULATES THE CARBAMOYL PHOSPHATE SYNTHETASE ACTIVITY OF THE MULTIFUNCTIONAL PROTEIN CAD

3.1 Introduction

The human Rad9, Rad1, and Hus1 proteins make a PCNA-like heterotrimericcomplex that has a ring structure and is thought to play a PCNA-like role as a DNA clamp specific for the DNA damage checkpoint response (reviewed in (Sancar et al., 2004)). It has been found that the checkpoint specific Rad17-RFC specifically binds to the 9-1-1 complex and clamps it around a DNA duplex (Bermudez et al., 2003; Ellison and Stillman, 2003; Majka and Burgers, 2003; Zou et al., 2003). Although the precise mechanism by which the Rad17-RFC/9-1-1 complex clamp loader/checkpoint clamp senses damage and initiates cell cycle arrest is not known, significant progress has been made in understanding the role of this complex.

Investigations into how the 9-1-1 complex may transduce a signal to downstream proteins in the checkpoint response have revealed that subunits of the complex, in particular Rad9, interact with a number of other cellular proteins with no obvious role in cell cycle arrest and have raised the possibility that these proteins might individually participate in other cellular functions as well. For example, Rad9 has recently been shown to bind to the androgen receptor and modulate its activity (Wang et al., 2004). Rad9 also binds to the kinases c-Abl (Yoshida et al., 2002) and PKCδ (Yoshida et al., 2003), which in turn regulate the binding of Rad9 to the antiapoptotic proteins Bcl-2 and Bcl-xL, suggesting that Rad9 may play a role in the apoptotic response to genotoxic stress (Komatsu et al., 2000).

In the course of our studies on the function of the 9-1-1 complex, we found that when Rad9 was purified by immunoaffinity chromatography from extracts of transiently transfected human cells, the purified Rad9 preparation contained a protein of 240 kDa as

a major contaminant. Mass spectrometric analysis was used to identify this protein as carbamoyl phosphate synthetase/aspartate transcarbamoylase/dihydroorotase (CAD), a multienzymatic protein that catalyzes the first three steps in *de novo* pyrimidine synthesis (Jones, 1980). The rate-limiting step in this pyrimidine synthesis pathway is catalyzed by the carbamoyl phosphate synthetase II (CPSase) of CAD, which is also the site of feedback inhibition by uridine nucleotides and activation by the allosteric ligand phosphoribosyl pyrophosphate (PRPP) (Carrey and Hardie, 1988). CPSase activity is increased in tumor cells (Reardon and Weber, 1985; Sigoillot et al., 2004) and is reported to be regulated by the protein kinase A and mitogen-activated protein kinase signaling pathways in a growth- and cell cycle-dependent manner (Graves et al., 2000; Huang and Graves, 2003; Sigoillot et al., 2003; Sigoillot et al., 2002a). We find that Rad9 binds to the CPSase domain and that this binding results in a two-fold stimulation of the CPSase activity of CAD. This is the first documented report of a protein-protein interaction with CAD regulating its CPSase activity. We find that CAD interacts with free Rad9, but not Rad9 within the 9-1-1 checkpoint complex. These findings suggest that Rad9 may have an additional role to its checkpoint function in ribonucleotide biosynthesis.

3.2 Experimental Procedure

3.2.1 Materials

Antisera that recognize various antigens were obtained as follows: rabbit anti-His_6 (H-15) and rabbit anti-hRad9 (M-389) from Santa Cruz Biotechnology (Santa Cruz, CA), mouse anti-Flag from Sigma (St. Louis, MO).

3.2.2 Transfections and immunoprecipitations

Human embryonic kidney 293T cells were grown in Dulbecco's modified Eagle's medium (Gibco BRL) supplemented with 10% fetal bovine serum, 100 U of penicillin and streptomycin per ml and were transfected with pcDNA3-FlaghRad9, pcDNA3-His_6FlagCAD, pcDNA3-His_6FlagCPSII, or pcDNA3-HA-hRad9 plasmids using the calcium phosphate transfection method as previously described (Lindsey-Boltz et al., 2001). Forty-eight hours after transfection, cells were washed with PBS and lysed in 20 packed cell volumes of Lysis Buffer (50 mM Tris-HCl (pH 7.5), 0.3 M NaCl, 0.5% Nonidet P-40 (NP-40), protease inhibitors (Roche Molecular Biochemicals). After incubating 15 minutes on ice, the cell lysate was centrifuged for 30 min at 32,000 x g. The supernatant was incubated with anti-Flag agarose (Sigma) (20 µl/ml of lysate) for 4 h at 4°C. The resin was then washed twice with Lysis Buffer, twice with TBS (50 mM Tris-HCl (pH 7.5), 150 mM NaCl), and the protein was eluted for 30 minutes at 4°C with TBS containing 0.2 mg/ml Flag peptide (Sigma).

3.2.3 Expression and purification of recombinant proteins

Baculoviruses were previously described for expression of full length Flag-Rad9, fragments of Rad9, and His_6-CAD. Monolayer High Five insect cells (Invitrogen) were infected with either theHis_6-CAD baculovirus alone or together with the Flag-Rad9 baculovirus and then harvested after 48 hours. The cells were washed with PBS and lysed in 20 packed cell volumes of lysis buffer (50 mM Tris-HCl (pH7.5), 300 mM NaCl, 15 mM imidazole, 0.5% Nonidet P-40 (NP40), and protease inhibitors). After incubating 15 minutes on ice, the cell lysate was centrifuged for 30 min at 32,000 x g. The supernatant was incubated with Ni-NTA agarose (Qiagen) (50 µl/ml of lysate) for 4 hours at 4°C. The

resin was then washed twice with lysis buffer, twice with elution buffer (50 mM Tris-HCl (pH 7.5), 10% glycerol, 0.3 M NaCl, 2 mM ATP), and then eluted with two volumes of elution buffer containing 100 mM imidazole.

3.2.4 Interactions between CAD and Rad9, 9-1-1, and Rad9 fragments

H5 insect cells were coinfected with baculoviruses expressing either His-CAD alone or together with either Flag-Rad9, or Flag-Hus1 and His-Rad1, or Flag-Hus1 and His-Rad1 and untagged Rad9, or the five fragments of Rad9 which were all previously described (Bermudez et al., 2003). After lysing the cells in 50 mM Tris-HCl (pH 7.5), 0.3 M NaCl, 0.5% NP40, the protein was then immunoaffinity purified using anti-Flag agarose. After washing the resin three times in the same buffer, the protein was eluted with Flag peptide and analyzed by western blotting.

3.2.5 CPSase activity assay

CPSase activity was measured essentially as described previously (Huang et al., 2002). Briefly, all of the reaction components except the cold and ^{14}C-labeled sodium bicarbonate (the initiation solution) were added to tubes on ice. These samples then were placed in a 37°C water bath for 10 minutes before the initiation mix was added to start the reaction. The 250 µl reaction was allowed to proceed for 30 minutes at 37°C before it was quenched by the addition of 125 µL of 80 % trichloroacetic acid. The unincorporated ^{14}C then was removed by gently heating the samples at 85° C for 2-3 hours. The incorporation of ^{14}C into the acid stable carbamoyl aspartate was then measured by scintillation counting. The reaction mixture, contained 7.5 µl of the elution buffer previously described containing approximately 0.11 µg of CAD, 87 mM Tris-HCl (pH

8.0), 87 mM KCl, 6.5% dimethyl sulfoxide, 2.2% glycerol, 0.87 mM dithiothreitol, 3.1 mM glutamine, 17.4 mM aspartate, 7 mM [^{14}C]$NaHCO_3$ (50 mCi/mmol), 2 mM excess of $MgCl_2$ over the addition of nucleotide and PRPP concentrations, and ATP concentrations (adjusted to ATP contained within the protein elution buffer) varying from 0.06 mM to 15 mM.

3.3 Results

3.3.1 Copurification of CAD with Rad9

In the course of our studies on the 9-1-1 complex, we found that when HEK293T cells were transfected with a plasmid expressing Flag-tagged Rad9 and the protein was purified with anti-Flag agarose, the preparation contained a major band of 240 kDa and a minor band of 110 kDa. These bands were not seen in immunoaffinity-purified extracts from control cells transfected with vector alone (Figure 3.1). Mass spectroscopic analysis of Rad9-copurifying bands revealed that the 240 kDa protein is CAD and the 110 kDa protein is the heat shock protein hsp110. As heat shock proteins often co-purify with ectopically expressed proteins, we concentrated our efforts on characterizing CAD, the major protein that copurifies with Rad9.

3.3.2 Mapping of CAD and Rad9 Domains Required for Binding

The human CAD protein catalyzes three separate reactions with three distinct structural domains, carbamoyl phosphate synthetase II (CPSase), aspartate transcarbamoylase (ATCase), and dihydroorotate reductase (DHOase) (Figure 3.2a). Similarly, human Rad9 has an N terminal PCNA-like domain and a C-terminal extension, which is heavily phosphorylated and is thought to play a role as an effector in checkpoint

signaling (Roos-Mattjus et al., 2003; St Onge et al., 2001; St Onge et al., 2003) (Figure 3.2b). To gain insight into the potential physiological significance of the CAD-Rad9 interaction, we mapped the interacting regions on both proteins by deletion analysis. In Figure 3.3, both full-length CAD and the CPSase domain of CAD were co-expressed with Rad9 in 293T cells and the CAD and CPSase immunoprecipitates were immunoblotted for Rad9. As seen in Figure 3.3 (right panel), Rad9 bound equally well to the full-length CAD and to the CPSase domain alone. To perform reciprocal experiments, insect cells were infected with baculoviruses expressing CAD together with regions of Rad9. The Rad9 fragments were immunoprecipitated and the precipitates were analyzed for CAD by immunoblotting. As seen in Figure 3.4, the N-terminal and the middle third, but not the C terminal third of Rad9 bound to CAD. The strongest binding was observed with the N terminal two-thirds of the protein. Interestingly, the C-terminal two-thirds bound CAD with less affinity than the middle third alone, suggesting that the C-terminal tail may negatively regulate the Rad9-CAD interaction. While the quantitative aspects of the data regarding the binding strength has certain limitations, this data unambiguously show that the PCNA-like domain of Rad9 binds to CAD whereas the C-terminal domain, which encompasses the major Rad9 phosphorylation sites and presumably acts as an effector in checkpoint signaling, does not.

3.3.3 CAD Binds to Free Rad9 But Not to Rad9 Within the 9-1-1 Complex

To investigate whether CAD may participate in Rad17-RFC/9-1-1 complex-mediated signal transduction, we tested the binding of CAD to the other members of the 9-1-1 complex, Rad1 and Hus1, as well as to the ternary Rad9-Rad1-Hus1 complex by co-infection of insect cells with combinations of baculoviruses that express these

proteins. The tagged 9-1-1 proteins were immunoprecipitated and the immunoprecipitates were tested for the other 9-1-1 proteins and for CAD. Figure 3.5 shows that Rad9 expressed in insect cells, like Rad9 expressed in mammalian cells, binds CAD, but Rad1 and Hus1 do not (lane 1 vs. lane 2). Most significantly, when Rad9 is co-immunoprecipitated as part of the 9-1-1 complex by using a Hus1 affinity tag, the immunoprecipitate does not contain any detectable CAD (lane 3). This was somewhat expected because Rad9 interacts with Rad1 and Hus1 through its PCNA-like domain suggesting that this domain is apparently blocked from binding to CAD within the 9-1-1 complex. These findings suggested that the Rad9-CAD interaction might have a role in cellular physiology other than DNA damage checkpoint signaling.

3.3.4 Modulation of Carbamoyl Phosphate Synthetase Activity

Since currently there is no specific assay for Rad9 activity, we tested for the possible modulation of CAD activity by Rad9 in the following series of experiments. Initially, we found that immunoaffinity purified Rad9-CAD complex exhibited higher CPSase activity than CAD alone (data not shown). To further examine the effect of Rad9 on CAD activity, we examined whether purified proteins could be combined to recapitulate this regulation. However, when combined *in vitro*, the two proteins did not form a stable complex, and we observed no change in the CPSase activity of CAD (data not shown). We reasoned that the two proteins may have to be co-expressed to form a complex, and therefore expressed CAD alone and CAD plus Rad9 in insect cells and purified these recombinant proteins using the His_6 tag on CAD for affinity purification. We obtained the protein preparations shown in Figure 3.6. The CAD protein levels obtained under the two conditions were quite similar, and the amount of CAD activity

was normalized to the amount of CAD protein in each sample as determined by quantitative western analysis. CPSase synthesizes carbamoyl phosphate from ATP, bicarbonate, and glutamine, and is the first enzymatic step in pyrimidine biosynthesis. CPSase is allosterically activated by phosphoribosyl pyrophosphate (PRPP) and inhibited by UTP (Jones, 1980). We tested the effect of Rad9 on CPSase activity in the presence of saturating amounts of PRPP with varying ATP concentrations. We observed that the Vmax of CAD was increased two-fold by Rad9 both in the presence or absence of PRPP (Figure 3.7 and Table 3.1). Kinetic analysis of CAD/Rad9 complexes revealed that Rad9 did not significantly change the apparent affinity for ATP (Km) in the presence or absence of PRPP. Likewise, a fragment of Rad9 lacking the C-terminal phosphorylation sites (fragment C in Figure 3.4) had a similar effect on the CPSase activity of CAD (Figure 3.7 and Table 3.1). Thus, it appears that Rad9 regulates the rate-limiting step of ribonucleotide biosynthesis by increasing the Vmax of the CPSase activity.

3.4 Discussion

Induction of ribonucleotide reductase (RNR) is one of the best characterized transcriptional response reactions to DNA damage and has been observed in organisms ranging from *Escherichia coli* to humans (Elledge et al., 1993). The upregulation of RNR activity by either transcriptional or post-transcriptional means increases the dNTP pools, and it has been shown that an increase in dNTP levels following DNA damage increases cellular survival in budding yeast (Chabes et al., 2003). Since rNTP pools are typically 100-fold higher than the dNTP pools, it has generally been assumed that changes in rNTP levels would not affect the dNTP pool and hence survival and mutation rate. This assumption, however, has not been experimentally tested. Furthermore, RNA synthesis,

which would be affected by rNTP levels, might contribute to cellular recovery from genotoxic stress. Such an outcome of a Rad9-CAD interaction would place this interaction within the general DNA damage response network. However, it is also plausible that the Rad9-CAD interaction is operational under physiological conditions to maintain cellular homeostasis and that this function is not related to the checkpoint function of Rad9 which occurs within the context of the 9-1-1 complex. Indeed, Rad9 has been found to associate with a number of proteins with diverse functions some of which are not related the DNA damage checkpoint response. Additionally, *de novo* pyrimidine biosynthesis is not only important in dividing cells for the production of new nucleic acids, but also for UDP-sugars and CDP-lipids, which are used for diverse cellular functions (reviewed in Huang and Graves, 2003). Therefore, the Rad9-induced increase in CAD activity could be important in many different areas of cell physiology.

We currently do not know the cellular location of the CAD-Rad9 interaction. While CAD is mainly cytoplasmic, some studies have provided evidence for a fraction of CAD being in the nucleus (Angeletti and Engler, 1998; Carrey et al., 2002; Sigoillot et al., 2003). Under normal cellular conditions, Rad9 is part of the nuclear 9-1-1 complex (Burtelow et al., 2000; Burtelow et al., 2001). However, Rad9 does appear to have an independent cytoplasmic function during apoptosis. It has been demonstrated that during apoptosis Rad9 is cleaved by caspase-3 and the N-terminal portion of Rad9 translocates to the cytosol where it interacts with Bcl-xL (Lee et al., 2003). Since CAD does not associate with the 9-1-1 complex (Figure 3.5), and all detectable nuclear Rad9 is in this complex (Burtelow et al., 2001), it is likely that the CAD-Rad9 interaction takes place in the cytoplasm.

CAD is a unique biosynthetic enzyme with three distinct enzymatic activities. The CPSase enzyme domain catalyzes the formation of carbamoyl phosphate from glutamine, bicarbonate, and two molecules of ATP. The ATCase region catalyzes the synthesis of carbamoyl aspartate from aspartate and carbamoyl phosphate. Finally, the formation of dihydroorotate is catalyzed by the DHOase domain (Carrey and Hardie, 1988). The assay used in these studies to measure CPSase activity is a coupled enzyme assay, which measures the incorporation of [^{14}C] into the acid stable chemical carbamoyl aspartate, which, as mentioned above, is catalyzed by the enzymatic activities of both the CPS II and ATC domains. However, since the CPSase activity is rate limiting (reviewed in (Jones, 1980), the observed changes in enzymatic activity are most likely due to changes in the CPSase activity of CAD.

The CPSase activity of CAD is highly regulated. As mentioned previously, it is allosterically activated by PRPP and inhibited by the product of pyrimidine-nucleotide synthesis, uridine 5‘-triphosphate (UTP). Moreover, phosphorylation can affect the allosteric regulation by PRPP and UTP An additional level of regulation of CPSase activity is by protein degradation induced by caspase 3 (Huang et al., 2002). The findings reported in this study add a previously unknown mode CPSase activity regulation. Our data reveal the first documented report that a protein-protein interaction with CAD can regulate CPSase activity. Although allosteric regulators (i.e. PRPP and UTP) decrease the Km for a CPSase substrate (ATP), our data suggests that Rad9 increases the Vmax of CPSase rather than changing the Km for ATP. Rad9 binding was also observed to increase the maximum velocity of CPSase activity in the presence of PRPP, but did not affect the percent activation by PRPP. We investigated the affect of Rad9 on UTP

induced inhibition of CPSase activity. Rad9 did not significantly decrease the inhibitory action of UTP, but this result varied between CAD protein preparations preventing us from making a conclusion from this data (data not shown).

The mechanism by which Rad9 increases CPSase activity is not known. Rad9 binding could increase the affinity of other CPS II substrates such as glutamine or bicarbonate. Another plausible hypothesis is that Rad9 increases the glutaminase activity of CPS II, thereby increasing the overall Vmax without affecting the affinity for ATP. However, this appears unlikely since experiments using ammonia as the nitrogen donor, thereby bypassing the need for the glutaminase activity, have shown that Rad9 still induced a two-fold increase in CPSase activity (data not shown). Alternatively, Rad9 binding may induce a conformational shift that affects the oligomeric (activated) form of the enzyme. Active CAD has been shown to be a hexamer (Qiu and Davidson, 2000), and Rad9 may increase CAD activity by increasing the amount of enzyme in the hexameric form. Dissociation of CAD to monomers did not affect the CPSase activity, but significantly reduced the Vmax of ATCase (Qiu and Davidson, 2000). It is therefore possible that Rad9 could be increasing CAD activity by stabilizing the oligomeric form of this enzyme and thereby increasing the Vmax of ATCase. However, this seems unlikely since the CPSase activity of CAD is the rate limiting step (Jones, 1980), and an increase in the ATCase rate would not be expected to increase the overall rate of our coupled enzyme reaction.

In summary, we find that the checkpoint protein Rad9 specifically interacts with the CPSase domain of CAD and increases its Vmax by at least a factor of two. The high specificity of the Rad9-CAD interaction strongly suggests that it is of significance to

normal cellular homeostasis. Further work is needed to determine the potential role of this interaction in regulating DNA damage checkpoints, ribonucleotide pools, or RNA and DNA synthesis.

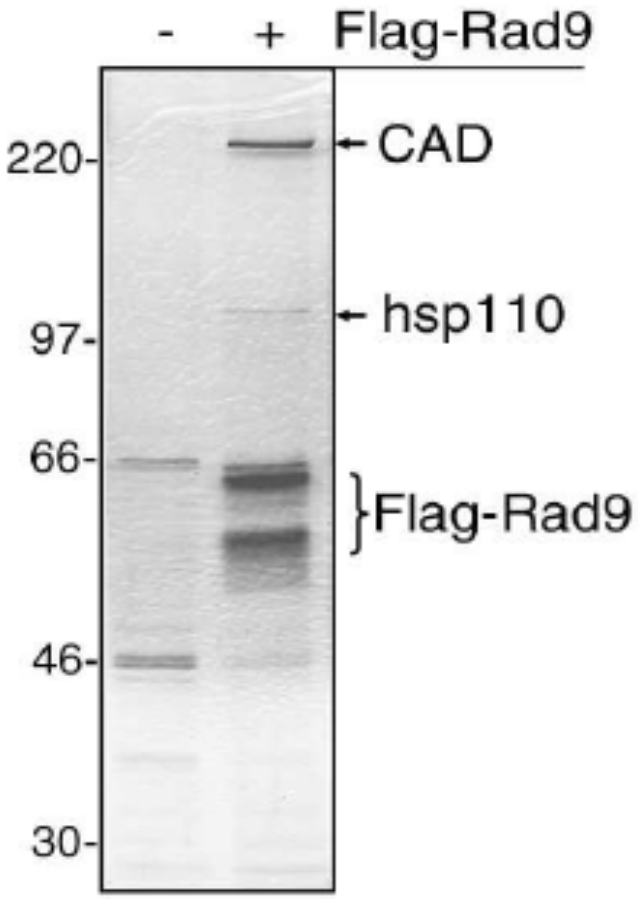

Figure 3.1. Copurification of CAD with Rad9. Copurification of CAD with Rad9. An aliquot of 3 X 10^6 293T cell were mock treated (-) or transfected with 6 μg pcDNA3-Flag-hRad9 (+). Protein was immunoprecipitated using anti-Flag agarose from whole cell extracts, and 10 % of the protein eluted with Flag peptide was visualized after SDS-PAGE by silver staining. Mass spectrometric analysis was performed by the University of North Carolina Mass Spectrometry Core Facility.

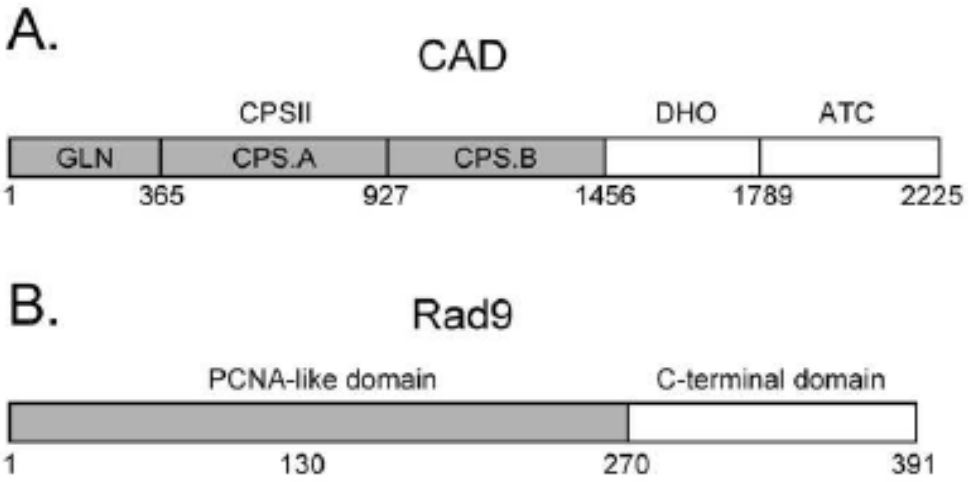

Figure 3.2 Structural organization of CAD and Rad9. (A) The human CAD protein has three distinct structural domains performing the three enzymatic activities, carbamoyl phosphate synthetase (CPS II), aspartate transcarbamoylase (ATC) and dihydroorotase (DHO). The CPS II domain is indicated with gray shading. (B) Human Rad9 has an N-terminal PCNA-like domain (gray shading) and a heavily phosphorylated C-terminal domain.

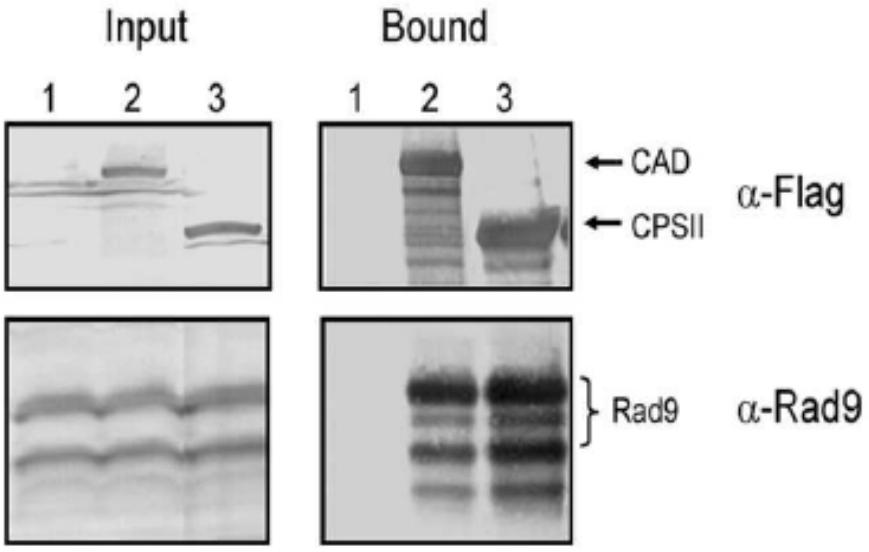

Figure 3.3. Rad9 interacts with the CPSII domain of CAD. An aliquot of $3 \cdot 10^6$ 293T cells was transfected with 6 mg of pcDNA3-HA-Rad9 alone (lane 1) or along with 6 mg of pcDNA3-Flag-CAD (lane 2), or pcDNA3-Flag-CPSII (lane 3). The proteins were immunoprecipitated with anti-Flag agarose and then analyzed by western blotting with anti-Rad9 and anti-Flag antibodies as indicated.

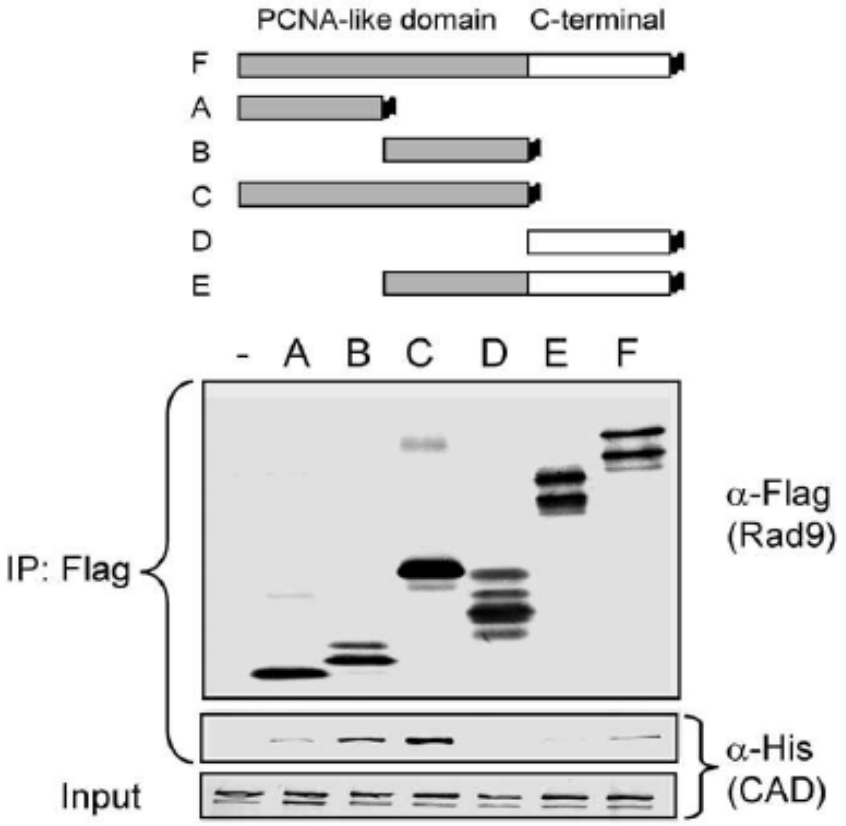

Figure 3.4. CAD interacts with the PCNA-like domain of Rad9. Insect cells were infected with His-CAD alone (-) or together with Flag-tagged fragments of Rad9 (fragment A contains amino acids 1–130, fragment B contains amino acids 130–270, fragment C contains amino acids 1–270, fragment D contains amino acids 260–391 and fragment E contains amino acids 130–391) or with full-length Rad9 (F). The proteins were immunoprecipitated with anti-Flag agarose and then analyzed by western blotting with anti-His and anti-Flag antibodies as indicated.

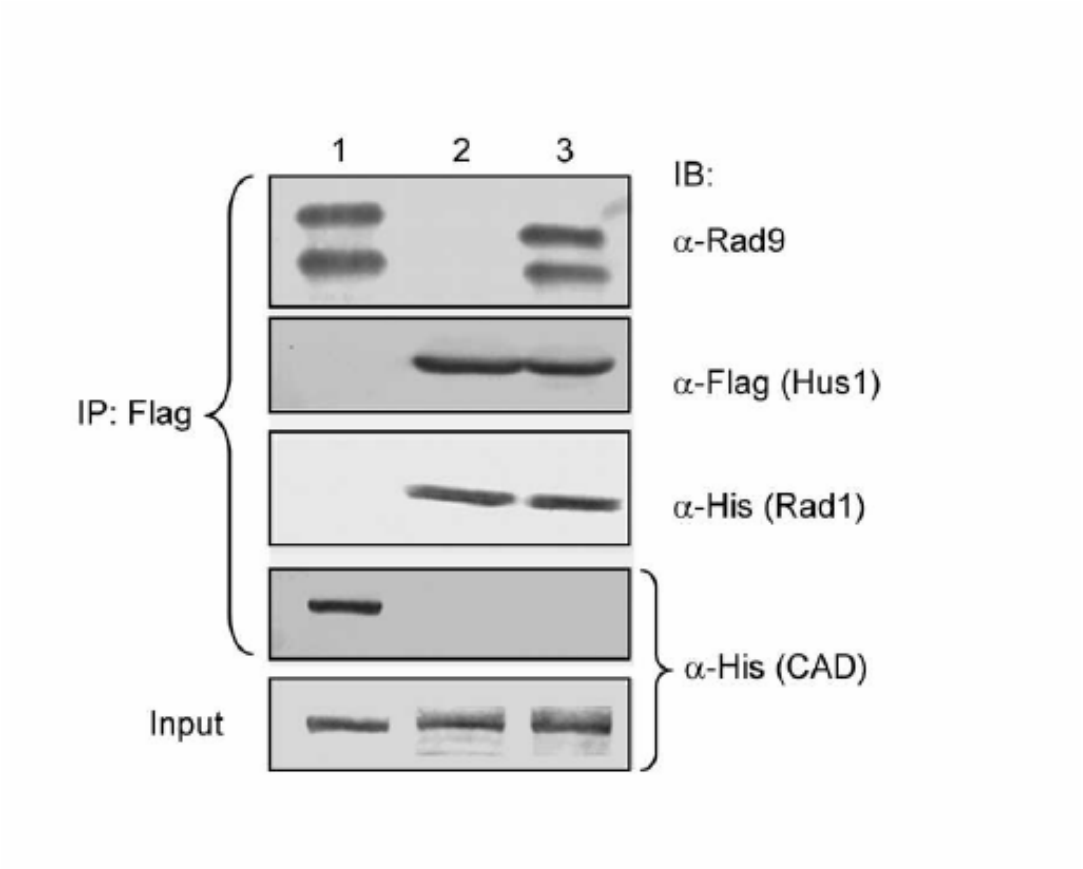

Figure 3.5. CAD binds to free Rad9, but not to Rad9 within the 9-1-1 complex. Insect cells were co-infected with His-CAD together with Flag-Rad9 (lane 1), or Flag-Hus1 and His-Rad1 and untagged-Rad9 (lane 3). The proteins were immunoprecipitated with anti-Flag agarose and then analyzed by western blotting with anti-His, anti-Rad9, and anti-Flag antibodies as indicated.

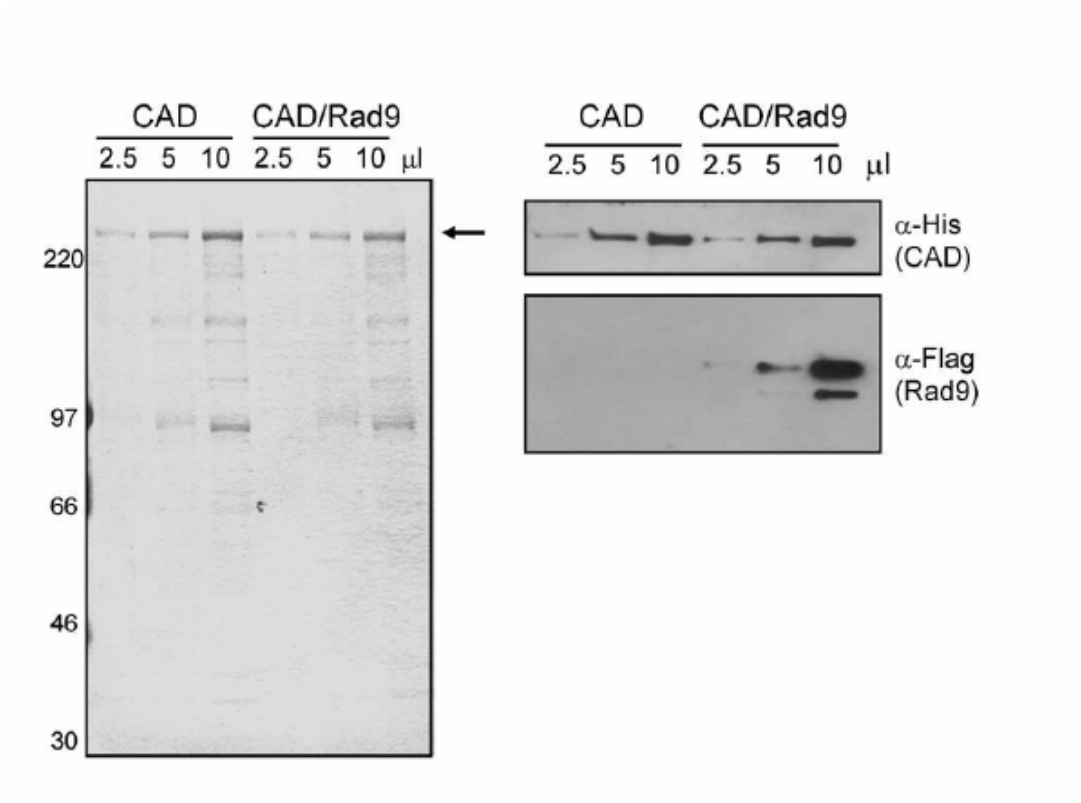

Figure 3.6. Purification of CAD with and without Rad9. Insect cells were infected with His-CAD alone or together with Flag-Rad9. The proteins were affinity purified with Ni-agarose and then analyzed by Coomassie staining (left panel) and western blotting (right panels). The arrow indicates the position of CAD. Aliquots of 2.5, 5, 10 ml from each sample was loaded which correlates to ~50, 100, 200 ng of CAD and 25, 50, 100 ng of Rad9 when quantitated using protein standards in the same gel.

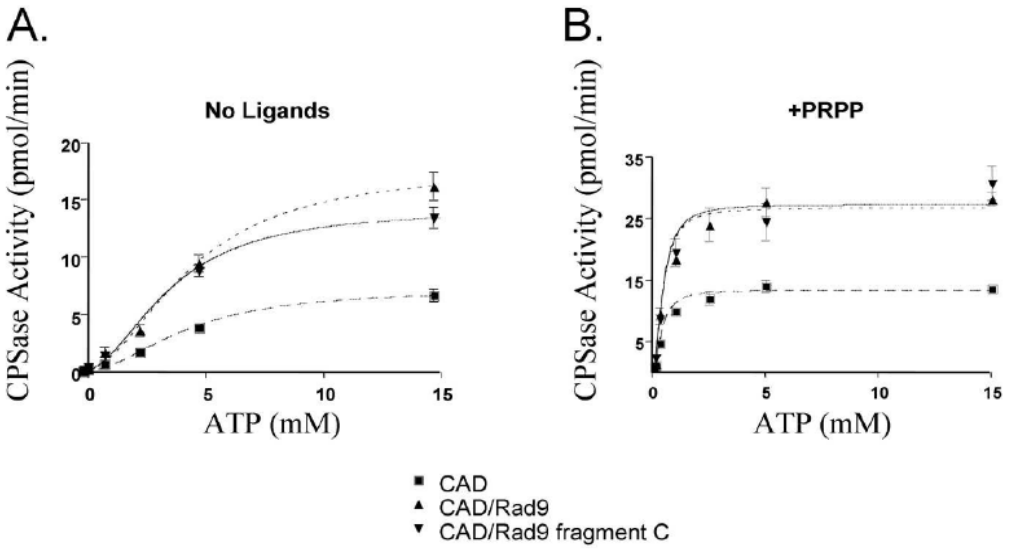

Figure 3.7. Rad9 increases the CPSase Vmax. CPSase activity was measured from purified CAD (square) expressed alone or co-expressed with full-length Rad9 (triangle) or Rad9 with a C-terminal deletion (upside-down triangle) in the absence (A) or presence (B) of 2mM PRPP with varying concentrations of ATP. The CAD and CAD/Rad9 data represent pooled results from five separate experiments, while the data from the CAD/Rad9 fragment C represent pooled data from two separate experiments. The curves were generated using GraphPad Prism version 4.01 for Windows (GraphPad Software, San Diego, CA, www.graphpad.com) by performing nonlinear regression analysis to fit the raw data to the equation $Y = Vmax * X^h/(K + X^h)$ where h is the Hill coefficient (set to 2) and K is the apparent Km.

	Ligand	Km	Vmax
CAD	None PRPP	4.5 +/- 0.43 0.4 +/- 0.05	7.3 +/- 0.38 13.4 +/- 0.43
CAD/Rad9	None PRPP	4.6 +/- 0.40 0.5 +/- 0.07	17.8 +/- 0.86 26.8 +/- 0.99
CAD/Rad9 fragment C	None PRPP	3.8 +/- 0.40 0.5 +/- 0.10	14.3 +/- 0.65 27.3 +/- 1.67

Table 3.1. Kinetic parameters of wild type CAD and CAD coexpressed with Rad9 and Rad9 fragment C. The kinetic parameters of the CPSase data from CAD and CAD/Rad9 represent pooled data from 5 separate experiments, while the data from the CAD/Rad9 fragment represents pooled data from 2 separate experiments. Km (mM ATP) is the apparent affinity for ATP, and Vmax ($pmol \bullet min^{-1}$) is the maximum CPSase velocity measured as a function of ATP concentration. These data are the numerical results from the graphs in Figure 4.7.

CHAPTER IV

CONCLUSIONS AND FUTURE DIRECTIONS

The studies in this dissertation were designed to investigate the regulation of CAD by phosphorylation and protein-protein interactions. While numerous studies on CAD phosphorylation have been performed, my work is the first comprehensive study of CAD phosphorylation. My data in Figure 2.7 demonstrated that CAD was not phosphorylated in response to ERK activation in HEK-293 cells, and thereby challenges the current dogma that the ERK-induced phosphorylation of CAD on Thr^{456} causes an increase in CAD activity and a consequent increase in intracellular pyrimidines (reviewed in (Evans and Guy, 2004). Furthermore, while we observed that CAD is phosphorylated on Ser^{1406} by PKA activation in HEK-293 cells, we did not detect the autophosphorylation at Thr^{1037}, as was proposed in (Sigoillot et al., 2002a). We discovered a previously unidentified CAD phosphorylation site contained in phosphopeptide spot three (Thr^{1772}) (Figure 2.3), but unfortunately were unable to determine the identity of the phosphopeptide in spot 2 on our 2D-phosphopeptide maps. However, by the process of elimination, we determined that it did not contain one of previously reported CAD phosphorylation sites (Olsen et al., 2006; Sigoillot et al., 2002a; Sigoillot et al., 2002b).

One of our aims was to elucidate the effect of CAD phosphorylation on enzymatic activity and allosteric regulation. CPSase II assays were performed on Flag-CAD immunoprecipitated from HEK-293 cells. While this method of CAD isolation does not give the purity of CAD that other methods might provide, the specific activity of CPSase II from CAD isolated using our method was similar to previously reported CPSase II specific activities (Shaw and Carrey, 1992; Sigoillot et al., 2002a). Therefore, this suggests that our method of CAD isolation and our CPSase II activity assays are valid.

As described above, we observed that CAD was phosphorylated on multiple residues in HEK-293 cells. To determine if the phosphorylation of CAD was important for the enzymatic activity, we compared CPSase II activity between Flag-CAD treated with or without alkaline phosphatase. As seen in Figure 2.5, the dephosphorylation of CAD significantly reduced CPSase II activity. Furthermore, CAD is phosphorylated during the 3-4 hours of [^{32}P]-orthophosphate labeling, and treatment of cells with the phosphatase inhibitor calyculin A caused a robust increase in the phosphorylation of phosphopeptides 1-4 (data not shown). Therefore, this dynamic regulation of CAD phosphorylation and the importance of CAD phosphorylation for enzyme activity, suggests that this post-translational modification is an important mechanism by which cells regulate CPSase II activity.

While the phosphatase treatment of CAD reduced the phosphorylation of phosphopeptides 1-4 (Figure 2.5B), we currently do not know if the dephosphorylation of one of these peptides is responsible for the reduction in CPSase II activity observed in Figure 2.5 C. Since spots 1 and 4 contain pSer^{1859} (Figure 2.2) and the phospho-null mutant S1859A did not affect CPSase II activity, the dephosphorylation of Ser^{1859} probably did not account for the decrease of CPSase II activity after phosphatase treatment. However, whether the dephosphorylation of phosphopeptide spot 3, which putatively contained pThr^{1772}, or phosphopeptide spot 2, accounted for the decrease in CPSase II activity remains to be tested. Therefore, it will be important to determine the identity of phosphopeptide spot 2, so that a phospho-null mutation can be created to test the affect on CPSase II activity. In addition, to conclusively prove that Thr^{1772} is the CAD phosphorylation site in phosphopeptide spot 3, and to know if the phosphorylation

of this site is important for CPSase II activity, we will need to create the T1772A mutant and perform 2D phosphopeptide mapping and CPSase II activity assays.

The mechanism by which CAD phosphorylation regulates CPSase II activity is not known. Since the functional unit of CAD in cells is a hexamer (Coleman et al., 1977; Lee et al., 1985; Qiu and Davidson, 2000), it is possible that the phosphorylation of CAD plays a role in the formation or maintenance of the hexamer. Although the crystal structure of CAD has not been solved, phosphorylation may influence inter- or intra-CAD protein domain contacts. Since the ATCase and DHOase regions appear to facilitate the CAD hexamer formation (Carrey, 1993; Qiu and Davidson, 2000), and the phosphorylation site Thr^{1772} is contained in the DHOase domain (Figure 1.6), the phosphorylation of this residue may play a role in hexamer formation. To test this hypothesis, we could purify the T1772A CAD mutant from HEK-293 cells and perform glycerol gradient ultracentrifugation to determine if CAD hexamer formation was inhibited.

While the identity of the kinase(s) that phosphorylated phosphopeptide spots 1-4 in HEK-293 cells is unknown, our data suggested that phosphopeptide spot 5 (Ser^{1406}) was phosphorylated by PKA in HEK-293 cells (Figure 2.6). Tatibana and colleagues first observed that the PKA-induced phosphorylation of CAD in vitro caused a slight increase in CPSase II activity. Carrey and colleagues determined that PKA phosphorylated CAD *in vitro* on Ser^{1406} and Ser^{1859}. Furthermore, they reported that the most significant effect of the phosphorylation of CAD by PKA was the reduction in the UTP-induced decrease in CPSase II activity. Subsequent studies demonstrated that CAD was phosphorylated in intact cells after the stimulation of PKA activity. While these data

suggested that the role of PKA-induced CAD phosphorylation was the activation of CPSase II activity, Evans and colleagues reported data that suggested that the PKA phosphorylation of CAD caused an overall decrease in CPSase II activity by decreasing the affinity for PRPP. Furthermore, it was proposed that PKA caused a decrease in CAD activity and total cellular pyrimidines as cells became quiescent or as cells progressed through the cell cycle after S-phase. To specifically determine if the phosphorylation of CAD by PKA in HEK-293 cells affected CAD activity, we stimulated HEK-293 cells with forskolin. We observed a significant increase in Ser^{1406} phosphorylation (Figure 2.6 B). The CPSase II activity assays, performed on Flag-CAD treated under these same conditions, demonstrated that PKA activation caused only a slight reduction in CPSase II activity and PRPP activation. Whether or not this slight reduction in enzymatic activity affects cellular pyrimidine synthesis remains to be tested. Since forskolin is an extremely potent stimulator of cAMP synthesis, which strongly activates PKA, it is also questionable how physiologically relevant this regulation is.

It is possible that the phosphorylation of Ser^{1406} by PKA serves a purpose other than modulating the acute CPSase II activity. Since CAD has been found in the nucleus, and the phosphorylation of proteins can regulate nuclear entry, the phosphorylation of Ser^{1406} could regulate the nuclear entry of CAD. Additionally, since the phosphorylation of CAD by PKA accelerated the cleavage of this multienzymatic protein by elastase and trypsin *in vitro* (Carrey and Hardie, 1988), the increase in CAD protein stability in cells may be a potential function for the PKA-induced phosphorylation of CAD. Interestingly, CAD protein is degraded during the differentiation of myoblasts into myocytes (Graves,

unpublished results). It could be that the phosphorylation or dephosphorylation of CAD facilitates the degradation of this protein during differentiation.

Additional studies have suggested that CPSase II activity is regulated by phosphorylation during cell cycle progression (Morford et al., 1994; Sigoillot et al., 2002a). While it is has been demonstrated that mitogen stimulation of human lymphocytes increased CPSase II activity (Ito and Uchino, 1973) and the CPSase II activity of rat hepatoma cells increased gradually over the G1 phase reaching a maximum in the S-phase of the cell cycle, whether or not this is due to CAD phosphorylation is not well established. Since resting primary human lymphocytes express undetectable levels of CAD mRNA and protein and there is a strong correlation between the mitogen-stimulated increase in CAD expression and the observed increase in CPSase II activity (Wauson unpublished observations and (Ito and Uchino, 1971). Thus it is possible that the main mechanism for the increase in CPSase II activity during the initial cell cycle progression is mediated by the increased expression of CAD. Interestingly, we observed that this increase in expression was blocked by U0126, the MEK-1 inhibitor (Eric Wauson unpublished results). However, this increase in CAD expression might only occur during the entry into the cell cycle from a G0 state and the phosphorylation of CAD might be important in subsequent cell divisions. Indeed, Guy and colleagues reported that the increase in PRPP stimulation of CPSase II activity and the decrease in UTP inhibition observed as the BHK 165-23 hamster cells proceeded through G1 and into S-phase and correlated with an increase in threonine phosphorylation of CAD (Sigoillot et al., 2003).

To investigate the role of CAD phosphorylation in the cell cycle, it will be important to determine the identity of the specific CAD residues phosphorylated during specific cell cycle phases. Therefore, phosphospecific antibodies that recognize pSer^{1406}, pThr^{1772,} pSer^{1859}, and the yet to be determined phosphorylated amino acid in spot 2, could be created. Cells could be synchronized and the phosphorylation of each of the above residues could be examined at each stage of the cell cycle. Additionally, the phosphorylation status of CAD from cancer cell lines that are known to have elevated CAD activity and/or *de novo* pyrimidine synthesis (Aoki et al., 1982a; Aoki and Weber, 1981; Karle et al., 1986; Sigoillot et al., 2004), could be profiled using these phosphospecific antibodies. Furthermore, the phosphorylation status of CAD from samples of primary cancer tissues could be investigated. This specific phosphorylation of CAD could also be examined in cells in normal rapidly growing tissues, such as regenerating liver, spleen, testis, thymus, and mitogen-stimulated lymphocytes (Aoki et al., 1982b; Ito and Uchino, 1971; Yip and Knox, 1970). These experiments would allow us to determine if there is a correlation between the phosphorylation of specific CAD residues and elevated CAD activity in numerous cell types. Ultimately, this approach would allow us to gain a better understanding of the physiological role of CAD phosphorylation.

To fully understand the role of CAD phosphorylation in cell physiology will require the identification of the kinase(s) that phosphorylate CAD. While our data from Figure 2.6 indicate that PKA phosphorylates CAD on Ser^{1406} Ser^{1859}, we do not know the kinase that phosphorylates Thr^{1772}, or the residue in spot 2 (Figure 2.2). Additionally, while our data suggests that ERK is not responsible for phosphorylating and regulating

the activity of CAD during the cell cycle as was reported (Sigoillot et al., 2003), there may be another kinase mediating the phosphorylation and activity of CAD during the cell cycle. Therefore, a future direction would be to determine which kinase(s) is responsible for the phosphorylation of CAD during the cell cycle. Since HeLa cells have been used extensively as a model to study cell cycle regulation, I propose to synchronize HeLa cells, release them into the cell cycle, and harvest them at multiple time points during the progression of the cell cycle. Kinase assays would be performed to identify the lysate that contained a CAD kinase activity. The lysate that contained a CAD kinase would be fractionated by size exclusion chromatography and kinase assays would be performed to find the fraction(s) that still contained a CAD kinase. This fraction then would be separated using SDS-PAGE, and the gel would be silver-stained. Since kinases autophosphorylate, autoradiography would be performed on the gel to identify potential kinases. The protein bands then could be identified by mass spectrometry. This method could allow us to identify putative cell cycle regulated kinase(s) that phosphorylated CAD. Since we observed evidence that suggested there was a basally active kinase in HEK-293 cells that phosphorylated CAD (Chapter II), we could use this approach to identify the kinase in HEK-293 cells. Finally, experiments using kinase inhibitors and RNAi designed to knockdown the putative CAD kinase(s) would be performed to determine if CAD was phosphorylated in intact cells by this kinase.

A cell model where endogenous CAD is not expressed would be useful in deciphering the role of CAD phosphorylation. The Chinese hamster ovary cell line that displays low levels of endogenous CAD activity (Musmanno et al., 1992) has been used in the past to test the function of CAD mutants (Banerjei and Davidson, 1997; Graves et

al., 2000). However, since these cells were created by chemical mutagenesis, they likely have additional mutations that could confound the interpretation of results. Consequently, another cell model would be favorable. Cells could be created that expressed siRNA that knocked-down WT-CAD expression. These cells then could be transfected with various CAD phosphorylation site mutants, which would be designed to not be recognized by the siRNA. The growth parameters, cell cycle progression, and intracellular pyrimidine levels would be tested in these cells to determine the effects of the phosphorylation site mutants on cell physiology. Furthermore, as done in previous studies (Sigoillot et al., 2005), the effect of CAD phosphorylation on the flux of precursors through the *de novo* pyrimidine pathway could also be investigated.

Another potential role of CAD phosphorylation may be the regulation of CPSase II activity during embryogenesis. Since the half-life of CAD protein is at least 24 hours (reviewed in Huang and Graves, 2003), and CPSase II enzymatic activity fluctuates relatively rapidly during *Drosophila* development (Mehl and Jarry, 1978), it is possible that the phosphorylation and/or other post-translational modifications of CAD protein are responsible for these changes in CPSase II activity. Furthermore, CAD expression is dynamically regulated during zebrafish embryogenesis, with CAD levels being high in the rapidly proliferating cells and low in tissues as cell growth slows and the cells exit the cell cycle. CAD expression is particularly high in the developing zebrafish retina, and the knockdown of CAD mRNA during zebrafish embryogenesis causes retinal malformation (Willer et al., 2005). In addition to CAD expression changes, the CPSase II activity during embryogenesis may be regulated by phosphorylation. The phosphorylation status of CAD during zebrafish embryogenesis could be investigated by

using phospho-specific CAD antibodies to perform immunohistochemistry on zebrafish embryos during different stages of embryogenesis.

In addition to phosphorylation, the CPSase II activity of CAD can be regulated by the interaction with hRad9. While we have demonstrated that hRad9 binds to CAD and this interaction increases enzymatic activity, future experiments are needed to determine the physiological role of this protein-protein interaction. It is interesting to speculate that upon DNA damage, hRad9 may bind to CAD; thereby, inducing an increase in pyrimidine nucleotides that may be needed to repair damaged DNA. Significant increases in cellular pools of deoxynucleoside triphosphates (dNTPs) in yeast have been observed to be necessary for survival after DNA damage induction. However, an increase in cellular pools of ribonucleoside triphosphates (NTPs) did not appear necessary for the increase in dNTPs. However, there are differences in how yeast and mammalian cells regulate their NTP and dNTP levels during normal cell cycle progression or following DNA damage. Therefore, while it is known that NTP levels fluctuate during normal cell cycle progression in mammalian cells (Schobitz et al., 1991; Sigoillot et al., 2003), whether or not NTP levels increase after DNA damage induction or other cellular stresses needs to be tested. Additionally, to determine if the hRad9/CAD interaction plays a role in mediating cellular pyrimidine NTP levels in cells, we could compare the rate of *de novo* pyrimidine synthesis and the concentrations of NTPs between the hRad9$^{-/-}$ and WT mouse embryonic stem cells (Hopkins et al., 2004).

While it is not clear if the hRad9/CAD interaction is involve in the DNA damage response, other recent data has suggested that CAD may be involved in the DNA damage response. For instance, CAD was found in a complex with the DNA damage

postreplicative mismatch repair enzyme PMS2 (Cannavo et al., 2007). Additionally, we demonstrated that caffeine, which inhibits the DNA damage inducible kinases ATM/ATR, inhibited Ser^{1859} phosphorylation (Figure 2.13). While ATM/ATR may not directly phosphorylate Ser^{1859}, since it is not a consensus site for these kinases, the Chk1/2 kinases, which are activated by ATM/ATR, may phosphorylate this residue. It is interesting to speculate that the role of the phosphorylation of Ser^{1859} by a caffeine sensitive DNA damage inducible kinase is to regulate the binding of CAD to either hRad9 and/or PMS2.

As discussed earlier, CAD either interacts with 14-3-3ζ directly, or with another protein that binds to 14-3-3ζ. The 14-3-3 proteins are a family of proteins containing seven isoforms that exert biological functions by binding to client proteins. The effects of the binding of 14-3-3 to client proteins are numerous and include, but are not limited to: modulation of enzymatic activity, changes in subcellular localization, and protection against protein degradation (reviewed in Aitken, 2006). Since we observed the CAD/14-3-3ζ interaction *in vitro* (Figure 2.14), it will be important to determine if this interaction occurs in intact cells. Experiments designed to determine the physiological role of the CAD/14-3-3ζ protein-protein interaction need to be performed. Since most of the 14-3-3 interactions occur at a phosphorylated residue, we would determine if one of the CAD phosphoamino acids mediates the CAD/14-3-3 interaction. As we did with the S1406A Flag-CAD mutant (Figure 2.14), we will determine if any of the other phosphorylation-null mutants prevent 14-3-3 binding. Additionally, to determine if 14-3-3ζ binding affects CAD activity in HEK-293 cells, we could knockdown 14-3-3ζ in cells to determine how CAD activity is affected.

Furthermore, since 14-3-3 binding can affect protein stability (Aitken, 2006), we could investigate the half-life of CAD in cells that were devoid of 14-3-3 ζ. Interestingly, Kido and colleagues discovered that of 14-3-3ζ was significantly upregulated in Drosophila after heat stress. Furthermore, they observed that 14-3-3ζ protected the enzyme citrate synthase against heat stress-induced inactivation. Since CAD is known to be thermally unstable (Guy and Evans, 1994b), the CAD/14-3-3ζ interaction may function to facilitate CAD stability at elevated temperatures.

In summary, we have performed a comprehensive analysis of CAD phosphorylation. We have identified major phosphorylation sites in CAD isolated from HEK-293 cells that appear to be important for enzymatic activity. Furthermore, we have shown that at least in HEK-293 cells, CAD is not phosphorylated in response to growth factor induced-ERK activation. Therefore, the current proposal that ERK-induced phosphorylation of CAD is responsible for the increase in cellular pyrimidines needed for cellular growth should be reevaluated. While we anticipated finding phosphorylation events that directly regulated CAD activity, our data suggests that phosphorylation may play a subtler role in stabilizing CAD activity. While some of the mutations that we examined abolished or significantly lowered CPSase II activity, it is possible that these mutants simply impaired the catalytic function of the CPSase II or ATCase domains by affecting residues necessary for catalysis. Future studies are needed to determine the role of CAD phosphorylation in cell physiology. Finally, we have discovered a novel protein-protein interaction between hRad9 and CAD that causes an increase in CPSase II activity. Further studies will be required to elucidate the physiological role of the hRad9-CAD interaction.

References

Aitken A (2006) 14-3-3 proteins: a historic overview. *Semin Cancer Biol* **16**:162-72.

Anderson CM and Parkinson FE (1997) Potential signaling roles for UTP and UDP: sources, regulation and release of uracil nucleotides. *Trends Pharmacol Sci* **18**:387-92.

Angeletti PC and Engler JA (1998) Adenovirus preterminal protein binds to the CAD enzyme at active sites of viral DNA replication on the nuclear matrix. *J Virol* **72**:2896-904.

Aoki T, Morris HP and Weber G (1982a) Regulatory properties and behavior of activity of carbamoyl phosphate synthetase II (glutamine-hydrolyzing) in normal and proliferating tissues. *J Biol Chem* **257**:432-8.

Aoki T, Sebolt J and Weber G (1982b) In vivo inactivation by acivicin of carbamoyl-phosphate synthetase II in rat hepatoma. *Biochem Pharmacol* **31**:927-32.

Aoki T and Weber G (1981) Carbamoyl phosphate synthetase (glutamine-hydrolyzing): increased activity in cancer cells. *Science* **212**:463-5.

Banerjei LC and Davidson JN (1997) Site-directed substitution of Ser1406 of hamster CAD with glutamic acid alters allosteric regulation of carbamyl phosphate synthetase II. *Somat Cell Mol Genet* **23**:37-49.

Bein K, Simmer JP and Evans DR (1991) Molecular cloning of a cDNA encoding the amino end of the mammalian multifunctional protein CAD and analysis of the 5'-flanking region of the CAD gene. *J Biol Chem* **266**:3791-9.

Bermudez VP, Lindsey-Boltz LA, Cesare AJ, Maniwa Y, Griffith JD, Hurwitz J and Sancar A (2003) Loading of the human 9-1-1 checkpoint complex onto DNA by the checkpoint clamp loader hRad17-replication factor C complex in vitro. *Proc Natl Acad Sci U S A* **100**:1633-8.

Beuneu C, Auger R, Loffler M, Guissani A, Lemaire G and Lepoivre M (2000) Indirect inhibition of mitochondrial dihydroorotate dehydrogenase activity by nitric oxide. *Free Radic Biol Med* **28**:1206-13.

Bodenmiller B, Mueller LN, Mueller M, Domon B and Aebersold R (2007) Reproducible isolation of distinct, overlapping segments of the phosphoproteome. *Nat Methods* **4**:231-7.

Boyd KE and Farnham PJ (1997) Myc versus USF: discrimination at the cad gene is determined by core promoter elements. *Mol Cell Biol* **17**:2529-37.

Brunschweiger A and Muller CE (2006) P2 receptors activated by uracil nucleotides--an update. *Curr Med Chem* **13**:289-312.

Burtelow MA, Kaufmann SH and Karnitz LM (2000) Retention of the human Rad9 checkpoint complex in extraction-resistant nuclear complexes after DNA damage. *J Biol Chem* **275**:26343-8.

Burtelow MA, Roos-Mattjus PM, Rauen M, Babendure JR and Karnitz LM (2001) Reconstitution and molecular analysis of the hRad9-hHus1-hRad1 (9-1-1) DNA damage responsive checkpoint complex. *J Biol Chem* **276**:25903-9.

Bush A, Mateyak M, Dugan K, Obaya A, Adachi S, Sedivy J and Cole M (1998) c-myc null cells misregulate cad and gadd45 but not other proposed c-Myc targets. *Genes Dev* **12**:3797-802.

Cannavo E, Gerrits B, Marra G, Schlapbach R and Jiricny J (2007) Characterization of the interactome of the human MutL homologues MLH1, PMS1, and PMS2. *J Biol Chem* **282**:2976-86.

Carrey EA (1993) Phosphorylation, allosteric effectors and inter-domain contacts in CAD; their role in regulation of early steps of pyrimidine biosynthesis. *Biochem Soc Trans* **21**:191-5.

Carrey EA, Campbell DG and Hardie DG (1985) Phosphorylation and activation of hamster carbamyl phosphate synthetase II by cAMP-dependent protein kinase. A novel mechanism for regulation of pyrimidine nucleotide biosynthesis. *Embo J* **4**:3735-42.

Carrey EA, Dietz C, Glubb DM, Loffler M, Lucocq JM and Watson PF (2002) Detection and location of the enzymes of de novo pyrimidine biosynthesis in mammalian spermatozoa. *Reproduction* **123**:757-68.

Carrey EA and Hardie DG (1988) Mapping of catalytic domains and phosphorylation sites in the multifunctional pyrimidine-biosynthetic protein CAD. *Eur J Biochem* **171**:583-8.

Cervera J, Bendala E, Britton HG, Bueso J, Nassif Z, Lusty CJ and Rubio V (1996) Photoaffinity labeling with UMP of lysine 992 of carbamyl phosphate synthetase from Escherichia coli allows identification of the binding site for the pyrimidine inhibitor. *Biochemistry* **35**:7247-55.

Chabes A, Georgieva B, Domkin V, Zhao X, Rothstein R and Thelander L (2003) Survival of DNA damage in yeast directly depends on increased dNTP levels allowed by relaxed feedback inhibition of ribonucleotide reductase. *Cell* **112**:391-401.

Chandra D, Bratton SB, Person MD, Tian Y, Martin AG, Ayres M, Fearnhead HO, Gandhi V and Tang DG (2006) Intracellular nucleotides act as critical prosurvival factors by binding to cytochrome C and inhibiting apoptosome. *Cell* **125**:1333-46.

Chaparian MG and Evans DR (1991) The catalytic mechanism of the amidotransferase domain of the Syrian hamster multifunctional protein CAD. Evidence for a CAD-glutamyl covalent intermediate in the formation of carbamyl phosphate. *J Biol Chem* **266**:3387-95.

Chen KF, Lai YY, Sun HS and Tsai SJ (2005) Transcriptional repression of human cad gene by hypoxia inducible factor-1alpha. *Nucleic Acids Res* **33**:5190-8.

Christopherson RI and Jones ME (1980) The overall synthesis of L-5,6-dihydroorotate by multienzymatic protein pyr1-3 from hamster cells. Kinetic studies, substrate channeling, and the effects of inhibitors. *J Biol Chem* **255**:11381-95.

Christopherson RI, Jones ME and Finch LR (1979) A simple centrifuge column for desalting protein solutions. *Anal Biochem* **100**:184-7.

Christopherson RI, Traut TW and Jones ME (1981) Multienzymatic proteins in mammalian pyrimidine biosynthesis: channeling of intermediates to avoid futile cycles. *Curr Top Cell Regul* **18**:59-77.

Clark KL, Oelke A, Johnson ME, Eilert KD, Simpson PC and Todd SC (2004) CD81 associates with 14-3-3 in a redox-regulated palmitoylation-dependent manner. *J Biol Chem* **279**:19401-6.

Clauser KR, Baker P and Burlingame AL (1999) Role of accurate mass measurement (+/- 10 ppm) in protein identification strategies employing MS or MS/MS and database searching. *Anal Chem* **71**:2871-82.

Coleman PF, Suttle DP and Stark GR (1977) Purification from hamster cells of the multifunctional protein that initiates de novo synthesis of pyrimidine nucleotides. *J Biol Chem* **252**:6379-85.

Connolly GP and Duley JA (1999) Uridine and its nucleotides: biological actions, therapeutic potentials. *Trends Pharmacol Sci* **20**:218-25.

Cuevas BD, Abell AN and Johnson GL (2007) Role of mitogen-activated protein kinase kinase kinases in signal integration. *Oncogene* **26**:3159-71.

Davidson JN, Chen KC, Jamison RS, Musmanno LA and Kern CB (1993) The evolutionary history of the first three enzymes in pyrimidine biosynthesis. *Bioessays* **15**:157-64.

Davies SP, Reddy H, Caivano M and Cohen P (2000) Specificity and mechanism of action of some commonly used protein kinase inhibitors. *Biochem J* **351**:95-105.

Denis-Duphil M, Lecaer JP, Hardie DG and Carrey EA (1990) Yeast carbamoyl-phosphate-synthetase--aspartate-transcarbamylase multidomain protein is phosphorylated in vitro by cAMP-dependent protein kinase. *Eur J Biochem* **193**:581-7.

Denton JE, Lui MS, Aoki T, Sebolt J, Takeda E, Eble JN, Glover JL and Weber G (1982) Enzymology of pyrimidine and carbohydrate metabolism in human colon carcinomas. *Cancer Res* **42**:1176-83.

Elledge SJ, Zhou Z, Allen JB and Navas TA (1993) DNA damage and cell cycle regulation of ribonucleotide reductase. *Bioessays* **15**:333-9.

Ellison V and Stillman B (2003) Biochemical characterization of DNA damage checkpoint complexes: clamp loader and clamp complexes with specificity for 5' recessed DNA. *PLoS Biol* **1**:E33.

Evans DR and Guy HI (2004) Mammalian pyrimidine biosynthesis: fresh insights into an ancient pathway. *J Biol Chem* **279**:33035-8.

Fox BA, Horii T and Bzik DJ (2002) Plasmodium falciparum: fine-mapping of an epitope of the serine repeat antigen that is a target of parasite-inhibitory antibodies. *Exp Parasitol* **101**:69-72.

Franks DM, Izumikawa T, Kitagawa H, Sugahara K and Okkema PG (2006) C. elegans pharyngeal morphogenesis requires both de novo synthesis of pyrimidines and synthesis of heparan sulfate proteoglycans. *Dev Biol* **296**:409-20.

Ganguly S, Weller JL, Ho A, Chemineau P, Malpaux B and Klein DC (2005) Melatonin synthesis: 14-3-3-dependent activation and inhibition of arylalkylamine N-acetyltransferase mediated by phosphoserine-205. *Proc Natl Acad Sci U S A* **102**:1222-7.

Gassmann MG, Stanzel A and Werner S (1999) Growth factor-regulated expression of enzymes involved in nucleotide biosynthesis: a novel mechanism of growth factor action. *Oncogene* **18**:6667-76.

Gattermann N, Dadak M, Hofhaus G, Wulfert M, Berneburg M, Loeffler ML and Simmonds HA (2004) Severe impairment of nucleotide synthesis through inhibition of mitochondrial respiration. *Nucleosides Nucleotides Nucleic Acids* **23**:1275-9.

Graves LM, Guy HI, Kozlowski P, Huang M, Lazarowski E, Pope RM, Collins MA, Dahlstrand EN, Earp HS, 3rd and Evans DR (2000) Regulation of carbamoyl phosphate synthetase by MAP kinase. *Nature* **403**:328-32.

Grayson DR and Evans DR (1983) The isolation and characterization of the aspartate transcarbamylase domain of the multifunctional protein, CAD. *J Biol Chem* **258**:4123-9.

Greer DA, Besley BD, Kennedy KB and Davey S (2003) hRad9 rapidly binds DNA containing double-strand breaks and is required for damage-dependent topoisomerase II beta binding protein 1 focus formation. *Cancer Res* **63**:4829-35.

Grem JL, King SA, O'Dwyer PJ and Leyland-Jones B (1988) Biochemistry and clinical activity of N-(phosphonacetyl)-L-aspartate: a review. *Cancer Res* **48**:4441-54.

Griffith JD, Lindsey-Boltz LA and Sancar A (2002) Structures of the human Rad17-replication factor C and checkpoint Rad 9-1-1 complexes visualized by glycerol spray/low voltage microscopy. *J Biol Chem* **277**:15233-6.

Guy HI and Evans DR (1994a) Cloning and expression of the mammalian multifunctional protein CAD in Escherichia coli. Characterization of the recombinant protein and a deletion mutant lacking the major interdomain linker. *J Biol Chem* **269**:23808-16.

Guy HI and Evans DR (1994b) Cloning, expression, and functional interactions of the amidotransferase domain of mammalian CAD carbamyl phosphate synthetase. *J Biol Chem* **269**:7702-8.

Guy HI and Evans DR (1994c) Function of the polypeptide chain segment connecting the dihydroorotase and aspartate transcarbamylase domains in the mammalian multifunctional CAD. *Adv Exp Med Biol* **370**:729-33.

Guy HI and Evans DR (1996) Function of the major synthetase subdomains of carbamyl-phosphate synthetase. *J Biol Chem* **271**:13762-9.

Herrmann ML, Schleyerbach R and Kirschbaum BJ (2000) Leflunomide: an immunomodulatory drug for the treatment of rheumatoid arthritis and other autoimmune diseases. *Immunopharmacology* **47**:273-89.

Hewagama A, Guy HI, Vickrey JF and Evans DR (1999) Functional linkage between the glutaminase and synthetase domains of carbamoyl-phosphate synthetase. Role of serine 44 in carbamoyl-phosphate synthetase-aspartate carbamoyltransferase-dihydroorotase (cad). *J Biol Chem* **274**:28240-5.

Hirai I and Wang HG (2002) A role of the C-terminal region of human Rad9 (hRad9) in nuclear transport of the hRad9 checkpoint complex. *J Biol Chem* **277**:25722-7.

Holden HM, Thoden JB and Raushel FM (1999) Carbamoyl phosphate synthetase: an amazing biochemical odyssey from substrate to product. *Cell Mol Life Sci* **56**:507-22.

Hoogenraad NJ, Levine RL and Kretchmer N (1971) Copurification of carbamoyl phosphate synthetase and aspartate transcarbamoylase from mouse spleen. *Biochem Biophys Res Commun* **44**:981-8.

Hopkins KM, Auerbach W, Wang XY, Hande MP, Hang H, Wolgemuth DJ, Joyner AL and Lieberman HB (2004) Deletion of mouse rad9 causes abnormal cellular responses to DNA damage, genomic instability, and embryonic lethality. *Mol Cell Biol* **24**:7235-48.

Huang M and Graves LM (2003) De novo synthesis of pyrimidine nucleotides; emerging interfaces with signal transduction pathways. *Cell Mol Life Sci* **60**:321-36.

Huang M, Kozlowski P, Collins M, Wang Y, Haystead TA and Graves LM (2002) Caspase-dependent cleavage of carbamoyl phosphate synthetase II during apoptosis. *Mol Pharmacol* **61**:569-77.

Huang X and Raushel FM (2000a) An engineered blockage within the ammonia tunnel of carbamoyl phosphate synthetase prevents the use of glutamine as a substrate but not ammonia. *Biochemistry* **39**:3240-7.

Huang X and Raushel FM (2000b) Restricted passage of reaction intermediates through the ammonia tunnel of carbamoyl phosphate synthetase. *J Biol Chem* **275**:26233-40.

Idzko M, Dichmann S, Ferrari D, Di Virgilio F, la Sala A, Girolomoni G, Panther E and Norgauer J (2002) Nucleotides induce chemotaxis and actin polymerization in immature but not mature human dendritic cells via activation of pertussis toxin-sensitive P2y receptors. *Blood* **100**:925-32.

Irvine HS, Shaw SM, Paton A and Carrey EA (1997) A reciprocal allosteric mechanism for efficient transfer of labile intermediates between active sites in CAD, the mammalian pyrimidine-biosynthetic multienzyme polypeptide. *Eur J Biochem* **247**:1063-73.

Ishida H, Mori M and Tatibana M (1977) Effects of dimethyl sulfoxide and glycerol on catalytic and regulatory properties of glutamine-dependent carbamoyl phosphate synthase from rat liver and dual effects of uridine triphosphate. *Arch Biochem Biophys* **182**:258-65.

Ishijima S, Kita K, Kinoshita N, Ishizuka T, Suzuki N and Tatibana M (1988) Evidence for early mitogenic stimulation of metabolic flux through phosphoribosyl pyrophosphate into nucleotides in Swiss 3T3 cells. *J Biochem (Tokyo)* **104**:570-5.

Ishikawa K, Ishii H, Murakumo Y, Mimori K, Kobayashi M, Yamamoto K, Mori M, Nishino H, Furukawa Y and Ichimura K (2007) Rad9 modulates the P21WAF1 pathway by direct association with p53. *BMC Mol Biol* **8**:37.

Ito K and Uchino H (1971) Control of pyrimidine biosynthesis in human lymphocytes. Induction of glutamine-utilizing carbamyl phosphate synthetase and operation of orotic acid pathway during blastogenesis. *J Biol Chem* **246**:4060-5.

Ito K and Uchino H (1973) Control of pyrimidine biosynthesis in human lymphocytes. Simultaneous increase in activities of glutamine-utilizing carbamyl phosphate synthetase and aspartate transcarbamylase in phytohemagglutinin-stimulated human peripheral lymphocytes and their enzyme co-purification. *J Biol Chem* **248**:389-92.

Jans DA and Hubner S (1996) Regulation of protein transport to the nucleus: central role of phosphorylation. *Physiol Rev* **76**:651-85.

Jarry B and Falk D (1974) Functional diversity within the rudimentary locus of Drosophila melanogaster. *Mol Gen Genet* **135**:113-22.

Jayaram HN, Cooney DA, Ryan JA, Neil G, Dion RL and Bono VH (1975) L-[alphaS, 5S]-alpha-amino-3-chloro-4,5-dihydro-5-isoxazoleacetic acid (NSC-163501): a new amino acid antibiotic with the properties of an antagonist of L-glutamine. *Cancer Chemother Rep* **59**:481-91.

Jones ME (1970) Regulation of pyrimidine and arginine biosynthesis in mammals. *Adv Enzyme Regul* **9**:19-49.

Jones ME (1980) Pyrimidine nucleotide biosynthesis in animals: genes, enzymes, and regulation of UMP biosynthesis. *Annu Rev Biochem* **49**:253-79.

Kalman SM, Duffield PH and Brzozowski T (1965) Identity in Escherichia Coli of Carbamyl Phosphokinase and an Activity Which Catalyzes Amino Group Transfer from Glutamine to Ornithine in Citrulline Synthesis. *Biochem Biophys Res Commun* **18**:530-7.

Karle JM, Cowan KH, Chisena CA and Cysyk RL (1986) Uracil nucleotide synthesis in a human breast cancer cell line (MCF-7) and in two drug-resistant sublines that contain increased levels of enzymes of the de novo pyrimidine pathway. *Mol Pharmacol* **30**:136-41.

Kelly RE, Mally MI and Evans DR (1986) The dihydroorotase domain of the multifunctional protein CAD. Subunit structure, zinc content, and kinetics. *J Biol Chem* **261**:6073-83.

Kempe TD, Swyryd EA, Bruist M and Stark GR (1976) Stable mutants of mammalian cells that overproduce the first three enzymes of pyrimidine nucleotide biosynthesis. *Cell* **9**:541-50.

Kensler TW, Reck LJ and Cooney DA (1981) Therapeutic effects of acivicin and N-(phosphonacetyl)-L-aspartic acid in a biochemically designed trial against a N-(phosphonacetyl)-L-aspartic acid-resistant variant of the Lewis lung carcinoma. *Cancer Res* **41**:905-9.

Khan S, Abdelrahim M, Samudio I and Safe S (2003) Estrogen receptor/Sp1 complexes are required for induction of cad gene expression by 17beta-estradiol in breast cancer cells. *Endocrinology* **144**:2325-35.

Kim C, Vigil D, Anand G and Taylor SS (2006) Structure and dynamics of PKA signaling proteins. *Eur J Cell Biol* **85**:651-4.

Kim H, Kelly RE and Evans DR (1992) The structural organization of the hamster multifunctional protein CAD. Controlled proteolysis, domains, and linkers. *J Biol Chem* **267**:7177-84.

Kim J, Howell S, Huang X and Raushel FM (2002) Structural defects within the carbamate tunnel of carbamoyl phosphate synthetase. *Biochemistry* **41**:12575-81.

Kim J and Raushel FM (2004) Perforation of the tunnel wall in carbamoyl phosphate synthetase derails the passage of ammonia between sequential active sites. *Biochemistry* **43**:5334-40.

Komatsu K, Miyashita T, Hang H, Hopkins KM, Zheng W, Cuddeback S, Yamada M, Lieberman HB and Wang HG (2000) Human homologue of S. pombe Rad9 interacts with BCL-2/BCL-xL and promotes apoptosis. *Nat Cell Biol* **2**:1-6.

Kotsis DH, Masko EM, Sigoillot FD, Gregorio RD, Guy-Evans HI and Evans DR (2007) Protein kinase A phosphorylation of the multifunctional protein CAD antagonizes activation by the MAP kinase cascade. *Mol Cell Biochem* **301**:69-81.

Lagoja IM (2005) Pyrimidine as constituent of natural biologically active compounds. *Chem Biodivers* **2**:1-50.

Lee L, Kelly RE, Pastra-Landis SC and Evans DR (1985) Oligomeric structure of the multifunctional protein CAD that initiates pyrimidine biosynthesis in mammalian cells. *Proc Natl Acad Sci U S A* **82**:6802-6.

Lee MW, Hirai I and Wang HG (2003) Caspase-3-mediated cleavage of Rad9 during apoptosis. *Oncogene* **22**:6340-6.

Lehmann F, Tiralongo E and Tiralongo J (2006) Sialic acid-specific lectins: occurrence, specificity and function. *Cell Mol Life Sci* **63**:1331-54.

Liao WS, Heller R, Green P and Stark GR (1986) Regulation of carbamoyl phosphate synthetase-aspartate transcarbamoylase-dihydroorotase gene expression in growing and arrested cells. *J Biol Chem* **261**:15577-81.

Lindsey-Boltz LA, Bermudez VP, Hurwitz J and Sancar A (2001) Purification and characterization of human DNA damage checkpoint Rad complexes. *Proc Natl Acad Sci U S A* **98**:11236-41.

Lindsey-Boltz LA, Wauson EM, Graves LM and Sancar A (2004) The human Rad9 checkpoint protein stimulates the carbamoyl phosphate synthetase activity of the multifunctional protein CAD. *Nucleic Acids Res* **32**:4524-30.

Lipscomb WN (1994) Aspartate transcarbamylase from Escherichia coli: activity and regulation. *Adv Enzymol Relat Areas Mol Biol* **68**:67-151.

Liu L, Li L, Rao JN, Zou T, Zhang HM, Boneva D, Bernard MS and Wang JY (2004) Polyamine-modulated expression of c-Myc plays a critical role in stimulation of normal intestinal epithelial cell proliferation. *Am J Physiol Cell Physiol*.

Liu X, Guy HI and Evans DR (1994) Identification of the regulatory domain of the mammalian multifunctional protein CAD by the construction of an Escherichia coli hamster hybrid carbamyl-phosphate synthetase. *J Biol Chem* **269**:27747-55.

Loegering D, Arlander SJ, Hackbarth J, Vroman BT, Roos-Mattjus P, Hopkins KM, Lieberman HB, Karnitz LM and Kaufmann SH (2004) Rad9 protects cells from topoisomerase poison-induced cell death. *J Biol Chem* **279**:18641-7.

Loffler M, Jockel J, Schuster G and Becker C (1997) Dihydroorotat-ubiquinone oxidoreductase links mitochondria in the biosynthesis of pyrimidine nucleotides. *Mol Cell Biochem* **174**:125-9.

Lyons SD, Sant ME and Christopherson RI (1990) Cytotoxic mechanisms of glutamine antagonists in mouse L1210 leukemia. *J Biol Chem* **265**:11377-81.

Mac SM and Farnham PJ (2000) CAD, a c-Myc target gene, is not deregulated in Burkitt's lymphoma cell lines. *Mol Carcinog* **27**:84-96.

Macdonald N, Welburn JP, Noble ME, Nguyen A, Yaffe MB, Clynes D, Moggs JG, Orphanides G, Thomson S, Edmunds JW, Clayton AL, Endicott JA and Mahadevan LC (2005) Molecular basis for the recognition of phosphorylated and phosphoacetylated histone h3 by 14-3-3. *Mol Cell* **20**:199-211.

Maher MJ, Huang DT, Guss JM, Collyer CA and Christopherson RI (2003) Crystallization of hamster dihydroorotase: involvement of a disulfide-linked tetrameric form. *Acta Crystallogr D Biol Crystallogr* **59**:381-4.

Majka J and Burgers PM (2003) Yeast Rad17/Mec3/Ddc1: a sliding clamp for the DNA damage checkpoint. *Proc Natl Acad Sci U S A* **100**:2249-54.

Maley JA and Davidson JN (1988) Identification of the junction between the glutamine amidotransferase and carbamyl phosphate synthetase domains of the mammalian CAD protein. *Biochem Biophys Res Commun* **154**:1047-53.

Meek SE, Lane WS and Piwnica-Worms H (2004) Comprehensive proteomic analysis of interphase and mitotic 14-3-3-binding proteins. *J Biol Chem* **279**:32046-54.

Meek TD, Karsten WE and DeBrosse CW (1987) Carbamoyl-phosphate synthetase II of the mammalian CAD protein: kinetic mechanism and elucidation of reaction intermediates by positional isotope exchange. *Biochemistry* **26**:2584-93.

Mehl Y and Jarry BP (1978) Developmental regulation of the first three enzymes of pyrimidine biosynthesis in Drosophila melanogaster. *Dev Biol* **67**:1-10.

Miles BW and Raushel FM (2000) Synchronization of the three reaction centers within carbamoyl phosphate synthetase. *Biochemistry* **39**:5051-6.

Milosevic J, Brandt A, Roemuss U, Arnold A, Wegner F, Schwarz SC, Storch A, Zimmermann H and Schwarz J (2006) Uracil nucleotides stimulate human neural precursor cell proliferation and dopaminergic differentiation: involvement of MEK/ERK signalling. *J Neurochem* **99**:913-23.

Miltenberger RJ, Sukow KA and Farnham PJ (1995) An E-box-mediated increase in cad transcription at the G1/S-phase boundary is suppressed by inhibitory c-Myc mutants. *Mol Cell Biol* **15**:2527-35.

Miran SG, Chang SH and Raushel FM (1991) Role of the four conserved histidine residues in the amidotransferase domain of carbamoyl phosphate synthetase. *Biochemistry* **30**:7901-7.

Mitchell AD and Hoogenraad NJ (1975) De novo pyrimidine nucleotide biosynthesis in synchronized rat hepatoma (HTC) cells and mouse embryo fibroblast (3T3) cells. *Exp Cell Res* **93**:105-10.

Morford G, Davidson JN and Snow EC (1994) Appearance of CAD activity, the rate-limiting enzyme for pyrimidine biosynthesis, as B cells progress into and through the G1 stage of the cell cycle. *Cell Immunol* **158**:96-104.

Musmanno LA, Jamison RS, Barnett RS, Buford E and Davidson JN (1992) Complete hamster CAD protein and the carbamylphosphate synthetase domain of CAD complement mammalian cell mutants defective in de novo pyrimidine biosynthesis. *Somat Cell Mol Genet* **18**:309-18.

Nagy M, Le Gouar M, Potier S, Souciet JL and Herve G (1989) The primary structure of the aspartate transcarbamylase region of the URA2 gene product in Saccharomyces cerevisiae. Features involved in activity and nuclear localization. *J Biol Chem* **264**:8366-74.

Norby S (1970) A specific nutritional requirement for pyrimidines in rudimentary mutants of Drosophila melanogaster. *Hereditas* **66**:205-14.

Norby S (1973) The biochemical genetics of rudimentary mutants of Drosophila melanogaster. I. Aspartate carbamoyltransferase levels in complementing and non-complementing strains. *Hereditas* **73**:11-6.

Nyunoya H and Lusty CJ (1983) The carB gene of Escherichia coli: a duplicated gene coding for the large subunit of carbamoyl-phosphate synthetase. *Proc Natl Acad Sci U S A* **80**:4629-33.

Obenauer JC, Cantley LC and Yaffe MB (2003) Scansite 2.0: Proteome-wide prediction of cell signaling interactions using short sequence motifs. *Nucleic Acids Res* **31**:3635-41.

Olsen JV, Blagoev B, Gnad F, Macek B, Kumar C, Mortensen P and Mann M (2006) Global, in vivo, and site-specific phosphorylation dynamics in signaling networks. *Cell* **127**:635-48.

Otsuki T, Mori M and Tatibana M (1981) Phosphorylation and dephosphorylation of carbamoyl-phosphate synthetase II complex of rat ascites hepatoma cells. *J Biochem (Tokyo)* **89**:1367-74.

Padgett RA, Wahl GM, Coleman PF and Stark GR (1979) N-(Phosphonacetyl)-L-aspartate-resistant hamster cells overaccumulate a single mRNA coding for the multifunctional protein that catalyzes the first steps of UMP synthesis. *J Biol Chem* **254**:974-80.

Pal S, Yun R, Datta A, Lacomis L, Erdjument-Bromage H, Kumar J, Tempst P and Sif S (2003) mSin3A/histone deacetylase 2- and PRMT5-containing Brg1 complex is involved in transcriptional repression of the Myc target gene cad. *Mol Cell Biol* **23**:7475-87.

Pappas A, Yang WL, Park TS and Carman GM (1998) Nucleotide-dependent tetramerization of CTP synthetase from Saccharomyces cerevisiae. *J Biol Chem* **273**:15954-60.

Pausch J, Keppler D and Decker K (1972) Activity and distribution of the enzymes of uridylate synthesis from orotate in animal tissues. *Biochim Biophys Acta* **258**:395-403.

Porter RW, Modebe MO and Stark GR (1969) Aspartate transcarbamylase. Kinetic studies of the catalytic subunit. *J Biol Chem* **244**:1846-59.

Powers SG, Griffith OW and Meister A (1977) Inhibition of carbamyl phosphate synthetase by P1, P5-di(adenosine 5')-pentaphosphate: evidence for two ATP binding sites. *J Biol Chem* **252**:3558-60.

Powers SG and Meister A (1978) Mechanism of the reaction catalyzed by carbamyl phosphate synthetase. Binding of ATP to the two functionally different ATP sites. *J Biol Chem* **253**:800-3.

Qiu Y and Davidson JN (2000) Substitutions in the aspartate transcarbamoylase domain of hamster CAD disrupt oligomeric structure. *Proc Natl Acad Sci U S A* **97**:97-102.

Raman M, Chen W and Cobb MH (2007) Differential regulation and properties of MAPKs. *Oncogene* **26**:3100-12.

Rao GN, Buford ES and Davidson JN (1987) Transcriptional regulation of the human CAD gene during myeloid differentiation. *Mol Cell Biol* **7**:1961-6.

Rao GN and Church RL (1988) Regulation of CAD gene expression in mouse fibroblasts during the transition from the resting to the growing state. *Exp Cell Res* **178**:449-56.

Rao GN and Davidson JN (1988) CAD gene expression in serum-starved and serum-stimulated hamster cells. *DNA* **7**:423-32.

Rawls JM and Fristrom JW (1975) A complex genetic locus that controls of the first three steps of pyrimidine biosynthesis in Drosophila. *Nature* **255**:738-40.

Reardon MA, Dixon JE and Weber G (1987) Increased messenger RNA concentration for carbamoyl-phosphate synthase II in hepatoma 3924A. *Biochem Biophys Res Commun* **147**:494-500.

Reardon MA and Weber G (1985) Increased carbamoyl-phosphate synthetase II concentration in rat hepatomas: immunological evidence. *Cancer Res* **45**:4412-5.

Reitsma PH, Rothberg PG, Astrin SM, Trial J, Bar-Shavit Z, Hall A, Teitelbaum SL and Kahn AJ (1983) Regulation of myc gene expression in HL-60 leukaemia cells by a vitamin D metabolite. *Nature* **306**:492-4.

Reyes P and Guganig ME (1975) Studies on a pyrimidine phosphoribosyltransferase from murine leukemia P1534J. Partial purification, substrate specificity, and evidence for its existence as a bifunctional complex with orotidine 5-phosphate decarboxylase. *J Biol Chem* **250**:5097-108.

Roos-Mattjus P, Hopkins KM, Oestreich AJ, Vroman BT, Johnson KL, Naylor S, Lieberman HB and Karnitz LM (2003) Phosphorylation of human Rad9 is required for genotoxin-activated checkpoint signaling. *J Biol Chem* **278**:24428-37.

Ruckemann K, Fairbanks LD, Carrey EA, Hawrylowicz CM, Richards DF, Kirschbaum B and Simmonds HA (1998) Leflunomide inhibits pyrimidine de novo synthesis in mitogen-stimulated T-lymphocytes from healthy humans. *J Biol Chem* **273**:21682-91.

Rush J, Moritz A, Lee KA, Guo A, Goss VL, Spek EJ, Zhang H, Zha XM, Polakiewicz RD and Comb MJ (2005) Immunoaffinity profiling of tyrosine phosphorylation in cancer cells. *Nat Biotechnol* **23**:94-101.

Sahay N, Guy HI, Liu X and Evans DR (1998) Regulation of an Escherichia coli/mammalian chimeric carbamoyl-phosphate synthetase. *J Biol Chem* **273**:31195-202.

Sancar A, Lindsey-Boltz LA, Unsal-Kacmaz K and Linn S (2004) Molecular mechanisms of mammalian DNA repair and the DNA damage checkpoints. *Annu Rev Biochem* **73**:39-85.

Sarkaria JN, Busby EC, Tibbetts RS, Roos P, Taya Y, Karnitz LM and Abraham RT (1999) Inhibition of ATM and ATR kinase activities by the radiosensitizing agent, caffeine. *Cancer Res* **59**:4375-82.

Schauer R (2000) Achievements and challenges of sialic acid research. *Glycoconj J* **17**:485-99.

Scheidtmann KH, Echle B and Walter G (1982) Simian virus 40 large T antigen is phosphorylated at multiple sites clustered in two separate regions. *J Virol* **44**:116-33.

Schobitz B, Wolf S, Christopherson RI and Brand K (1991) Nucleotide and nucleic acid metabolism in rat thymocytes during cell cycle progression. *Biochim Biophys Acta* **1095**:95-102.

Shabb JB (2001) Physiological substrates of cAMP-dependent protein kinase. *Chem Rev* **101**:2381-411.

Shaw SM and Carrey EA (1992) Regulation of the mammalian carbamoyl-phosphate synthetase II by effectors and phosphorylation. Altered affinity for ATP and magnesium ions measured using the ammonia-dependent part reaction. *Eur J Biochem* **207**:957-65.

Shikano S, Coblitz B, Sun H and Li M (2005) Genetic isolation of transport signals directing cell surface expression. *Nat Cell Biol* **7**:985-92.

Shoaf WT and Jones ME (1971) Initial steps in pyrimidine synthesis in Ehrlich ascites carcinoma. *Biochem Biophys Res Commun* **45**:796-802.

Shoaf WT and Jones ME (1973) Uridylic acid synthesis in Ehrlich ascites carcinoma. Properties, subcellular distribution, and nature of enzyme complexes of the six biosynthetic enzymes. *Biochemistry* **12**:4039-51.

Sigoillot FD, Berkowski JA, Sigoillot SM, Kotsis DH and Guy HI (2003) Cell cycle-dependent regulation of pyrimidine biosynthesis. *J Biol Chem* **278**:3403-9.

Sigoillot FD, Evans DR and Guy HI (2002a) Autophosphorylation of the mammalian multifunctional protein that initiates de novo pyrimidine biosynthesis. *J Biol Chem* **277**:24809-17.

Sigoillot FD, Evans DR and Guy HI (2002b) Growth-dependent regulation of mammalian pyrimidine biosynthesis by the protein kinase A and MAPK signaling cascades. *J Biol Chem* **277**:15745-51.

Sigoillot FD, Kotsis DH, Masko EM, Bame M, Evans DR and Evans HI (2007) Protein kinase C modulates the up-regulation of the pyrimidine biosynthetic complex, CAD, by MAP kinase. *Front Biosci* **12**:3892-8.

Sigoillot FD, Kotsis DH, Serre V, Sigoillot SM, Evans DR and Guy HI (2005) Nuclear localization and mitogen-activated protein kinase phosphorylation of the multifunctional protein CAD. *J Biol Chem* **280**:25611-20.

Sigoillot FD, Sigoillot SM and Guy HI (2004) Breakdown of the regulatory control of pyrimidine biosynthesis in human breast cancer cells. *Int J Cancer* **109**:491-8.

Simmer JP, Kelly RE, Rinker AG, Jr., Scully JL and Evans DR (1990a) Mammalian carbamyl phosphate synthetase (CPS). DNA sequence and evolution of the CPS

domain of the Syrian hamster multifunctional protein CAD. *J Biol Chem* **265**:10395-402.

Simmer JP, Kelly RE, Rinker AG, Jr., Zimmermann BH, Scully JL, Kim H and Evans DR (1990b) Mammalian dihydroorotase: nucleotide sequence, peptide sequences, and evolution of the dihydroorotase domain of the multifunctional protein CAD. *Proc Natl Acad Sci U S A* **87**:174-8.

Simmer JP, Kelly RE, Scully JL, Grayson DR, Rinker AG, Jr., Bergh ST and Evans DR (1989) Mammalian aspartate transcarbamylase (ATCase): sequence of the ATCase domain and interdomain linker in the CAD multifunctional polypeptide and properties of the isolated domain. *Proc Natl Acad Sci U S A* **86**:4382-6.

Simmons AJ, Rawls JM, Piskur J and Davidson JN (1999) A mutation that uncouples allosteric regulation of carbamyl phosphate synthetase in Drosophila. *J Mol Biol* **287**:277-85.

Simmons CQ, Simmons AJ, Haubner A, Ream A and Davidson JN (2004) Substitutions in hamster CAD carbamoyl-phosphate synthetase alter allosteric response to 5-phosphoribosyl-alpha-pyrophosphate (PRPP) and UTP. *Biochem J* **378**:991-8.

Smith CL, Pilarski LM, Egerton ML and Wiley JS (1989) Nucleoside transport and proliferative rate in human thymocytes and lymphocytes. *Blood* **74**:2038-42.

St Onge RP, Besley BD, Park M, Casselman R and Davey S (2001) DNA damage-dependent and -independent phosphorylation of the hRad9 checkpoint protein. *J Biol Chem* **276**:41898-905.

St Onge RP, Besley BD, Pelley JL and Davey S (2003) A role for the phosphorylation of hRad9 in checkpoint signaling. *J Biol Chem* **278**:26620-8.

Stevens RC, Chook YM, Cho CY, Lipscomb WN and Kantrowitz ER (1991) Escherichia coli aspartate carbamoyltransferase: the probing of crystal structure analysis via site-specific mutagenesis. *Protein Eng* **4**:391-408.

Swyryd EA, Seaver SS and Stark GR (1974) N-(phosphonacetyl)-L-aspartate, a potent transition state analog inhibitor of aspartate transcarbamylase, blocks proliferation of mammalian cells in culture. *J Biol Chem* **249**:6945-50.

Tasken K and Aandahl EM (2004) Localized effects of cAMP mediated by distinct routes of protein kinase A. *Physiol Rev* **84**:137-67.

Thoden JB, Holden HM, Wesenberg G, Raushel FM and Rayment I (1997) Structure of carbamoyl phosphate synthetase: a journey of 96 A from substrate to product. *Biochemistry* **36**:6305-16.

Traut TW (1994) Physiological concentrations of purines and pyrimidines. *Mol Cell Biochem* **140**:1-22.

Traut TW and Jones ME (1977) Kinetic and conformational studies of the orotate phosphoribosyltransferase:orotidine-5'-phosphate decarboxylase enzyme complex from mouse Ehrlich ascites cells. *J Biol Chem* **252**:8372-81.

Trotta PP, Platzer KE, Haschemeyer RH and Meister A (1974) Glutamine-binding subunit of glutamate synthase and partial reactions catalyzed by this glutamine amidotransferase. *Proc Natl Acad Sci U S A* **71**:4607-11.

Wahl GM, Padgett RA and Stark GR (1979) Gene amplification causes overproduction of the first three enzymes of UMP synthesis in N-(phosphonacetyl)-L-aspartate-resistant hamster cells. *J Biol Chem* **254**:8679-89.

Walsh DA, Perkins JP and Krebs EG (1968) An adenosine 3',5'-monophosphate-dependant protein kinase from rabbit skeletal muscle. *J Biol Chem* **243**:3763-5.

Wang L, Hsu CL, Ni J, Wang PH, Yeh S, Keng P and Chang C (2004) Human checkpoint protein hRad9 functions as a negative coregulator to repress androgen receptor transactivation in prostate cancer cells. *Mol Cell Biol* **24**:2202-13.

Wang W, Lindsey-Boltz LA, Sancar A and Bambara RA (2006) Mechanism of stimulation of human DNA ligase I by the Rad9-rad1-Hus1 checkpoint complex. *J Biol Chem* **281**:20865-72.

Wellner VP, Anderson PM and Meister A (1973) Interaction of Escherichia coli carbamyl phosphate synthetase with glutamine. *Biochemistry* **12**:2061-6.

Wiley JS, Snook MB and Jamieson GP (1989) Nucleoside transport in acute leukaemia and lymphoma: close relation to proliferative rate. *Br J Haematol* **71**:203-7.

Willer GB, Lee VM, Gregg RG and Link BA (2005) Analysis of the Zebrafish perplexed mutation reveals tissue-specific roles for de novo pyrimidine synthesis during development. *Genetics* **170**:1827-37.

Williams NK, Simpson RJ, Moritz RL, Peide Y, Crofts L, Minasian E, Leach SJ, Wake RG and Christopherson RI (1990) Location of the dihydroorotase domain within trifunctional hamster dihydroorotate synthetase. *Gene* **94**:283-8.

Wisdom R and Lee W (1990) Translation of c-myc mRNA is required for its post-transcriptional regulation during myogenesis. *J Biol Chem* **265**:19015-21.

Yeilding NM, Procopio WN, Rehman MT and Lee WM (1998) c-myc mRNA is down-regulated during myogenic differentiation by accelerated decay that depends on translation of regulatory coding elements. *J Biol Chem* **273**:15749-57.

Yin Y, Zhu A, Jin YJ, Liu YX, Zhang X, Hopkins KM and Lieberman HB (2004) Human RAD9 checkpoint control/proapoptotic protein can activate transcription of p21. *Proc Natl Acad Sci U S A* **101**:8864-9.

Yip MC and Knox WE (1970) Glutamine-dependent carbamyl phosphate synthetase. Properties and distribution in normal and neoplastic rat tissues. *J Biol Chem* **245**:2199-204.

Yoshida K, Komatsu K, Wang HG and Kufe D (2002) c-Abl tyrosine kinase regulates the human Rad9 checkpoint protein in response to DNA damage. *Mol Cell Biol* **22**:3292-300.

Yoshida K, Wang HG, Miki Y and Kufe D (2003) Protein kinase Cdelta is responsible for constitutive and DNA damage-induced phosphorylation of Rad9. *Embo J* **22**:1431-41.

Zhang J, Visser F, King KM, Baldwin SA, Young JD and Cass CE (2007) The role of nucleoside transporters in cancer chemotherapy with nucleoside drugs. *Cancer Metastasis Rev* **26**:85-110.

Zou L, Liu D and Elledge SJ (2003) Replication protein A-mediated recruitment and activation of Rad17 complexes. *Proc Natl Acad Sci U S A* **100**:13827-32.